Exploring the role of methionine aminopeptidase 2 and other noncaspase proteases in programmed cell death of *Leishmania donovani*

A Thesis
Submitted in Partial
Fulfillment of the Requirements for the Degree of

DOCTOR OF PHILOSOPHY

By

Mr. Ritesh Kumar

Department of Biosciences and Bioengineering
Indian Institute of Technology Guwahati
Guwahati-781039, Assam, India

MAY 2017

Exploring the role of methionine aminopeptidase 2 and other noncaspase proteases in programmed cell death of *Leishmania donovani*

A Thesis Submitted

By

Mr. Ritesh Kumar

126106036

In Partial Fulfillment of the Requirements for the Degree of

Doctor of Philosophy

Department of Biosciences and Bioengineering

Indian Institute of Technology Guwahati

Guwahati -781039, Assam, INDIA

MAY 2017

TH-1832_126106036

Dedicated
to
My Parents and Supervisor
for
constant support and encouragement

TH-1832_126106036

INDIAN INSTITUTE OF TECHNOLOGY GUWAHATI

DEPARTMENT OF BIOSCIENCES AND BIOENGINEERING

STATEMENT

I hereby declare that the matter embodied in this thesis titled **"Exploring the role of methionine aminopeptidase 2 and other noncaspase proteases in programmed cell death of *Leishmania donovani*"** is the result of investigations carried out by me in the Department of Biosciences and Bioengineering, Indian Institute of Technology Guwahati, Assam, India under the supervision of **Prof. Vikash Kumar Dubey**.

In keeping with the general practice of reporting scientific observations, due acknowledgements have been made wherever the work of other investigators are referred. Further the data in the thesis are collected by me. I certify that there is no fabrication or manipulation of data in the thesis.

Date: May, 2017

Ritesh Kumar
(126106036)

TH-1832_126106036

INDIAN INSTITUTE OF TECHNOLOGY GUWAHATI

DEPARTMENT OF BIOSCIENCES AND BIOENGINEERING

CERTIFICATE

It is certified that the work described in this thesis **"Exploring the role of methionine aminopeptidase 2 and other noncaspase proteases in programmed cell death of *Leishmania donovani*"** by **Mr. Ritesh Kumar** (Roll No. **126106036**), submitted to Indian Institute of Technology Guwahati, India for the award of degree of Doctor of Philosophy, is an authentic record of results obtained from the research work carried out under my supervision at the Department of Biosciences and Bioengineering, Indian Institute of Technology Guwahati, India and this work has not been submitted elsewhere for a degree.

Prof. Vikash Kumar Dubey

(Thesis Supervisor)

TH-1832_126106036

Acknowledgement

I would like to begin by thanking Prof. Vikash Kumar Dubey, my PhD supervisor without whom this journey would be impossible. He is an epitome of sincerity and never shies away from working hard. He is approachable and knows exactly what to say to motivate his students. He has cultivated an ambience in the lab which propagates the idea to work independently. This further helps in developing abilities to apply the idea which has benefitted me immensely. I am immensely grateful to him as I cannot imagine completing my PhD without his support.

I would like to thank my Doctoral committee: Dr. Shankar Prasad Kanaujia, Dr. Manish Kumar, and Prof. Parameswar K. Iyer for reviewing my thesis work constantly and providing critical comments to improve and evolve my thesis in a better way. They made sure that I was always on the right track and also, helped me understand the nuances of research. I would also like to extend my special thanks to the Heads of the Department: Prof. K. Pakshirajan and Prof. V. V. Dasu for providing a sustainable working environment for me through their administrative abilities. I would also like to extend my thanks to the technical and non-technical staffs of the department for their support and assistance during my Ph.D studies.

I am very grateful to Prof. Stephen Beverley, Washington University in St. Louis for gifting pXG expression vectors to prepare knock out constructs. I am also thankful to Prof. Shyam Sundar, Banaras Hindu University for generously providing Leishmania donovani strain.

A major pillar for building any scientific venture is infrastructure and instruments. I would like to thank the Department of Biosciences and Bioengineering, Central Instrument Facility and Indian Institute of Technology Guwahati for establishing this durable pillar to aid my PhD. A major assistance in completing my research work came from Guwahati Biotech Park in the form of confocal microscopy imaging facility. I am truly indebted to Ministry of Human Resource and Development (MHRD) for the perennial financial support offered throughout the course of my PhD.

A heartfelt gratitude to all my current and past lab members: Dr. Jay Prakash, Kartikeya, Shyamali, Kamalesh, Adarsh, Gundappa, Jiban, Prachi, Chayanika, Buddhadev, Dr. Suresh Kumar, Dr. Ruchika Bhardwaj, Dr. Shalini Singh, Dr. Mousumi Das, Dr. Sushant Singh, Dr. Saudagar Prakash, Dr. Abhay N Singh, Vidyadhar, Ashish, Ankur, Ekta and Sona. They truly stuck with me through thick-and-thin. Thank you for the awesome lab environment and help during several experiments. When I turn back and look at my PhD journey, it will always be painted with the endearing memories I created

TH-1832_126106036

with Sudhir, Balwant, Ajay and all other friends in Department of Biosciences and Bioengineering. They made all the joy enjoyable and all the pain bearable. I would also like to thank to my friend Bishal and Gayathri for their constant support and motivation during difficult times.

During hectic schedule of PhD work, the one thing that never failed to refresh me was Bani Mandir Coffee corner. Your coffee and condiments powered me through the time when I was stressed out with hectic research schedule.

A note of gratitude will never be complete without the mention of my family: my parents, my wife Deepti, and my brother Rohit. They believed in my dreams long before I envisioned them. They believed in me when I ceased to believe in myself. They shaped my identity. They sowed the seeds of dreams in my mind, they nurtured those dreams, and they protected the dreams from adversities. Sometimes, they had to sacrifice their own happiness to turn my dreams into reality. All the words in the English language put together will be insufficient to thank you.

Ritesh Kumar
May, 2017

TH-1832_126106036

Abbreviations

Ld	:	*Leishmania donovani*
7-AMC	:	7-amido-4-methylcoumarin
Ac-DEVD-AMC	:	N-acetyl-Asp-Glu-Val-Asp-7-amino-4-methylcoumarin
Ac-LEHD-AFC	:	N-acetyl-Leu-Glu-His-Asp-7-amino-4-methylcoumarin
Ac-VEID-AMC	:	N-acetyl-Val-Glu-Iso-Asp-7-amino-4-methylcoumarin
AIDS	:	Acquired immunodeficiency syndrome
AmB	:	Amphotericin B
Apaf-1	:	Apoptotic protease activating factor
Bid	:	BH3 interacting-domain
BLAST	:	Basic Local Alignment Search Tool
BRENDA	:	Braunschweig Enzyme Database
$CaCl_2$	:	Calcium chloride
CDC	:	Centers for Disease Control and Prevention
CELLO	:	subCELlular LOcalization predictor
CL	:	Cutaneous Leishmaniasis
CTLs	:	Cytotoxic T lymphocytes
$CuCl_2$	:	Copper(II) chloride
Cyt. c	:	Cytochrome c
DAB	:	3,3'-Diaminobenzidine
DEVD	:	Aspartyl-glutamyl-valyl-aspartate
DISC	:	Death induced signaling complex
DMSO	:	Dimethyl sulfoxide
ECD	:	Electron Coupled Dye
EDTA	:	Ethylenediaminetetraacetic acid
eIF2α	:	Eukarytic initiation factor 2α
ER	:	Endoplasmic reticulumn
FADD	:	Fas activated death domain
FBS	:	Fetal bovine serum
FITC	:	Fluorescein isothiocyanate
FSC	:	Forward scatter
FURA 2AM	:	Fura-2-acetoxymethyl ester
H_2O_2	:	Hydrogen peroxide
HCl	:	Hydrochloric acid
HIV	:	Human immunodeficiency virus
ICE	:	Interleukin -1β converting enzyme
IP_3R	:	Inositol triphosphate
IPTG	:	Isopropyl β-D-1-thiogalactopyranoside

TH-1832_126106036

KCl	:	Potassium chloride
K_i	:	Inhibitory constant
K_m	:	Michaelis-Menten constant
LB medium	:	Luria-Bertani medium
*Ld*MT	:	*Leishmania donovani* miltefosine transporter
MAP1	:	Methionine aminopeptidase 1
MAP2	:	Methionine aminopeptidase 2
MCL	:	Muco-cutaneous leishmaniasis
Met-AMC	:	L-Methionine 7-amido-4-methylcoumarin
$MgCl_2$	:	Magnesium chloride
$MnCl_2$	:	Manganese(II) chloride
MOMP	:	Mitochondrial outer membrane permeabilization
MOPS	:	(3-(N-morpholino) propanesulfonic acid)
MTT	:	3-(4,5-dimethylthiazol-2-yl)-2,5-diphenyltetrazolium bromide
NaCl	:	Sodium chloride
$NiCl_2$	:	Nickel(II) chloride
Ni-NTA	:	Nickel-Nitrilotriacetic acid
$NiSO_4$	:	Nickel(II) sulfate
NK cells	:	Natural Killer cells
N-s-LLVY-AMC	:	N-succinyl-leu-leu-val-tyr-7-amido-4-methylcourmarin
PAGE	:	Polyacrylamide gel electrophoresis
PCD	:	Programmed cell death
PI	:	Propidium iodide
PVDF	:	Polyvinylidene fluoride
ROS	:	Reactive oxygen species
SbV	:	Pentavalent antimonials
SDS	:	Sodium dodecyl sulfate
SSC	:	Side scatter
t-Bid	:	Truncated-BH3 interacting-domain
TNP-470	:	5-methoxy-4-(2-methyl-3-(3-methyl-2-butenyl)oxiranyl)-1-oxaspiro(2,5)oct-6-yl(chloroacetyl) carbamate
VL	:	Visceral leishmaniasis
V_{max}	:	Maximum velocity
WHO	:	World health organization
Z-DEVD-fmk	:	Benzoylcarbonyl-aspartyl-glutamyl-valyl-aspartyl-fluoromethyl ketone
$ZnCl_2$	:	Zinc chloride
Z-VAD-fmk	:	Benzyloxycarbonylvalyl-alanyl-aspartyl fluoromethyl ketone

TH-1832_126106036

CONTENTS

TH-1832_126106036

TH-1832_126106036

TH-1832_126106036

TH-1832_126106036

भारतीय प्रौद्योगिकी संस्थान गुवाहाटी • Indian Institute of Technology Guwahati •

TH-1832_126106036

LIST OF FIGURES

TH-1832_126106036

TH-1832_126106036

TH-1832_126106036

TH-1832_126106036

TH-1832_126106036

TH-1832_126106036

TH-1832_126106036

LIST OF TABLES

TH-1832_126106036

Chapter I

Review of literature on *Leishmani*a apoptosis, current perspectives and future scope*

1.1 Abstract

Visceral Leishmaniasis (referred to as Kala-azar) is caused by *Leishmania donovani* which is a dimorphic protozoan parasite. The disease claims numerous lives worldwide annually. All the efforts directed to ameliorate the progression of this fatal disease have gone in vain over the years owing to drug resistance and toxicity related issues. Worldwide concerns have spurred a series of investigations by the scientific community to explore novel drug targets and to investigate the vital pathways in the parasite. Apoptotic or programmed cell death pathway of the *L. donovani* has largely remained unexplored and it promises to bring out novel insights in the drug discovery process for Leishmaniasis. The review brings together available literature about *Leishmania,* Leishmaniasis, available drugs and programmed cell death in the parasite. Methionine aminopeptidase 2 (MAP2) has emerged to be a key player in the apoptotic pathway of *L. donovani*. Key molecular underpinnings have been uncovered in the current work which holds significance in therapeutic interventions. Glimpses of a plethora of caspase and non caspase proteases in the programmed cell death of the parasite have been presented in the current work.

*** Part of the review submitted for publication**

TH-1832_126106036

1.2 Introduction

1.2.1 History of leishmaniasis: Leishmaniasis is a vector borne disease caused by more than 20 species of protozoan parasite of genus *Leishmania (Croan et al., 1997)*. The parasite *Leishmania* was first described by Alexander Russell in 1756 *(Hide et al., 2007)* and termed this disease "Aleppo boil". In year 1898, Peter Borovsky has presented the first explanation of interaction of parasite to host tissue and referred this parasite to protozoa (*Hoare, 1938*). In Indian subcontinent the disease is known as Kala-azar (kala meaning black and azar meaning fever). Later in the year 1901, William Boog Leishman discovered ovoid bodies in the spleen of the patient having fever, anemia and splenomegaly while working in Dum Dum, a place in Kolkata and termed this disease as dum-dum fever. This finding has been published in year 1903 (*Leishman, 1903*). In same year, Charles Donovan also demonstrated the similar ovoid bodies in the splenic tissue of kala-azar patients and independently published his findings (*Donovan, 1903*). Later, Ronald Ross named these ovoid bodies as Leishman-donovan bodies and the species responsible for the disease became known as *Leishmania donovani* (*Ross, 1903*).

1.2.2 Classification of Leishmania: *Leishmania* parasite has been classified into kingdom protista, sub kingdom protozoa, phylum sarcomastigophora, subphylum mastigophora, class zoomastigophora, order kinetoplastida, family trypanosomatidae and genus *Leishmania.* The genus *Leishmania* uses flagella for their locomotion and contains kinetoplast which is unique form of DNA present in mitochondria. It takes up food through pinocytosis as well as phagocytosis processes. Based on the site of location in sand fly vectors, genus *Leishmania* is further sub divided into sub genus *Leishmania* (hindgut and foregut of the sand fly) and sub genus *Viannia* (limited to midgut of sand fly). Parasite of subgenus *Leishmania* mainly consists of *L. donovani complex, L. tropica complex* and *L. mexicana complex*, whereas subgenus *Viannia* consists of *L. braziliensis complex.*

1.2.3 Vectors of Leishmania: The disease leishmaniasis is mainly transmitted by bite of female sand flies. More than 700 species of sand flies are reported till date, but only 30 species of sand flies belonging to genus *Phlebotomus* and *Lutzomyia* have been reported for transmitting the parasite into mammalian host. Sand flies of genus *Phlebotomus* are reported

TH-1832_126106036

to transmit the disease in old world countries mainly Asia, Africa and Europe whereas *Lutzomyia* are reported to transmit in new world countries (South America and Central America). *Phlebotomus* species are mainly present in desert or semi arid region whereas *Lutzomyia* species found in forest area (*Sharma and Singh, 2008; Claborn, 2010*). The systematic positions of the sand flies are: Phylum Arthropoda, Family Psychodidae, Class Insecta, Order Diptera, Family Psychodidae, Subfamily Phlebotominae, Genus *Phlebotomus* and *Lutzomyia*. The morphology of *Phlebotomus* and *Lutzomyia* are shown in Figure 1.1.

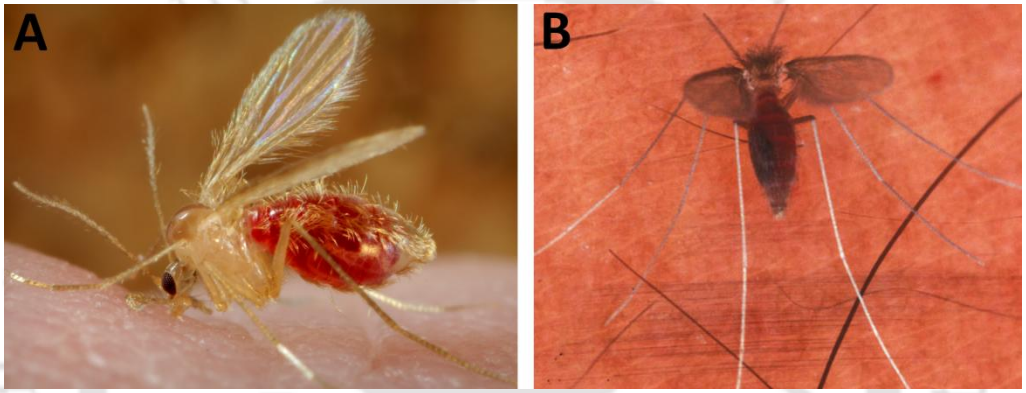

Figure 1.1: Vectors of leishmaniasis. (A) *Phlebotomus papatasi* and (B) *Lutzomyia shannoni*. Both sand flies are similar in their morphology, 2-3 mm in length. The parasite *Leishmania* is transmitted via bite of female sand fly to mammalian host. *Phlebotomus* species are mainly present in desert or semi arid region whereas *Lutzomyia* species found in forest area. (Figure A is adopted from Centre for disease control and prevention CDC,https://phil.cdc.gov/phil/details.asp?pid=10275%20 whereas Figure B is taken from http://entomology.ifas.ufl.edu/creatures/misc/flies/Lutzomyia_shannoni.htm).

1.2.4 Life cycle of Leishmania parasite: *Leishmania* has digenetic life cycle which completes its life in between mammalian hosts and sand flies. During its life cycle stage, parasites undergo morphological changes which include promastigotes stage and amastigotes stage. Promastigote is extracellular form, having flagella at its anterior end and motile in nature, present in sand fly whereas amastigote (2-4 µm in diameter) is intracellular form, reside inside the mammalian host (macrophages) and devoid of flagella as shown in Figure 1.2 *(Bogitsh et al., 1999; HerwaLdt, 1999).* Sand fly transfers the metacyclic promastigotes into mammalian host during its blood meal phase. Inside the mammalian host, these metacyclic promastigotes are recognized by macrophages and dendritic cells and transformed

TH-1832_126106036

into intracellular amastigote form inside the macrophages. Amastigotes divide inside the macrophages by binary fission; cell bursts and further infects other macrophages *(Dostalova and Volf, 2012).* When sand fly bites the infected mammalian host, it ingests infected macrophages containing amastigotes. These amastigotes are taken up to midgut of sand fly vector where it transforms into motile, flagellated and elongated forms called promastigotes. Promastigotes undergo metacyclogenesis to convert into infective metacyclic promastigotes within seven days, and accumulate into the proboscis of sand fly along with promastigote secretory gel. When sand fly bites the mammalian host, it regurgitates the metacyclic promastigotes along with promastigote secretory gel into the blood (*Kamhawi, 2006, Hide et al., 2007*). The life cycle of *Leishmania* parasite in mammalian host and sand fly is shown in Figure 1.3.

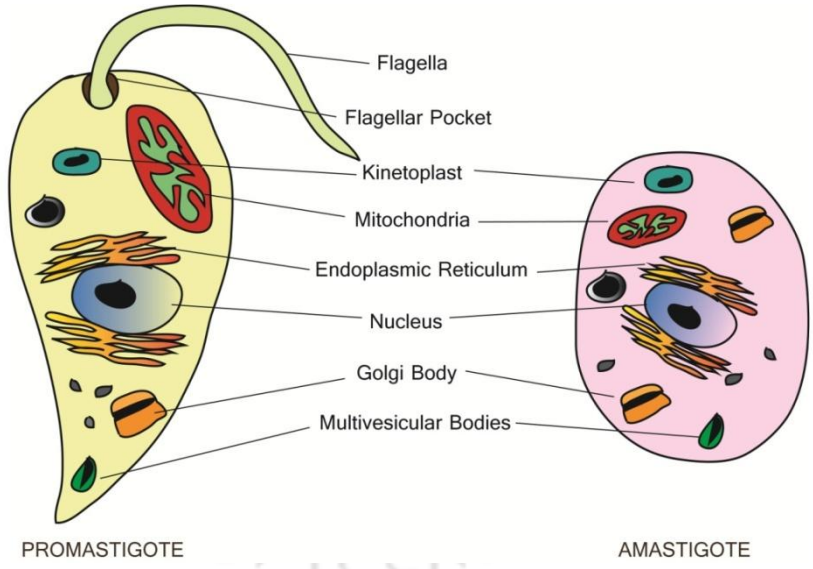

Figure 1.2: Cartoon image showing morphology of two different stages of *Leishmania* parasite. Promastigote is the sand fly stage of parasite which is motile in structure because of flagella present at its anterior end. It is long and slandered shape in shape. Amastigote form is mammalian stage of parasite, nonmotile in structure. It is ovoid in shape, smaller than promastigotes and devoid of flagella.

TH-1832_126106036

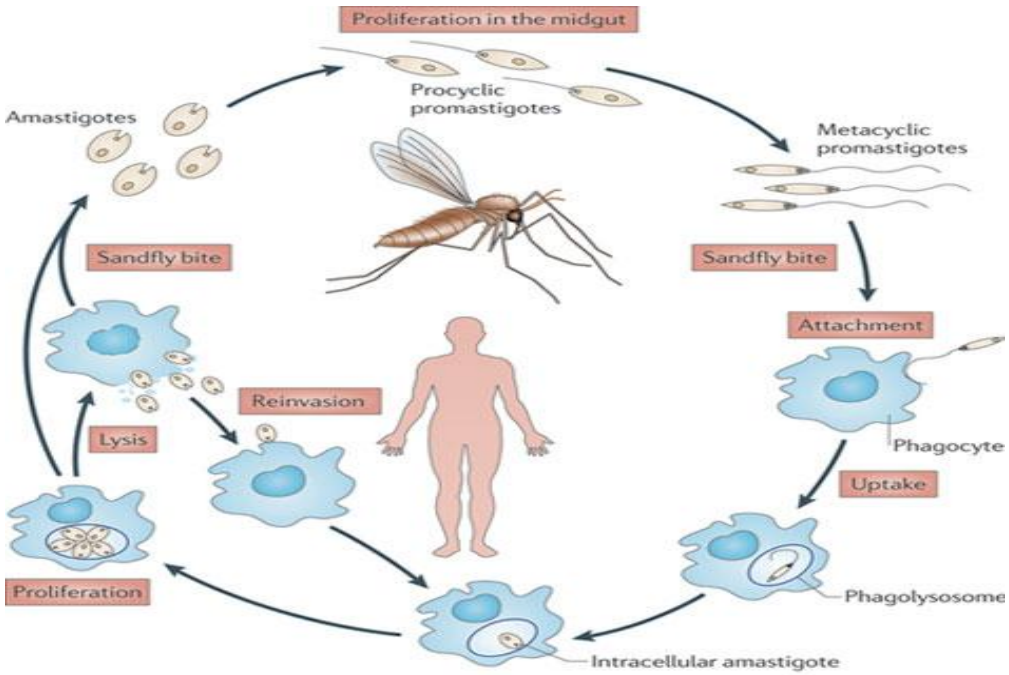

Figure 1.3: Life cycle of *Leishmania* parasite in sand fly and mammalian host. When sand fly takes the blood meal, it transfers the promastigotes inside the host which are taken up by macrophages. Inside the macrophages, the promastigotes convert into amastigote stage and undergoes cell division, cell bursts; infects the surrounding macrophages and infection progresses. During blood meal phase, sand fly ingests the infected macrophages containing amastigotes. Amastigotes transform into metacyclic promastigotes inside the gut of sand fly and it completes the life cycle of parasite (Adapted with permission from *Nature Reviews Microbiology* **9**, 604-615).

1.2.5 Leishmaniasis: Leishmaniasis is one of the most neglected tropical diseases caused by protozoan parasite of genus *Leishmania* which belongs to order kinetoplastida and family trypanosomatidae. The disease is caused by more than 20 species of protozoan parasite of genus *Leishmania (Croan et al., 1997). Leishmania* is an obligate intracellular parasite which is transmitted by bite of female sand fly, *Phlebotomus argentipes* and *Lutzomyia longipalpis*. According to the tropism of the disease, leishmaniasis is mainly classified into three different clinical forms: cutaneous leishmaniasis, muco-cutaneous leishmaniasis and visceral leishmaniasis. Different clinical manifestations of the disease are shown in Figure 1.4.

Cutaneous leishmaniasis (CL) is the most common form of the disease which mainly affects the exposed body parts. It is characterized by mainly ulcerative skin lesions at the site of infection which are self healing in nature whereas some requires treatment to heal

TH-1832_126106036

completely *(Hide et al., 2007).* However, the residual scars associated with skin lesions are associated with social stigma in several societies (CDC). It is mainly caused by *L. braziliansis, L. amazonensis, L. Mexicana* etc in new world countries and by *L. tropica, L. major etc* in old world countries *(Bañuls et al, 2007; MacMorris-Adix, 2008).*

Muco-cutaneous leishmaniasis (MCL) is the most severe form of cutaneous leishmaniasis which mainly affects the mucous membrane of the mouth, nose and throats etc. *(Sangueza et al., 1993; James et al., 2006).* It is mainly characterized by formations of lesions on the mucous membrane and if untreated, causes serious disFigureuration and deformities. It is mainly caused by *L. panamensis, L. guyanensis, L. braziliansis* etc. *(Hide et al, 2007; MacMorris-Adix, 2008).*

Visceral leishmaniasis is the most severe form of the disease which mainly affects the internal organs of body and characterized by hepatomegaly, splenomegaly, anemia, weight loss and fever *(MacMorris-Adix, 2008; Stockdale and Newton, 2013)*. The mortality rate by visceral leishmaniasis is as high as approximately 80 % of untreated cases are fatal *(Jha et al., 2005).* It is also known as kala-azar because of blackening of the skin associated with this disease. Nowadays the chances of co-infection of visceral leishmaniasis in HIV patients are very high. Because of compromised immunity in HIV patients, the chances of treatment are very less and eventually the mortality rate is high in co-infected patients *(Lachaud et al., 2009)*. Its etiological agents mainly include *L. donovani, L. infantum* etc (CDC).

Figure 1.4: Three different types of leishmaniasis. (A) the most common form is cutaneous leishmaniasis (B) less common form is muco-cutaneous leishmaniasis and (C) most prevalent form in India is visceral leishmaniasis. Cutaneous leishmaniasis is the most commonly found form of diseases whereas muco-cutaneous leishmaniasis is the advanced form of cutaneous leishmaniasis. Visceral leishmaniasis is the most prevalent form of the disease in India. All representative images are taken from WHO.

TH-1832_126106036

1.2.6 Epidemiology of leishmaniasis: Leishmaniasis is prevalent in 88 countries with reportedly 1.3 million new cases and causing death of approximately 20,000 to 40,000 people worldwide every year *(Alvar et al., 2012).* It is widely spread throughout the globe, ranging from tropical regions of Asia, America to temperate zones of Asia, Southern Europe and South America, as shown in Figure 1.5 *(Dawit et al., 2013).* According to world health organization (WHO) data, around 12 million people are infected with leishmaniasis and approximately 350 million people are at risk of the infection (WHO). Out of that, 90 % cases are reported from eleven countries namely India, Bangladesh, Nepal, Afghanistan, Iran, Saudi Arabia, Brazil, Sudan, Bolivia and Peru *(Hide et al., 2007).* Cutaneous Leishmaniasis is found in approximately 70 countries of the world and majorly in countries like Afghanistan, Pakistan, Peru, Algeria, Brazil, Syria and Saudi Arabia *(Reithinger et al., 2007).* Muco-cutaneous leishmaniasis is mainly prevalent in Bolivia, Brazil and Peru (*Hide et al., 2007)* whereas visceral leishmaniasis is mostly prevalent in India, Sudan, Nepal, Brazil and Bangladesh (*Murray et al., 2005).* According to National Vector Borne Disease Control Programme (NVBDCP Annual report 2014-15), Government of India; kala-azar is reported to be endemic in 54 districts in 4 states whereas in Bihar, it is endemic in 33 districts. Nowadays the global concerns associated with leishmaniasis are the chances of getting infected in immune-compromised patients such as HIV. The co-infection in such patients with *Leishmania* parasite further complicates the treatment procedure, as both infections further destroy the immunity (WHO 2007). According to WHO report, around 70% of adult visceral leishmaniasis cases in southern Europe are co-infected with HIV *(Desjeux et al., 2003).* The details of HIV co-infection along with leishmaniasis are shown in Figure 1.6.

1.2.7 Available arsenal of drugs for the treatment of leishmaniasis: Due to unavailability of potential vaccines for the prevention of leishmaniasis, the current treatment is mainly relying on chemotherapeutics. The available drugs for the treatment of leishmaniasis are mainly pentavalent antimonials, amphotericin B, pentamidine sulfate and miltefosine. These available drugs are known to have severe toxicity, high cost and the mode of administration is through intramuscular or intravenous injection *(Croft and Coombs, 2003; Croft et al., 2006).* In addition, the emerging resistance in *Leishmania* parasite against the available drugs is a major concern.

TH-1832_126106036

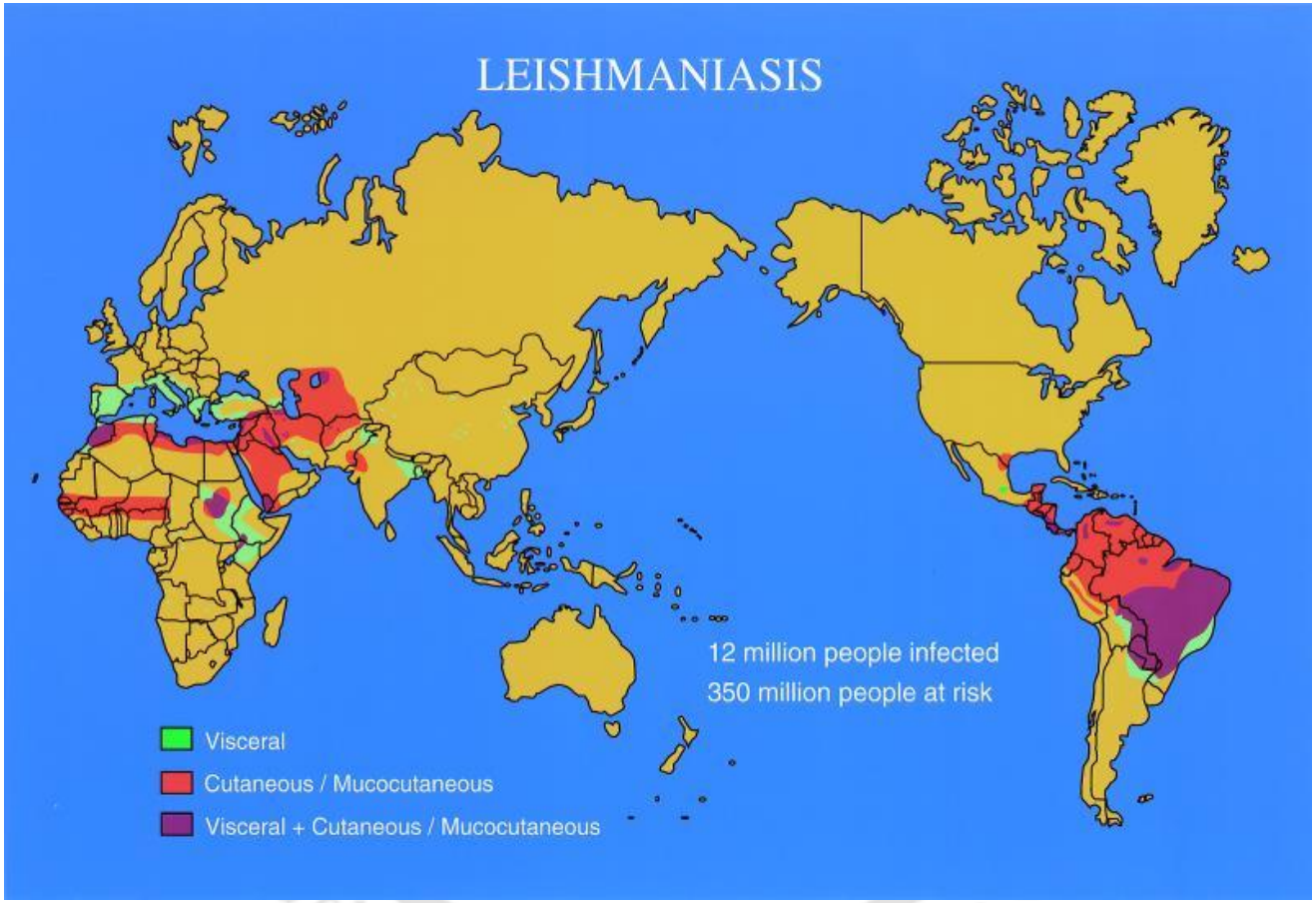

Figure 1.5: Epidemiology of visceral, cutaneous and muco-cutaneous leishmaniasis. Leishmaniasis is endemic in many countries and widely spread throughout the globe, ranging from tropical regions of Asia, America to temperate zones of Asia, Southern Europe and South America. Approximately 12 million people are affected across the globe with leishmaniasis whereas 350 million people are at risk of this disease. In India, visceral leishmaniasis is the most prevalent form of disease. (Adapted with permission from *Clin Microbiol Rev*. 2001;14:229-43)

TH-1832_126106036

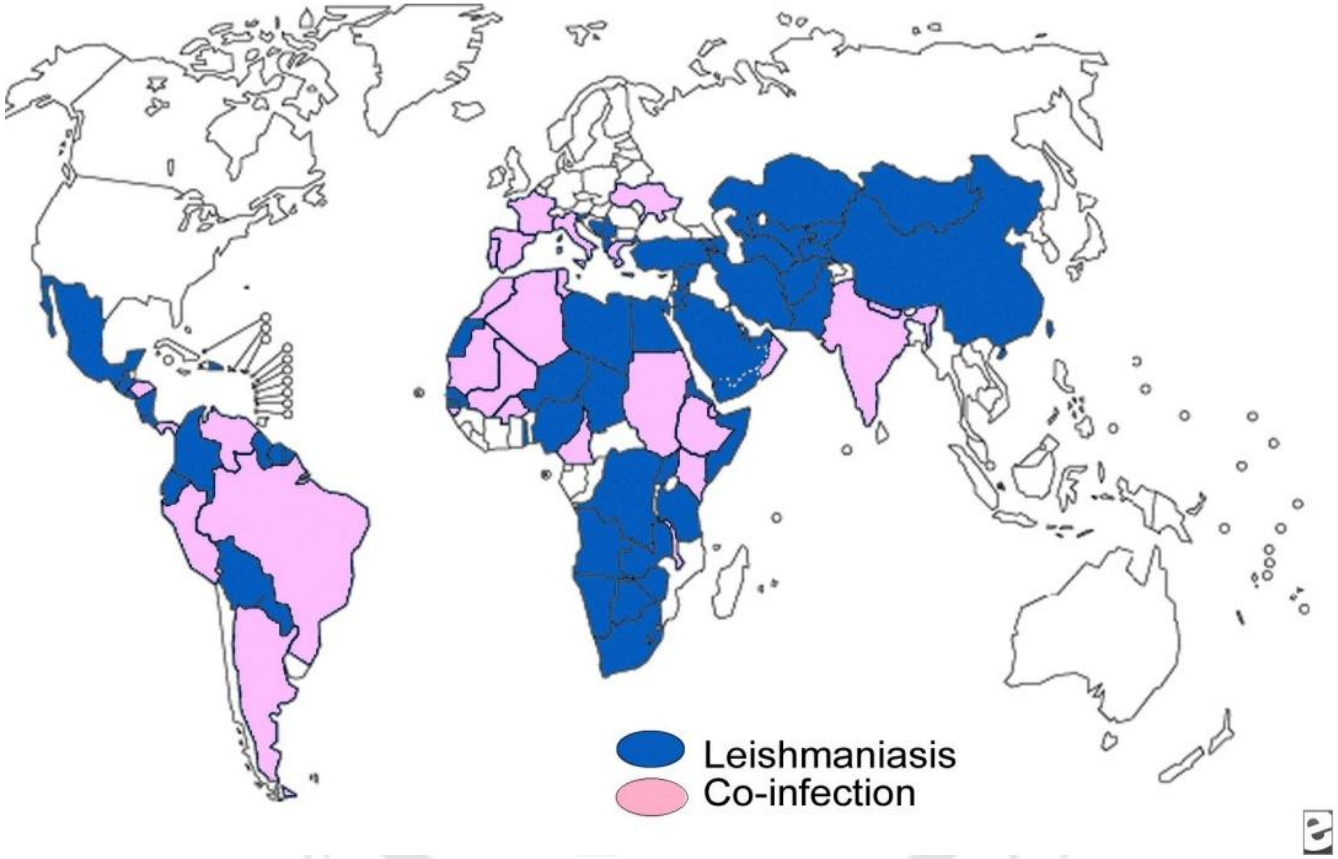

Figure 1.6: Geographical distribution of leishmaniasis co-infection. The blue color on map shows infection with leishmaniasis whereas pink color shows co-infection with HIV/AIDS. The cases of co-infection of leishmaniasis with HIV/AIDS are reported from 35 countries across the globe. Around 70% of adult visceral leishmaniasis cases in southern Europe are co-infected with HIV. (Adapted with permission from *Ann Trop Med Parasitol.* 2003; 97:1:3-15)

TH-1832_126106036

Miltefosine is the only available oral drug with limited toxicity but it also has certain limitations for the treatment of pregnant women due to teratogenic in nature *(Sundar et al., 2007).* The primary choice of drug for the treatment of cutaneous and visceral leishmaniasis is pentavalent antimonials in Indian subcontinent *(Croft et al., 2006).* The very first antimonials discovered were Sodium stibogluconate (pentostam) in the year 1945 *(Goodwin, 1995).* Because of increase in antimony resistance especially in North Bihar, the uses of pentavalent antimonials are stopped in these areas *(Sunder, 2001; Sunder et al., 2001).* Antimonials are still the primary drug of choice in areas where drug resistance has not emerged. The pentavalent antimonials (SbV) converted into SbIII by action of reductase enzyme which is the active form of drug *(Ephros et al., 1999).* The loss of reductase activity in parasite leads to drug resistance against the SbV compounds. The possible reason of acquired resistance against the SbV compounds is the widespread availability of this drug in North Bihar and nearby areas *(Maltezou, 2010).*

The areas where antimony resistance is emerged, Amphotericin B (AmB) and its liposomal formulations have been used as a second line of drug for the treatment of leishmaniasis *(Bern et al., 2006).* AmB is a macrolide polyene antifungal compound, initially used for the treatment of systemic fungal infections. The drug AmB is obtained from *Streptomyces nodsus* and has affinity towards ergosterol *(Caffrey et al., 2001).* Ergosterol is a major component of cell membrane of fungus as well as *Leishmania*. Binding of AmB to ergosterol, resulting in loss of membrane integrity and ultimately cell death of parasite *(McCall et al., 2015).* The toxicity of AmB is masked by using different formulations as liposomal AmB (Ambisome), AmB colloidal dispersion (Amphocil) and AmB lipid complex (Abelcit) *(Hamill et al., 2013).* The cost of these formulations is very high and as the sufferer of this disease is from very poor background, they cannot afford expensive drugs. In addition to high efficacy, AmB formulations are associated with high toxicity as it nephrotoxic in nature and emerging drug resistance *(Fanos et al., 2000; Sabra and Branch, 1990).* The drug resistance against AmB is associated with lack of ergosterol on cell membrane of resistant *Leishmania* strain. Moreover, AmB resistance *Leishmania* shows decrease in the uptake and rapid efflux of AmB *(Mbongo et al., 1998; Purkait et al., 2012).*

Miltefosine is the only available oral drug which is a hexadecylphosphocholine, initially developed for the treatment of cancer *(Croft et al., 1987; Croft and Coombs, 2003).*

TH-1832_126106036

Miltefosine is highly effective drug for the treatment of visceral leishmaniasis in endemic regions but also has certain limitations. The half life of miltefosine is approximately 150 hours and teratogenic in nature so cannot be given to pregnant ladies *(Maltezou. 2010).* Due to longer half life and low rate of clearance, the chances of getting acquired resistance in *Leishmania* parasites against miltefosine are relatively higher. The combination of Miltefosine and AmB are also used for the treatment of leishmaniasis but due to high toxicity associated with the combinatorial therapy leads to serious concern of their uses. Miltefosine are reported to inhibit the cell proliferation by changing the membrane sterol and phospholipids composition *(Urbina, 1997).* The emerging resistance in parasite against miltefosine is reported to have low expression of *Leishmania donovani* miltefosine transporter (*Ld*MT) and protein *Ld*Ros3 *(Dorlo et al., 2012). Ld*MT and *Ld*Ros3 proteins facilitate the uptake of miltefosine in the parasite. Low expression of both proteins leads to poor uptake of miltefosine and hence no effect against the drug. The available reports also signify that the miltefosine causes the cell death of parasite via apoptotic mediated pathways *(Verma and Dey. 2004; Paris et al., 2004; Verma et al., 2007; Marinho et al., 2011)*. The chemical structure of sodium stibogluconate, amphotericin B and miltefosine is shown in Figure 1.7.

1.3 Cell death processes of parasite

Apoptosis or programmed cell death (PCD) is characterized by DNA degradation, chromatin condensation, exposure of phosphatidyl serine on cell surface, change in mitochondrial transmembrane potential, cell shrinkage and release of cytochrome c from mitochondria *(Jiménez et al., 2010).* In mammals, apoptosis plays a crucial role in various physiological processes; to control the number of cells, remove the unwanted or damaged cells and in immune system functions. Caspases have been shown a central role for PCD in higher eukaryotic organisms, but till now no caspase gene have been recognized in plants, yeast and protozoan. However, several reports suggesting that caspase like activity also appear in many metazoan parasites including trypanosome species, *Leishmania donovani* (*Saudagar et al., 2013; Saudagar and Dubey, 2014*), plasmodium (*Ch'ng et al., 2010*), *Entamoeba histolytica* (*Villalba et al., 2007*), *Toxoplasma gonodii* (*Peng et al., 2003*), *Trichomonas vaginalis* (*Chose et al., 2002*) and *Giardia* species (*Ghosh et al., 2009*). In

TH-1832_126106036

Trypanosoma and *Leishmania* species, features suggesting apoptosis have been reported in response to various kinds of stimulus such as antiparasitic drug such as miltefosine (*Paris et al., 2004*), treatment with H_2O_2 (*Das et al., 2001*), reactive oxygen species, heat and stress (*Gannavaram and Debrabant, 2012*). There are several biochemical evidences of PCD in trypanosomatids reported in the literature. Some of the biochemical evidences of PCD in trypanosomatids are listed as follow:

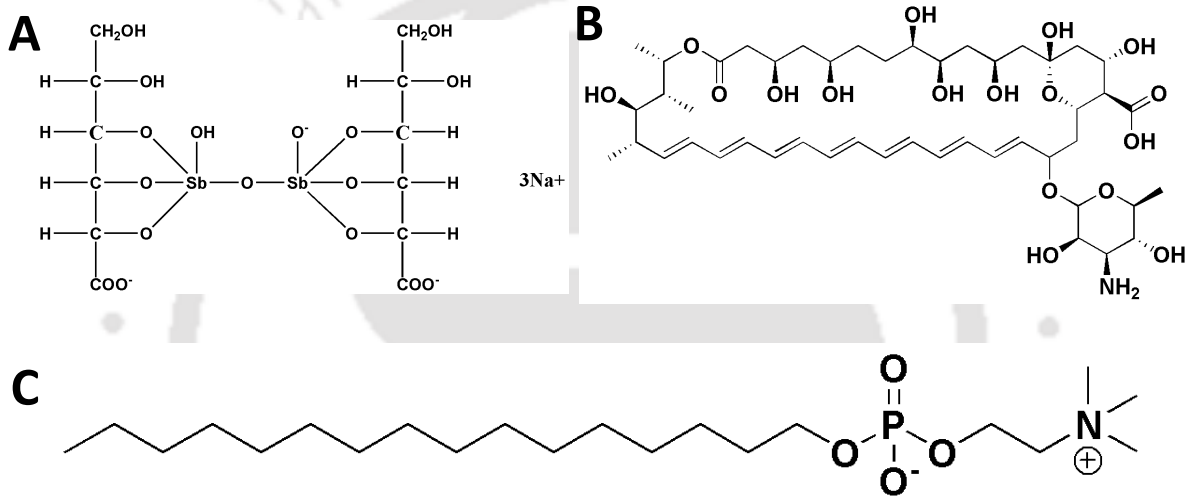

Figure 1.7: Current available drugs which are used for the treatment of different forms of leishmaniasis. (A) Sodium stibogluconate (pentostam), first line of drug against leishmaniasis. In North Bihar, leishmaniasis patients are unresponsive against antimonials. (B) Amphotericin B, second line of drug which is used for the cure of unresponsive leishmaniasis against antimonials. (C) Miltefosine, only available oral drug and contains hexadecylphosphocholine moiety. These available drugs are known to have high toxicity, high cost and emerging drug resistance in *Leishmania* parasite. The structures are redrawn by ChemDraw Ultra software.

1.3.1 Exposure of Phosphatidyl serine on cell surface: Phosphatidyl serine is present in the inner leaflet of plasma membrane in normal cells. In case of apoptotic cells, asymmetry of plasma membrane is lost and as a result there is exposure of phosphatidyl serine on outer membrane and can be detected by labeling with Annexin-V conjugated with FITC. It has high binding affinity with phosphatidyl serine as well as anionic phospholipids. Along with propidium iodide (PI), Annexin-V FITC can distinguish between apoptotic cells, necrotic cells and normal cells. Apoptotic cells are characterized by Annexin-V positive, PI negative;

TH-1832_126106036

necrotic cells are Annexin-V negative and PI positive; and normal cells are Annexin-V negative as well as PI negative *(Martin et al., 1995).* Several studies have shown that exposure of Phosphatidyl serine on cell surface in response of miltefosine, heat, ROS and stress in case of *Leishmania* promastigotes *(Jiménez et al., 2010).*

1.3.2 Change in morphology of cell: Life cycle of *Leishmania* parasites has been well characterized. It goes through a series of distinct morphological changes to complete its life cycle in mammalian hosts and sand fly vectors. Changes in cell volume with intact plasma membrane have been described in metazoan programmed cell death and considered as a hall mark of apoptotic processes whereas, in necrotic death loss of cell volume is normally a result of non-intact plasma membrane *(Galluzzi et al., 2012).* Some of the groups have reported the morphological changes during programmed cell death of *Leishmania* parasite but are not well characterized.

1.3.3 Oligonucleosomal DNA fragmentation: In *Leishmania,* no caspase gene have been identified till now, so it is highly unlikely to have caspase dependent DNases in their genome whereas, apoptosis inducing factor and endonuclease G are involved in case of mammalian apoptosis. Endonuclease G is mitochondrial protein and involved in DNA fragmentation of apoptotic cells. Similar to higher eukaryotic organisms, it is localized in the mitochondria of trypanosomes and released from mitochondria when apoptotic signal is generated from dying cells. Interestingly, genes encoding endonuclease G have been recognized in the genome database of *Leishmania major* (LmjF10.0610) and *Trypanosoma brucei* (Tb927.8.4040, Tb927.8.4090). It has also been reported that H_2O_2 and reactive oxygen species triggers release of endonuclease G from mitochondria as a result there is fragmentation of DNA suggesting role of endonuclease G in *Leishmania* programmed cell death (*Li et al., 2001; BoseDasgupta et al., 2008*).

1.3.4 Mitochondrial alterations and release of Cytochrome C: Release of cytochrome c from mitochondria is one of the characteristic features of apoptosis in higher eukaryotic organisms, which binds to adaptor protein, apoptotic protease activating factor (Apaf-1) form apoptosome complex and activates caspase-9 (*Hüttemann et al. 2011*). Mitochondrial

TH-1832_126106036

alterations include change in transmembrane potential, disruption of electron transport chain which subsequently disrupts oxidative phosphorylation and ATP production which can be measured fluorometrically by using various commercial kits *(Green et al., 1998).* However, very few studies have reported decreased level of ATP as an apoptotic marker; therefore this should be considered with caution. In addition, change in mitochondrial transmembrane potential also triggers intrinsic programmed cell death pathway resulting in release of cytochrome c from mitochondria. In several species of trypanosomatids, release of cytochrome c from the mitochondria to the cytosol has been reported in response to various apoptotic stimuli such as treatment with miltefosine, novobiocin and withaferin A. Similarly, release of cytochrome c was also observed when the proapoptotic mammalian Bax protein was exogenously expressed in *Trypanosoma brucei (Esseiva et al., 2004).*

1.3.5 Increase in the total cytosolic pool of calcium ions: Change in $\Delta\Psi m$ in apoptotic like cell death of parasite results in release of cytochrome C from the mitochondria into the cytosol. Cyt. c binds to inositol triphosphate (IP_3R) receptor present on endoplasmic reticulumn (ER). Binding of IP3R further enhance the release of calcium ions form ER and cause a global increase in cytoplasmic calcium concentration inside the parasite. Increased calcium ions inside the cytosol acts on mitochondria and increases the permeability and further release of Cyt.c. Cyt.c along with other factors forms apoptosome in which caspase-3 is activated and cell death occurs via apoptosis. The increase in cytosolic calcium concentration in miltefosine treated *Leishmania* undergoing apoptotic cell death *was* reported by several groups *(Kulkarni et al., 2009; Dolai et al., 2011).*

.

TH-1832_126106036

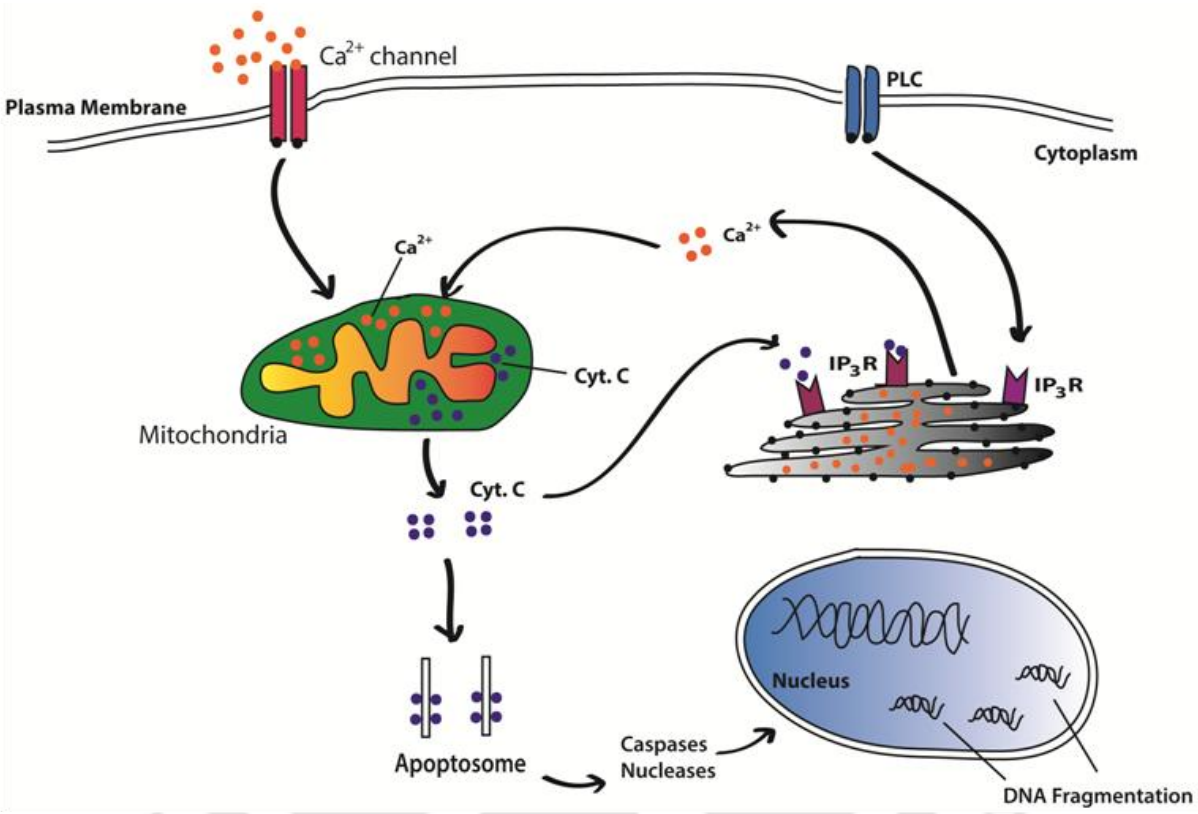

Figure 1.8. The schematic image of increase in the cytosolic pool of calcium ions during apoptosis. During cellular insult, calcium channel opens up and Ca^{2+} enters inside the cell through calcium pores or phospholipase C (PLC) mediated signaling pathway. Ca^{2+} bind to IP_3R receptor present on endoplasmic reticulum to further release of Ca^{2+} into the cytosol causes global rise of calcium concentration. The increase in the cytosolic calcium triggers the release of Cytochrome c from mitochondria which activates caspases and nucleases via apoptosome formation. Caspases and nucleases cleave cellular proteins and nuclear lamins leading to apoptosis cell death. (Reproduced with permission from *Nat Cell Biol.* 2003; 5:1041-3)

TH-1832_126106036

1.3.6 Caspase 3/7 protease like activity: Caspases are the most important regulators of the apoptotic processes in higher eukaryotic organisms but is absent in genome of *Leishmania*. In protozoan parasites, no caspase gene is identified till now. However, several groups have reported the extensive evidence of caspase like activities associated with programmed cell death in trypanosomatids. These groups have reported the activation of proteases in cell lysates of *Leishmania* undergoing programmed cell death which are able to degrade the classical caspase substrates. These reports usually analyzed the cleavage of flurogenic tagged DEVD which is the classical substrate of caspase-3 by flurometric analysis. Several groups have incubated the cell lysates with inhibitors of caspase-3 (Z-DEVD-fmk) and reported the decreased fluorescence signal showing as a strong evidence of caspase-3 like activity in *Leishmania* parasites *(Saudagar et al., 2013; Saudagar and Dubey, 2014).*

1.4 Role of Caspases in programmed cell death

Role of proteases in cell death processes via apoptosis is determined by biochemical and genetic analysis. The first report on the role of intracellular proteases in apoptotic cell death is established in *C. elegans* as genetic analysis showed that the product of gene responsible for cell death have significant homology to human interleukin -1β converting enzyme (ICE) *(Cerretti et al., 1992; Yuan et al., 1993).* Further studies on mammalian proteases leads to identification of 13 proteases similar to ICE and termed as caspases *(Alnemri et al., 1996).* Total 13 caspases are reported till date and named as caspase-1 to caspase-13 with varying functions as mentioned in Table 1. Caspases are cysteine proteases which cleave after aspartic acid residues in a peptide chain. They all are synthesized as inactive proenzymes and convert into its active form in case of apoptotic stimuli. Caspases contains three domains; a large subunit of 20 kDa, small subunit of 10 kDa and an amino terminal domain. According to available crystal structure, two heterodimers of caspases associate to form tetramer having two catalytically active site which functions independently (*Walker et al., 1994; Wilson et al., 1994; Rotonda et al., 1996*). After activation and proteolytic processing of inactive caspases, both large subunits associate with small subunits and form substrate binding sites for the catalysis. Mainly initiator and executioner caspases are involved in the apoptotic processes. Initiator caspases are caspase-8 or -9 where as executioner caspases are caspase -3 or -7 *(Almeri, 1996; Thornberry, 1998).* In case of

TH-1832_126106036

apoptotic stimuli, inactive initiator caspases undergo proteolytic processing to become active which in turn cleave and activate executioner caspases *(Thornberry, 1998)*. Downstream activation of executioner caspases leads to cascade of caspase activation which ultimately cleaves cellular proteins and series of molecular and biochemical effects leading to cell death. There are two different pathways are reported; Extrinsic pathway and Intrinsic pathway, also known as mitochondrial pathway. Extrinsic pathway acts through binding of death ligands to Fas death receptors which in turn recruits Fas activated death domain (FADD), procaspase-8 and form death induced signaling complex (DISC). Inside the complex procaspase-8 get cleaved and form active caspase-8. In intrinsic pathway, various cellular stresses generate the apoptotic stimuli inside the cell which cleaves the proapoptotic proteins into apoptotic. Apoptotic proteins act on mitochondria to increase the mitochondrial outer membrane permeabilization (MOMP) and further release cyt.c along with other proteins. Cyt. c binds to Apaf-1 and upon binding it recruits procaspase-9; form apoptosome complex and cleaves procaspase-9 into active caspase-9. Both caspase-8 and caspase-9 converge to activate executioner caspases (caspase-3 and caspase-7). Activated caspase-3 cleaves cytosolic proteins, nuclear lamins etc leading to cell death. The mechanistic pathway of caspase dependent cell death is mentioned in Figure 1.9. These events of cell death mainly include exposure of phosphatidyl serine on plasma membrane, membrane blebbing, cell shrinkage, chromatin condensation, oligonucleosomal DNA fragmentation and formation of apoptotic bodies as membrane enclosed vesicles *(Raff, 1992).* Apoptotic bodies are engulfed by phagocytic cells and prevent the release of intracellular contents to further inhibit the complications of inflammation and immunological response.

1.5 Role of noncaspase proteases in programmed cell death

As caspases are important to execute the cell death processes, several other proteases are also reported to have role in programmed cell death. These proteases are mainly cathepsins *(Guicciardi et al., 2000),* calpains *(Wang, 2000),* metacaspases *(Madeo et al., 2002),* Granzymes *(Froelich et al., 2004),* proteasomes *(Orlowski et al., 1999)* and certain metalloproteases *(Levkau et al., 2002)*. Several reports suggest that the expression level of noncaspase proteases is increased after apoptotic stimuli *(Guenette et al., 1990)*. Moreover, inhibition of noncaspase proteases by specific inhibitors delay the apoptotic processes *(Schotte et al., 1999)*

TH-1832_126106036

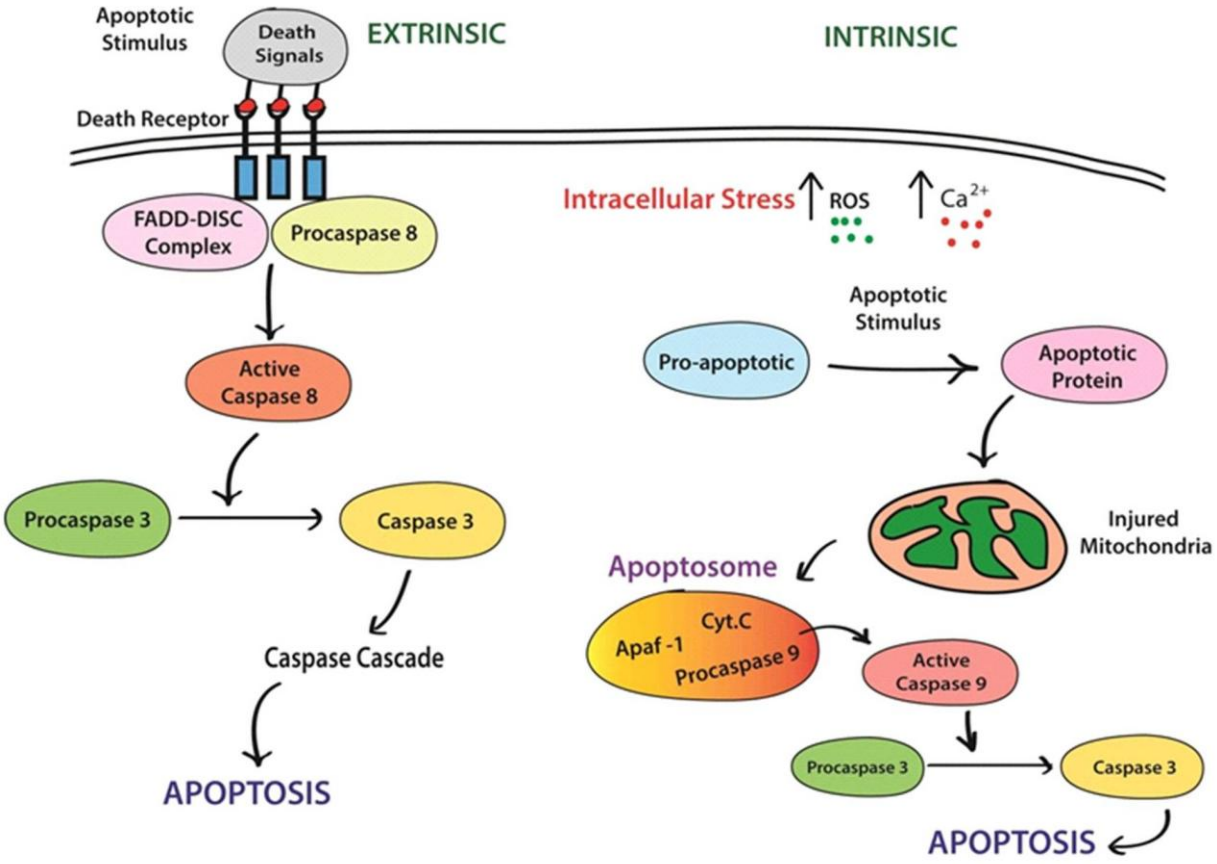

Figure 1.9: Two major pathways in mammalian apoptosis. Extrinsic pathway is triggered by death signals when bind to Fas-death receptors present on plasma membrane. Upon binding, it recruits Fas activated death domain (FADD) and procaspase-8 to form Death initiation signaling complex (DISC). This assembly cleaves the procaspase-8 into active caspase-8 which in turn activates caspase-3.
Intrinsic pathway, also known as mitochondrial pathway activates in response to cellular stress, DNA damage, and increased ROS etc. The apoptotic stimuli convert proapoptotic protein into apoptotic which acts on mitochondria and releases Cyt c. It binds with Apoptotic protease activating factor-1 (Apaf-1) along with procaspase-9 to form apoptosome and activates caspase-9. Activated caspase-9 cleaves procaspase-3 into caspase-3 which leads to cascade of reactions and causes cell death via apoptosis (Reproduced with permission from *Cell.* 1998; 94:695-8).

TH-1832_126106036

Table 1: Functional role of identified mammalian caspases

Type of caspases	Functional role
Capase-1	Inflammation
Capase-2	May be Initiator or Effector
Capase-3	Effector
Capase-4	No known role in apoptosis
Capase-5	No known role in apoptosis
Capase-6	Effector
Capase-7	Effector
Capase-8	Initiator
Capase-9	Initiator
Capase-10	May be Initiator
Capase-11 (Murine homologs)	Inflammation
Capase-12 (Murine homologs)	No known role in apoptosis
Capase-13	No known role in apoptosis

1.5.1 Role of metacaspases in apoptosis: Apoptotic like cell death processes in *Leishmania* parasite are reported with increased caspase3/7 protease like activity after chemotherapy or radiations. In case of plants and lower eukaryotes including yeast and trypanosomatids, caspase gene is absent in their genome. Metacaspases are reported in plants, fungi and parasitic protozoa whereas paracaspases in metazoans and dictyostellium *(Uren et al., 2000).* These metacaspases are absent in mammals. Metacaspases are belonging to cysteine protease family and structurally related to caspases. The active site residues forming the cysteine-histidine catalytic dyad are conserved in metacaspases as in caspases and thought to have precursor of caspases *(Carmona-Gutierrez et al., 2010).* Since caspases are absent in the genome of plants, fungi and protozoan parasites, the involvement of metacaspases in programmed cell death of plants and fungi are established *(Mottram et al., 2003; Bozhkov et al., 2005).* The studies in *Arabidopsis thaliana* validate that the metacaspases were not able to cleave any caspase specific substrates but were able to cleave the substrates containing lysine or arginine residues present at P1 position *(Vercammen et al., 2004; Watanabe et al., 2005).* In addition, these metacaspases were insensitive to any caspase specific inhibitors

TH-1832_126106036

such as Z-VAD-fmk. However, the plant metacaspases expressed in *E. coli* were inhibited by serine protease inhibitor such as antipain and leupeptin and were insensitive to caspase specific inhibitors *(Vercammen et al., 2004)*. The studies on yeast metacaspases also suggest the similar substrate specificity and insensitivity to pan-caspase inhibitors *(Watanabe et al., 2005).* Similar studies were done in *Leishmania* parasite to check the involvement of metacaspases in programmed cell death of protozoa. Even in *L. donovani* parasite, metacaspases were not able to cleave any caspase specific substrates rather they were cleaved the substrate containing lysine and arginine residues present at P1 position. Caspase specific substrates primarily Ac-DEVD-AMC, Ac-LEHD-AFC and Ac-VEID-AMC were used to check the activity *(Lee et al., 2007).* These findings imply that metacaspases are not responsible for caspase like activities in fungi, plants and protozoan parasites as *Leishmania*. They may have involved as an effector molecule in programmed cell death as increased activity is found in apoptotic conditions.

1.5.2 Role of cathepsins in apoptosis: Cathepsins are proteases contain 11 different members in this family *(Schwartz, 1995)* and are subdivided into three subgroups depending on amino acid present on active site residues. These subgroups are mainly: (i) serine proteases containing cathepsins A and G, (ii) aspartate proteases contains cathepsins D and E, and (iii) cysteine protease which mainly contains cathepsins B, C, H, K, L, S and T. Cathepsins are synthesized as proenzymes and during stimuli it undergoes proteolytic cleavage to become active enzymes *(Capony et al., 1989; Fujita et al., 1991).* Cathepsin B and Cathepsin D are extensively studied in their role in apoptotic cell death processes. Cathepsin B belongs to cysteine protease family whereas cathepsin D belongs to aspartate proteases family *(Godbold et al., 1998).* Their subcellular localization is primarily in endosomes or lysosomes. Cathepsins are known to digest the proteins or peptides in lysosomal compartment. In addition, these peptidases are also secreted outside and are known to cleave the apoptotic signaling cascades. The role of cathepsins B and D in execution of apoptosis is confirmed by using specific inhibitors of cathepsin B and cathepsin D in bile salts induced apoptosis in liver cells. After treatment of hepatocytes with bile salts shows the apoptotic mediated cell death processes. But when the same sets of cell were treated with specific inhibitor of cathepsin B (CA-074-Me) and inhibitor of cathepsin D (pepstatin A), the induced apoptosis

TH-1832_126106036

was markedly inhibited suggests the role of cathepsins in apoptosis *(Roberts et al., 1997; Roberts et. al., 1999).* In the study conducted by Nishimura *et al* and Rowan *et al*, report that cathepsins are activated in similar cascade fashion as in caspases and cathepsin D are required for the processing and activation of cathepsin B *(Nishimura et.al. 1988; Rowan et al., 1992).* Role of cathepsin D in execution of apoptotic pathways are reported in TNF-α- and INF-γ- induced apoptosis in HeLa cells and U937 lymphoma cells *(Deiss et al., 1996).* In addition, Cathepsin D is also involved in drug induced apoptotic pathways as upregulation of the mRNA transcript and protein were observed in doxorubicin and etoposide treated cells *(Wu et al., 1998).* Roberts *et al* further showed the increased activity of cathepsin B and cathepsin D in Hep3B cell line in campotheticin induced apoptosis which were inhibited by CA-074-Me and pepstatin A. In *Leishmania* parasite, apoptotic like cell death processes were diminished after incubation with caspase inhibitor Z-VAD-fmk. The study conducted by El-Fadili *et al* report that the pan-caspase inhibitor binds to cathepsin B like protease mainly cysteine protease C (CPC) of *Leishmania (El-Fadili et al., 2010).* The interaction was further confirmed that binding of Z-VAD-fmk is absent in gene knockout *L. major* devoid of cathepsin B like protease (CPC). In addition, *cpc* knockout *Leishmania* survive better than wild type after exposure of H_2O_2, further suggest the role of cathepsin B in PCD of *Leishmania* parasite.

1.5.3 Role of calpains in apoptosis: Calpains belonging to a family of Ca^{2+} dependent cysteine proteases *(Guroff, 1964; Murachi et al., 1981).* Calpains are expressed ubiquitously as well in tissue specific manner *(Sorimachi et al., 1994).* It primarily contains two domains; 80 kDa and 30 kDa subunits *(Sasaki et al., 1983).* Ca^{2+} is required for the activity of calpains and so Ca^{2+} binding domains are available in both the subunits. The role of calpains in apoptotic processes are established as increased mRNA transcript and activity were observed in apoptotic cell death *(Squier et al., 1994; Waterhouse et al., 1998).* Moreover, the apoptosis was inhibited after induction with various calpain inhibitors. In most of studies, N-s-LLVY-AMC was used as a flurogenic substrate the check the activity of calpains where as leupeptin, E64, E64d- cell permeable inhibitor, calpeptin and N-acetyl-leu-leu-norleucinal was used as an inhibitor of calpains *(Xie et al., 1997; Aoyagi et al., 1969; Barrett et al., 1981; Wang, 1990; Mehdi, 1991).* More specific inhibitors PD150606 has recently been used which binds

TH-1832_126106036

to Ca^{2+} binding domains of calpains. Studies on mouse photoreceptor cell line have shown that Ca^{2+} influx leading to activation of calpains which in turn executes PCD by augmenting caspase-3 activity *(Sharma and Rohrer, 2004).* Calpains have also been involved in several disease progressions as increased expression of calpains were observed in brain tissue of Alzheimer's diseases and in Parkinson's disease *(Saito et al., 1993; Nixon et al., 1994; Mouatt-Prigent et al., 1996).* Debiasi *et al* observed that following treatment with calpain inhibitor I and PD150606 in nonhematopoietic cells, retrovirus induced apoptosis was blocked in murine cells. In contrast, treatment of *L. amazonensis* parasite with calpain inhibitor MDL28170 has shown to induce apoptosis like cell death in parasite with increased expression of apoptotic markers such as genomic DNA fragmentation and increased Annexin-V positive cells *(Marinho et al., 2014).* The proposed mechanism of role of calpain in apoptotic processes are shown in Figure 1.10.

TH-1832_126106036

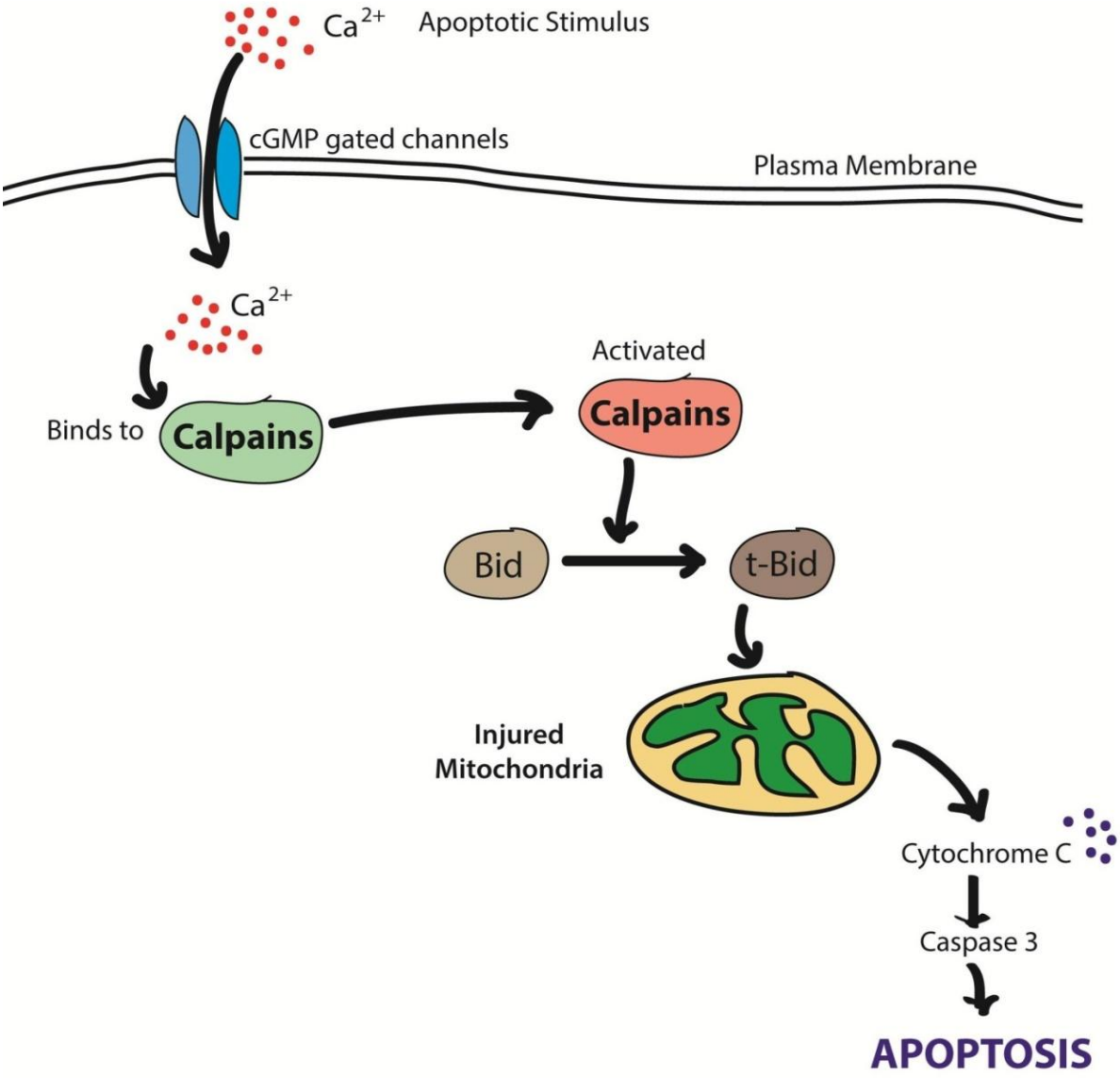

Figure 1.10: The proposed mechanism of execution of calpain in apoptotic processes. An Apoptotic stimulus triggers the cell to influx of calcium ions through plasma membrane channels such as PLC or cGMP-gated channels and activation of death receptors. Ca^{2+} binds through the calcium binding motifs available on calpains which in turn activates calpains. Activated calpains promote the cleavage of Bid protein into t-Bid resulting in increased membrane permeability of mitochondria. Thereby, promoting the release of Cyt.c from the mitochondria into cytosol, which enhances the cascade of events leads to activation of caspase-3 activity and ultimately cell death via apoptosis (Reproduced with permission from *J Biol Chem*. 2004; 279:35564-72).

TH-1832_126106036

1.5.4 Role of perforin and granzymes in apoptosis: Granzymes A and B are abundantly present within the granules of Cytotoxic T lymphocytes (CTLs) and Natural Killer (NK) cells. Granzymes are belonging to serine protease family with unique substrate specificity (*Smyth and Trapani 1995).* Granzyme A cleaves the substrate after arginine or lysine residues whereas Granzyme B cleaves if aspartate residue is present at P1 position *(Gershenfeld and Weissman, 1986; Masson et al., 1986; Odake et al., 1991).* Both Granzymes and perforins induce the cell death pathways in synergistic manner. Perforins a 70 kDa proteins are primarily a membrane disrupting protein which binds to the phosphorylcholine group of plasma membrane and forms pores after oligomerization *(Masson and Tschopp, 1985; Young et al., 1986; Tschopp et al., 1989).* Upon induction of apoptosis, Granzyme B diffuse into the target cell via perforin pores and cleaves the procaspases leading to activation of PCD. Granzymes are also reported to internalize inside the target cells via perforin independent mechanism. Very small amount of perforins are required for the execution of apoptosis as perforins help granzymes to translocate into the nucleus. In addition, granzyme B were able to cleave procaspase-3,-6,-7,-8,-9 and -10 *(Darmon et al., 1995; Quan et al., 1996; Gu et al., 1996; Duan et al., 1996).* Studies have shown that the cells incubated with granzyme B and perforin undergoes apoptotic cell death processes via activation of caspases with oligonucleosomal DNA fragmentation, cleavage of PARP and lamin B in target cells *(Medema et al., 1997; Van et al., 1997; Talanian et al., 1997; Andrade et al., 1998).* The cleavage of all these proteins was inhibited after incubation with pan-caspase inhibitors. Target cells co-incubated with granzyme A and perforin have shown caspase independent cell death modalities with single stranded DNA nicks and nuclear condensation and were insensitive to caspase specific inhibitors *(Hayes et al., 1980; Beresford et al., 1999).* In case of protozoan infections, CTLs and NK cells release granzymes and perforin to eliminate the pathogen infected cells and inhibits the further spread of disease. The author termed this killer cell mediated cell death as microptosis or microbe-programmed cell death. In protozoan parasite, microptosis is caspase independent apoptotic like cell death causing DNA fragmentation, chromatin condensation, phosphatidyl serine exposure on plasma membrane and change in transmembrane potential of mitochondria *(Dotiwala et al., 2016).* The schematic representation of granzyme dependent cell death modalities are shown in Figure 1.11.

TH-1832_126106036

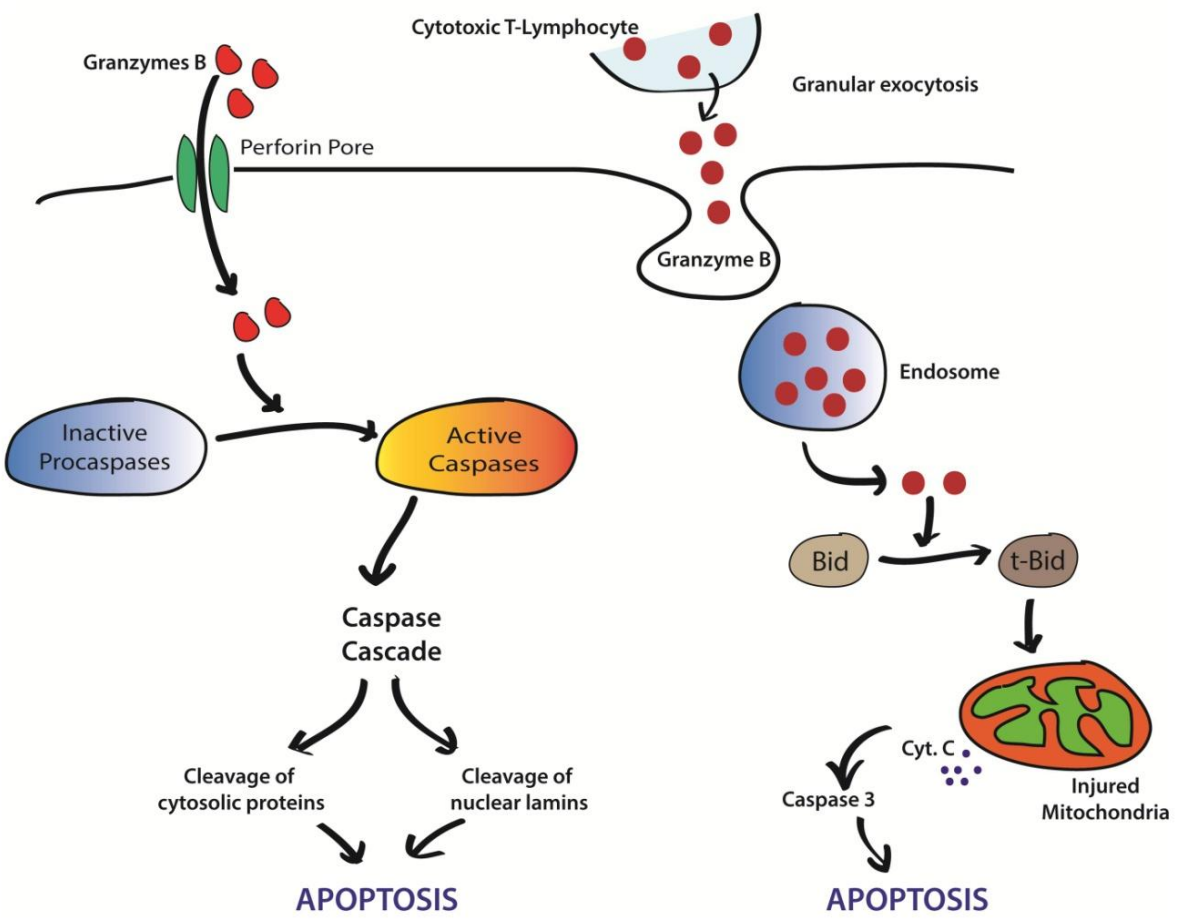

Figure 1.11: Proposed model for the apoptotic cell death pathway via granzymes and perforin. After induction of apoptosis, Granzymes B enter inside the cell via perforin pore and cleaves inactive procaspases to become active caspases. Active caspase, which in turn cleave cytosolic proteins and nuclear lamins, leads to cell death by apoptosis. Cytotoxic T lymphocytes and NK cell s contains granzyme B. Upon active, granular exocytosis takes place; granzymes are internalized by endocytosis and form endosomes. Active Granzymes cleave proapoptotic Bid protein into t-Bid (truncated-Bid), which acts on mitochondria to release cytochrome C and other proteins. These all proteins cause the cell death by caspase-3 mediated apoptosis processes. (Reproduced with permission from *Nat Rev Immunol*. 2002; 2:735-47)

TH-1832_126106036

1.6 Insights into the physiological implications of Methionine aminopeptidase

Methionine aminopeptidases (MAPs) are bifunctional enzyme that catalyzes the release of N-terminal methionine residues from nascent peptide and arylamides *(Ben-Bassat et al., 1987; Jackson and Hunter, 1970; Solbiati et al., 1999).* In eukaryotes, two types of MAPs are reported; MAP1 and MAP2 whereas in prokaryotes only one MAP gene is present *(Giglione et al., 2004).* Studies conducted in *E. coli* have shown that knockout of *map* gene is lethal, suggesting their important role in growth and survival of bacteria *(Chang et al, 1989).* MAP2 has shown a significant role in cell proliferation and growth in eukaryotes also *(Griffith et al., 1997; Sin et al., 1997).* During post translational modifications, removal of methionine is vital for amino terminal modifications such as addition of myristoyl group at N-terminal glycine residue by N-myristoyl transferase enzyme, addition of acetyl group by N-alpha acetyl transferase etc *(Boutin, 1997; Farazi, 2002).* These modifications are important for the biological activity of proteins, sub cellular localization and cell cycle progression *(Bradshaw et al., 1998).* In myristoylation process, myristic acid covalently binds to amino terminal glycine residues via amide linkage in both membrane bound and soluble proteins *(Aitken et al, 1982; Ozols et al., 1984; Schultz et al., 1985; Buss et al., 1987).* Several other proteins involved in signal transduction pathways and in regulatory pathways are myristoylated such as calcineurin, G-proteins, cAMP dependent protein kinases, proteins involved in ADP ribosylation and several oncoproteins *(Carr et al., 1982; Aitken et al., 1982; Schultz et al., 1987; Johnson et al., 1995).* Myristoylation of proteins increases the hydrophobicity and helps to anchor on the plasma membrane *(Resh, 2013).* Initially, MAP2 were reported to associate with eukaryotic initiation factor 2α (eIF2α) and regulate the protein synthesis pathway required for cell growth and survival. Bound MAP2 with eIF2α protects the inhibitory phosphorylation of eIF2α and in turn regulate the cell growth *(Li et al., 1996).*

Angiogenesis, the growth of new blood vessels, imparts an essential role for the development of tumor and metastasis. It is also vital for inflammation, wound healing and several other pathological conditions as diabetes retinopathy and rheumatoid arthritis. The role of MAP2 in angiogenesis is established as specific inhibitors of MAP2 inhibit the endothelial cell proliferation *(Griffith et al., 1997).* Fumagillin, isolated from fungus *Aspergillus fumigates* was discovered serendipitously to act as a potent inhibitor of MAP2. It

TH-1832_126106036

significantly inhibits the angiogenesis processes. Several synthetic analogs of fumagillin are synthesized by chemical approaches such as AGM-1470 (TNP-470), PPI-2458, XMT-1191 and beloranib *(Griffith et al., 1997*; *Liu et al., 1998; Arico-Muendel et al., 2013; Bernier et al., 2004; Howland, 2015).* Ovalicin, another analog of fumagillin, was isolated from fungus *Pseudorotium ovalis.* The structure of fumagillin and related analogs are shown in Figure 1.12. Several studies have reported the effect of fumagillin and its analogs in tumor growth and metastasis. Sheen *et al* have shown that the fumagillin treatment inhibits the hepatoma in rats *(Sheen et al., 2005).* High mRNA transcript and expression of MAP2 was found in malignant mesothelioma cells, malignant lymphomas, neuroblastomas, and colorectal carcinomas *(Catalano et al., 2001; Kanno et al., 2002; Morowitz et al., 2005; Selvakumar et al., 2004).* The higher expression of MAP2 in numerous tumor cells suggests that the dependence of tumor cell on MAP2 for uncontrolled growth. MAP2 inhibitors are successfully demonstrated to inhibit angiogenesis and tumor growth in carcinoma, sarcoma, neuroblastoma and arthritis. MAP2 inhibitors such as fumagillin and TNP 470 are in clinical and preclinical trials and found to be safe and effective *(Ingber et al., 1990; Kusaka et al., 1991; Shusterman et al., 2001).*

The structure of human MAP2 contains two pairs of α helices and a central β sheet *(Liu et al., 1998).* 165 residues N-terminal extension is found in human MAP2 than *E. coli* MAP2 which are not involve in removal of amino terminal methionine residues *(Griffith et al., 1997).* The studies suggest that the N-terminal extension may involve in association with intracellular organs such as ribosomes. The crystal structure of human MAP2 suggests that the active site of MAP2 buried deep inside and contains two Co^{2+} ions. These cobalt ions are associated with Asp251, Asp262, His331, Glu364 and Glu459 along with water molecules *(Liu et al., 1998).* The metal coordinated residues are conserved in all MAP2 sequences. Several biochemical analyses revealed that different metal ions are required for the optimum activity of MAPs. In yeast MAP1, Zn^{2+} is required for better activity whereas in *E. coli* MAP1 Fe^{2+} or Co^{2+} is required *(Roderick et al., 1993; Chai et al., 2008; Walker et al., 1998).* Mn^{2+} is found to be cofactor for maximum activity in human MAP2 (*Wang et al., 2003*). Fumagilin, a potent inhibitor of MAP2 binds covalently with the enzyme. Fumagilin contains spirocyclic epoxide group in its structure and this group binds to the His231 of the MAP2. His339 residue moves away by rotating its side chain to avoid the close proximity of

TH-1832_126106036

fumagillin epoxide group. Now side chain of fumagillin occupies in the active site pocket and His339 makes hydrophobic contacts along with other amino acids near active site. Both His231 and His339 residues are present in close proximity at active site and conserved in all MAPs (*Liu et al., 1998*). His231 acts as general base in acid-base catalysis reaction in which it performs nucleophilic attack along with metal coordinated ions to activate water molecules. Activated water molecule acts on amide bond of a peptide where another His residue acts as general acid and protonate the amide nitrogen. Protonation of amide nitrogen helps the proteolytic cleavage of peptide bonds. The schematic mechanism of proteolytic cleavage of peptide bonds and inhibition by fumagillin is shown in Figure 1.13. Binding of epoxide group of fumagillin and its analogues block the active site pocket of MAP2 and hence prevents the substrate binding and catalytic efficiency. His231 is conserved in both MAP1 and MAP2. But binding of epoxide group of fumagillin with His231 is exclusive for MAP2 only, suggesting the role of other amino acids present at the active site pocket in substrate binding and catalysis (*Liu et al., 1998*). Specific binding of fumagillin analogues to MAP2 may suggest the molecular and biochemical events preventing endothelial cell proliferation and tumor progression by this inhibitors.

TH-1832_126106036

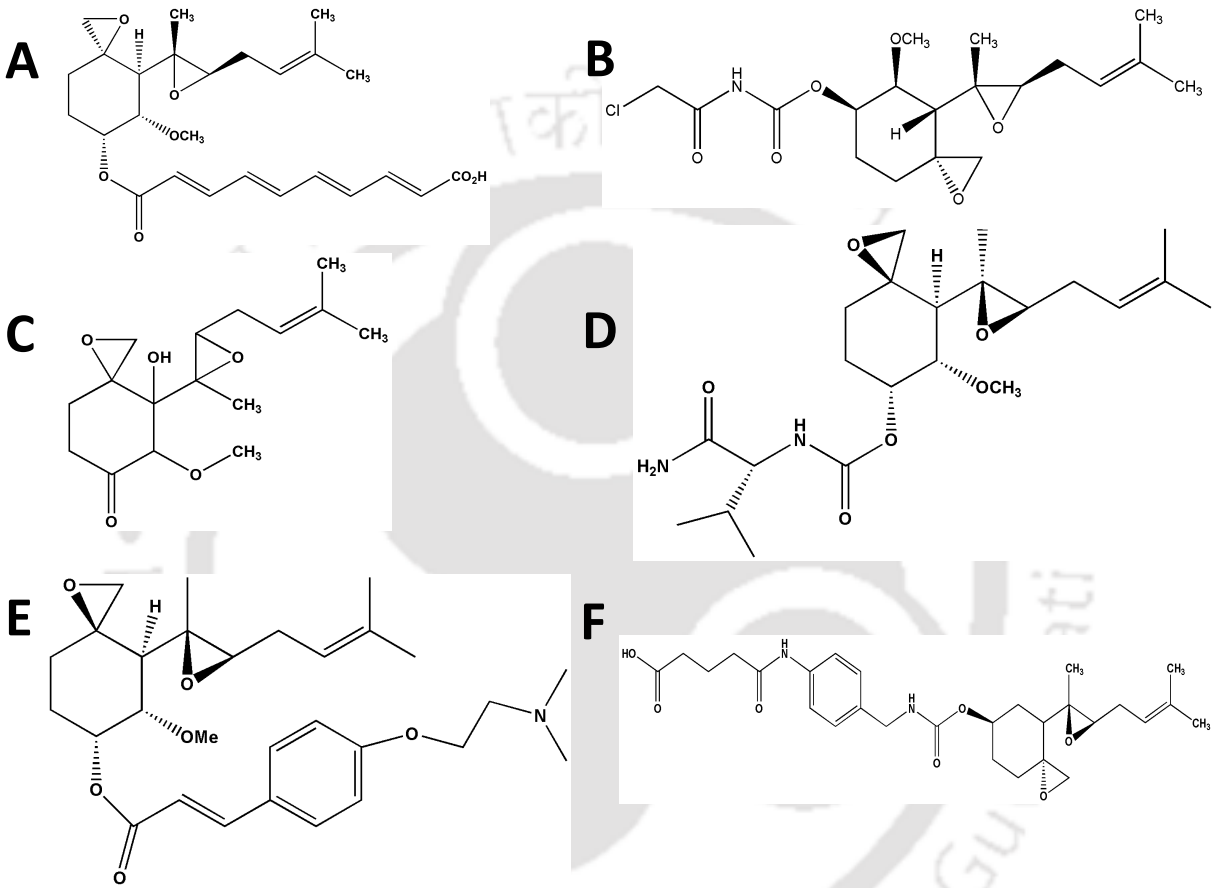

Figure 1.12: Chemical structure of MAP2 inhibitors **(A)** fumagillin, a natural MAP2 inhibitor obtained from fungus *Aspergillus fumigates* **(B)** TNP-470, a fumagillin analogue **(C)** Ovalicin, obtained from *Pseudorotium ovalis* **(D)** PPI-2458 (E) Beloranib (F) XMT-1191. The chemical structures are redrawn using ChemDraw Ultra software.

TH-1832_126106036

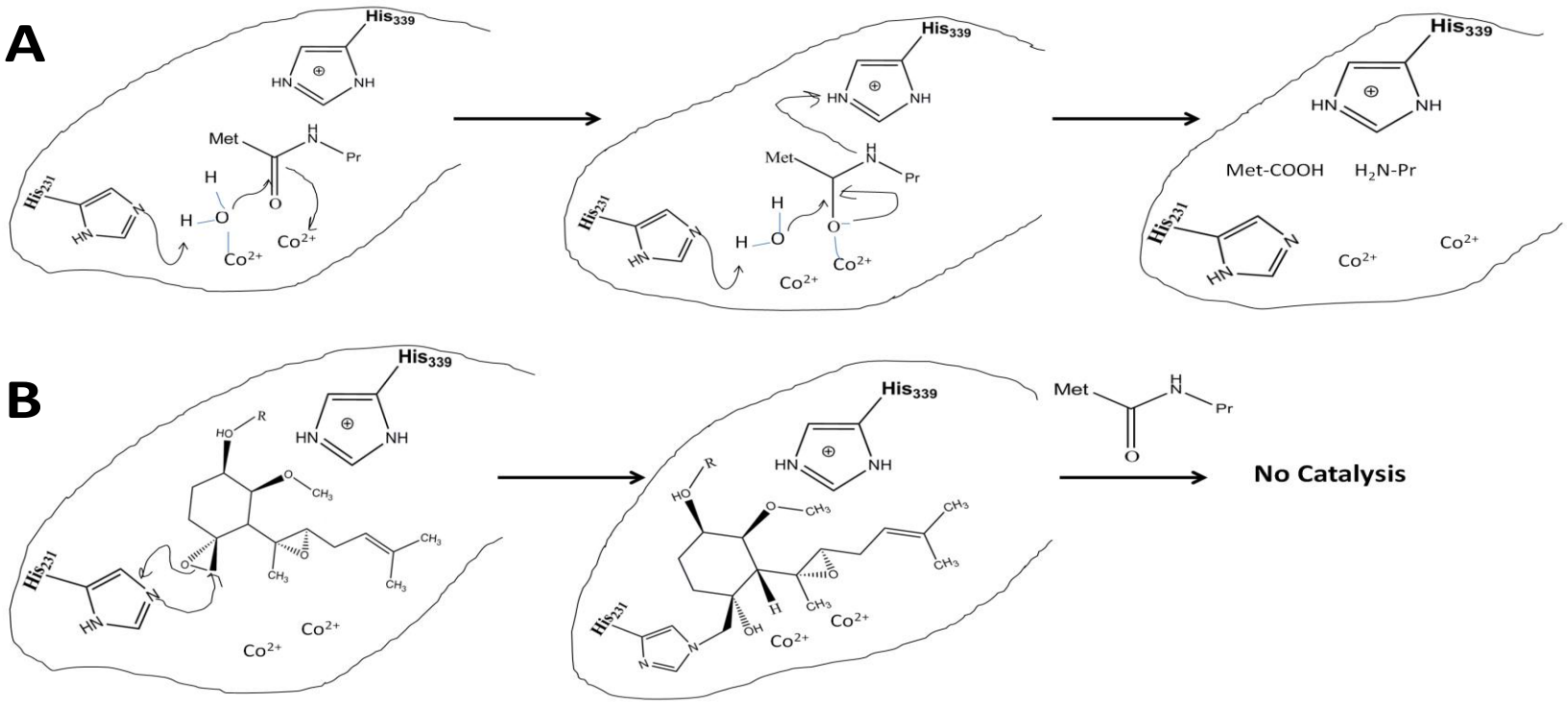

Figure 1.13: Reaction mechanism of methionine aminopeptidase 2 and inhibition by fumagillin. (A) Enzyme catalysis showing removal on N-terminal methionine residues from nascent peptide. (B) Fumagilin binds to active site residues of MAP2 and inhibits enzyme catalysis reaction. His231 acts as general base in acid-base catalysis reaction in which it performs nucleophilic attack along with metal coordinated ions to activate water molecules. Activated water molecule acts on amide bond of a peptide where another His residue acts as general acid and protonate the amide nitrogen. Protonation of amide nitrogen helps the proteolytic cleavage of peptide bonds. Binding of epoxide group of fumagillin and its analogues block the active site pocket of MAP2 and hence prevents the substrate binding and catalytic efficiency. (Pr: Nascent Protein) (Reproduced with permission from *Proc Natl Acad Sci U S A.* 1998; 95:15183-8)

TH-1832_126106036

1.7 Significance of present research work and defining the research problem

Apoptotic mediated cell death processes of the parasite are well documented by several groups after treatment with various leishmanicidal molecules or drugs. In most of the studies, the cell death pathway is reported *via* increase in caspase like activity. Caspases are known to be important regulator of programmed cell death in higher eukaryotic organisms. Activation of caspases leads to cleavage of cytosolic proteins, nuclear lamins and ultimately cell death by apoptosis. Genome sequencing of *L. donovani* has been completed and it provided an avenue to analyze the entire genome sequences of parasite. The submitted genome sequence of *Leishmania* revealed that no caspase gene is present. Metacaspases, belongs to cysteine proteases and structurally similar to caspases are present in the genome of parasite. Detailed biochemical characterization of metacaspases suggests that the metacaspases are not responsible for caspase like activity, as metacaspases were not able to cleave any caspase specific substrates. As caspase gene is absent and metacaspases are not responsible for caspase like activity, the available literature point out towards the role of other proteases in PCD of parasite. Moreover, the role of various proteases in PCD of parasite is not well explored. Based on this background and available literature, we explored the possible function of various proteases in PCD of parasite. Searching for the role of proteases in PCD, we have observed that the mRNA transcript of *Ld*MAP2 was up-regulated in miltefosine treated parasite. This data led us to investigate the involvement of *Ld*MAP2 in the apoptotic pathway of the *L. donovani*. The apoptotic condition was induced in parasite by miltefosine. Upon inhibition of *Ld*MAP2 with small molecule inhibitor, the parasite did not show apoptotic mediated cell death processes. We further validate the role of *Ld*MAP2 in PCD of parasite *via* gene knock out approach. Biochemical and genetic approaches revealed the role of MAP2 in the apoptotic processes of the parasite. Further, genetic approaches suggest that the parasite shows miltefosine unresponsive phenotype after knock out of *map2* gene. The current work promises to uncover key molecular underpinnings of the programmed cell death pathway of *L. donovani* as well as gaining a broad understanding of the process of apoptosis as a whole in the dimorphic parasites.

TH-1832_126106036

The Ph.D work presented in the thesis aims to answer the following important questions:

1. To explore the total proteases of *Leishmania donovani* genome and gene expression analysis of proteases under apoptotic condition.

2. To explore the role of Methionine aminopeptidase 2 in programmed cell death of parasite by using small molecule inhibitor.

3. To further validate the role of Methionine aminopeptidase 2 in programmed cell death of parasite by using gene knock out approach.

TH-1832_126106036

Chapter II

Exploring realm of proteases of *Leishmania donovani* genome and gene expression analysis of proteases under apoptotic condition*

2.1 Abstract

Proteases are known to be among key players in the apoptotic pathways. Many publications have reported apoptotic death in trypanosomatids including *Leishmania donovani*. However, various proteases involved in apoptotic pathways of trypanosomatids in general and *Leishmania donovani* in specific remains uncharacterized. Genomic analysis of *Leishmania donovani* has shed light on various proteases in the parasite genome, their classification and sub-cellular localization. Under apoptotic condition of the parasite, gene expression analyses of representative protease(s) from each clan show altered expression levels of various proteases. The data indicates possible role of various proteases in apoptotic process, directly or indirectly. Over-expression of autophagy related protease genes under apparent apoptotic conditions show some crosstalk between autophagy and apoptosis like cell death of *Leishmania* parasite. The counter-regulation of these two processes in trypanosomatids in general and *Leishmania* in specific needs further investigation.

***Part of the work is published in *Journal of Proteomics and Bioinformatics*, 2016; 9:200-208.**

TH-1832_126106036

2.2 Introduction

Apoptotic like cell death in *Leishmania* is well established under various stress conditions, including oxidative stress *(Das et al., 2008; Saudagar et al., 2013; Saudagar and Dubey, 2014).* Roles of various proteases, including caspases, are recognized for cell death mechanism in different organisms and human cell lines *(Patel et al., 2004; Tang and Grimm, 2004).* However, in *Leishmania*, studies remains focused on possible role of caspases and metacaspases in the apoptotic processes. Extensive studies about possible role of other proteases in the apoptotic processes of parasites are not reported. Thus, the mechanism of cell death with respect to role of proteases remains elusive. Caspases are the most important regulators of the apoptotic processes in higher eukaryotic organisms. Several groups have reported evidence of caspase like activities associated with apoptotic cell death in *Leishmania (Das et al., 2008; Saudagar et al., 2013; Saudagar and Dubey, 2014; Zangger et al., 2002).* However, caspase that has essential role in apoptosis in higher eukaryotic organism is absent in genome of *Leishmania (Uren et al., 2000; Berriman et al., 2005).* Metacaspases are cysteine proteases distinctly related to caspase are found in *Leishmania* (but absent in mammal), was initially thought to be responsible for caspase like activity. However, they are recently reported to have trypsin like activity rather than caspase like activity *(Lee et al., 2007).* Metacaspases do not seem to have role in apoptosis mediated cell death of parasite *(Castanys-Muñoz et al., 2012).* Thus, it remains crucial to rigorously analyze possible enzyme that may responsible for caspase like activity in the pathogen. It is possible that some other protease in *Leishmania* genome has evolved to perform additional function *i.e.* caspase like activity. Identification of enzyme cleaving caspase substrate may provide fundamental insights into apoptotic pathways in *Leishmania*. Furthermore, role of other proteases in the apoptotic cell death of *Leishmania* is also not extensively explored. To get the insight of the mechanism of apoptotic cell death and possible role of peptidases in the process, real time q-PCR analysis of various peptidase genes of *L. donovani* was done in miltefosine treated cells and compared with control cells (untreated cells) to know the change in mRNA expression level. It is worth mentioning that miltefosine is known to trigger apoptotic cell death in parasite *(Paris et al., 2004).*

TH-1832_126106036

2.3 Methods

2.3.1 Parasites, cell lines and chemicals: The *Leishmania donovani* (MHOM/IN/2010/BHU1081) promastigotes culture was obtained from Prof. Shyam Sundar, Banaras Hindu University. The apoptosis detection kit was procured from Calbiochem. Power SYBR Green PCR master mix was obtained from Life Technologies. AMV first strand cDNA synthesis kit and DNase I was purchased from New England Biolabs. RNeasy Mini Kit was obtained from Qiagen. All the chemicals used in the experiments were of the highest grade procured from Sigma-Aldrich or Merck.

2.3.2 Sequence retrieval and Classification of Peptidases: We have analyzed the genome of *L. donovani* available in GeneDB database (http://www.genedb.org/) where 8,021 proteins are found to be annotated *(Downing et al., 2011).* Total 141 proteins (Table 2.2) are identified/predicted as peptidases by blast in UniprotK *(Apweiler et al., 2004)* (http://www.uniprot.org/help/uniprotkb); and classified in respective clan and family using MEROPS database (http://merops.sanger.ac.uk/) *(Rawlings et al., 2014).* Some other family prediction tools namely SVMProt: Protein Functional Family Prediction tool (*Cai et al., 2003)* (http://jing.cz3.nus.edu.sg/cgi-bin/svmprot.cgi), ProtoNet tools *(Rappoport et al., 2012)* (http://www.protonet.cs.huji.ac.il/) and SUPERFAMILY *(Gough et al., 2001)* (http://supfam.cs.bris.ac.uk/) are used for the peptidases which are not enlisted in MEROPS.

2.3.3 Sub-cellular localization: Uniprot database (http://www.uniprot.org/) and BRENDA-Enzyme database (http://www.brenda-enzymes.org/) are used to check the experimental information about the sub-cellular localization of proteins. If experimental data of sub cellular localization is not available, various bioinformatics tools are used to predict the localization. Signal P 4.1 server (http://www.cbs.dtu.dk/services/SignalP/) has been used for predicting presence and location of signal peptide sequences. TMHMM tools (http://www.cbs.dtu.dk/services/TMHMM-2.0/) are used for prediction of transmembrane helices. LocTree 3 (https://rostlab.org/services/loctree2/) and CELLO v 2.5 (http://cello.life.nctu.edu.tw/) are used for predicting the sub cellular localization based on

TH-1832_126106036

two level support vector machine (SVM) system, sequence similarity and gene ontology information.

2.3.4 Apoptosis detection: Apoptotic assay was performed as reported earlier to confirm the apoptotic condition after miltefosine treatment *(Saudagar and Dubey, 2014).* In brief, *L. donovani* promastigote cells were treated with 50 µM of miltefosine for 24 hr. After treatment, cells were harvested by centrifugation at 3000 rpm for 10 min and washed twice by cold PBS. Similarly, untreated cells were also centrifuged and washed by cold PBS. Both treated and untreated cells were suspended in 500 µl of 1X binding buffer, stained with Annexin V-FITC and propidium iodide (PI) as per manufacturer instructions. After staining, the cells were analyzed using BD FACS Calibur flow cytometer and the fraction of cell population in different quadrants was analyzed by quadrant statistics using CellQuest software.

2.3.5 Expression level analysis of various peptidase genes by Real time PCR: Total RNA was extracted from untreated cells (control) and treated cells (50 µM miltefosine for 24 hrs) using RNeasy Mini Kit – QIAGEN according to the manufacturer's protocol. In brief, the RNA was treated with DNase I-NEB for 30 min at 37°C and heat inactivated at 70°C for 5min before cDNA preparation to remove contamination of genomic DNA. RNA was quantified by nanodrop at 260 nm absorbance and purity was accessed at A260/A280 ratio (>1.8). Equal amount of RNA was taken for first strand cDNA synthesis using AMV First Strand cDNA Synthesis Kit – NEB. Random hexamer primers were used for cDNA synthesis. Cycling parameters were 70°C for 5 min, followed by 25°C for 15 min and final extension at 42°C for 45 min. The quality of cDNA was assessed by generating expression profiles of *L. donovani* housekeeping α-tubulin genes with real time PCR. Out of all proteases identified and classified (Figure 1), representative protease(s) from each clan was taken for expression analysis under induced apoptotic condition. Only one clan PB (threonine protease) which primarily includes proteasomes subunits is excluded. mRNA sequences for various *L. donovani* peptidases were taken from GeneDB (http://www.genedb.org) and primers were designed with primer 3 – Biotools *(Rozen et al., 2000).* Accession number and primer sequences are shown in Table 2.1.

TH-1832_126106036

SYBR Green PCR assays were performed on Applied Biosystems 7500 Real-Time PCR System. All quantitative assays were performed with housekeeping α-tubulin gene as endogenous control as reported in literature *(Carter et al., 2006).* Cycling parameters were run at initialization at 50°C for 2 min, 95°C for 10 min to activate the DNA polymerase, 40 cycles of denaturation at 95°C for 30 sec, annealing at 60°C for 30 sec and then extension at 72°C for 30 sec. Melt curve was included and analyzed to access the specificity of PCR product. All results were normalized to the expression of alpha-tubulin gene in control and miltefosine treated cells. In addition to this, the PCR product was run on 1% agarose gel to check the amplicon size and nonspecific amplifications. Data were analyzed using Applied Biosystems SDS v2.0.6 software.

Table 2.1: List of Primers used for gene expression analysis

S.No	Name of Primers	Sequences	Name of peptidases	Gene DB Accession no.	Clan	Family
01.	PrAP-F	GTCGTGGAGTTTCTGTATGGTGAG	Presenilin-like aspartic peptidase, putative	LdBPK_151600.1	AA	A22
	PrAP-R	GAGCACAAAGACGACAGTAGAGAG				
02.	SPP–F	GCGTACACTCTGAGTCTTGTGAAC	Signal peptide peptidase, putative	LdBPK_290990.1	AD	A22
	SPP-R	CAGCAGAGAATGTGACGAGAAG				
03.	CCP-F	CGATCTACTACGTCAACGACTACG	Calpain-like cysteine peptidase, putative	LdBPK_040430.1	CA	C1
	CCP-R	GACGATGTTATCACCGATCTCC				
04.	CPB -F	CCCTCTTATAGACGCACTTACCAG	Cysteine peptidase B (CPB)	LdBPK_070600.1	CA	C1
	CPB –R	GGACACACTCCTCGTTGATGAT				
05.	CPA-F	GCAGACAGCCTACTTCCTCAAT	Cysteine peptidase A (CPA)	LdBPK_191460.1	CA	C1
	CPA-R	CGTAGTAGTTGGGGTTCAGGTACA				
06.	CPC-F	GGCTACAAGAGTGGAGTGTACAAG	Cysteine peptidase C (CPC)	LdBPK_290860.1	CA	C1
	CPC-R	GGATCAGGAAGTAGCCTTTGTC				
07.	UbH-F	GAGAGCGGCTACTATGACCTGT	Ubiquitin hydrolase, putative	LdBPK_310150.1	CA	C19
	UbH-R	GCCACTTGTCTGCTTTCTTACC				
08.	ATG4.1-F	AGCACACTTTCAAACAGGGG	AUT2/APG4/ATG4 cysteine	LdBPK_300270.1	CA	C54

TH-1832_126106036

	ATG4.1-R	GGCTGCTCCATCAGTTTTTC	peptidase, putative			
09.	ATG4.2-F	CATCCAAAACGCCTACACCT	AUT2/APG4/ATG4 cysteine	LdBPK_324040.1	CA	C54
	ATG4.2-R	ATTAGTGGAAACGCCACGAG	peptidase, putative			
10.	MCas-F	TCGACCTGTACAAGCCCTTC	Metacaspase, putative	LdBPK_351580.1	CD	C14
	MCas-R	CGGTACGTGGACTGGGTAAC				
11.	PGP-F	GGTGTCTTCATTCACGTTGTCG	Pyroglutamyl-peptidase I (PGP), putative	LdBPK_341750.1	CF	C15
	PGP-R	ACGTGGTCATCAAAGACAGCAG				
12.	PAP-F	CCTCGTTGACTGTATCGT	Puromycin-sensitive aminopeptidase-like protein	LdBPK_120830.1	MA	M1
	PAP-R	TCGTAGATGTAGAGGTAGGG				
13.	ZnMP1-F	GATCCAGTTTAGCACCTACTACCC	Mitochondrial ATP-dependent zinc metallopeptidase, putative	LdBPK_341130.1	MA	M41
	ZnMP1-R	GAACGTAAACCGACTCTTCTCC				
14.	ZnCP-F	GCACCTTCTACTTTCAGGAGGAC	Zinc carboxypeptidase, putative	LdBPK_342670.1	MC	M14
	ZnCP-R	GTGTACATGCGGTAGTGGAAGAC				
15.	PMP-F	GTACCCCTTCTCGACTACCAATC	Pitrilysin-like metalloprotease	LdBPK_070250.1	ME	M16
	PMP-R	CTCCTGCTTGAAGTCCTCCTCT				
16.	MLP-F	GACGTACCCGATTATCCAGCTC	Metalloprotease-like protein	LdBPK_040820.1	ME	M67
	MLP-R	CATCGATGGGTACTGGTAGTAGTG				
17.	APP-F	CCTGGCTGCTACTTTAAC	Aminopeptidase P, putative	LdBPK_352400.1	MG	M24
	APP-R	CAAGACGTCACTCTCGAT				
18	MAP1-F	CTGTGCCAAAGGAGATAG	Methionine aminopeptidase, putative	LdBPK_190540.1	MG	M24
	MAP1-R	GGCGTTGTTGTAGTCTTC				
18.	MAP2-F	CACCTCATGAACCTGAAC	Methionine aminopeptidase 2, putative	LdBPK_210960.1	MG	M24
	MAP2-R	CGAGGTAGATCGTGTGTT				
20.	PepT-F	AAGTACGTTGGACAGGAC	Peptidase t, putative	LdBPK_170250.1	MH	M10
	PepT-R	GTGCTTCTCCTTACTGGA				
21.	AAP-F	CATGGAGGACCTGTTATC	Aspartyl aminopeptidase, putative	LdBPK_292470.1	MH	M18
	AAP-R	CTCTTGGATGGGTATGTC				

TH-1832_126106036

22.	ZnMP2-F	GCTACGAACTTTGTGGAC	ATP-dependent zinc metallopeptidase, putative	LdBPK_191620.1	MH	M41
	ZnMP2-R	CGGCTAAGATAGTGGTTG				
23.	SerP-F	GATCGATCACTCCTACACTCTGC	Serine peptidase, putative	LdBPK_120920.1	SC	S10
	SerP-R	GTTACGACACGCTCTCGAAGTATC				
24.	SP1-F	GTGGAGCAGGACATGATTATCG	Signal peptidase type I, putative	LdBPK_080460.1	SF	S26
	SP1-R	GTGGAGGTCAGCATAAAGAAGC				
25.	AT-F	CTACGGCAAGAAGTCCAAGC	Alpha tubulin	LdBPK_130330.1		
	AT-R	CAATGTCGAGAGAACGACGA				

2.4 Results

2.4.1 Classification of Peptidases: Total 141 proteins are annotated as peptidases in *L. donovani*. The number of identified proteases are close to the number of proteases reported from another species *i.e. L. major* (154 peptidases). Majorly five classes of peptidases are present in parasite namely aspartic peptidase, cysteine peptidase, metallopeptidase, serine and threonine peptidase. We have found two families of aspartic peptidases, ten families of cysteine peptidases, twenty one families of metallopeptidases, seven families of serine peptidases and one family of threonine peptidases in *L.donovani*. Cysteine peptidase is the largest clan containing 60 peptidases followed by metallopeptidases - 52, serine peptidases - 15, threonine peptidases - 13 and aspartic peptidases containing only two peptidases as shown in Figure 2.1. All peptidases are classified with high confidence and are reported in Table 2.2.

TH-1832_126106036

Table 2.2: List of all peptidases of *L. donovani* with their accession number (GeneDB ID). Nomenclature of peptidases is done on the basis of MEROPS databases. Subcellular localization(s) are predicted by LocTree3 and CELLO v 2.5 web server. Any transmembrane helices and signal peptide sequences are predicted by TMHMM server and Signal P.

Clans of Aspartic peptidases								
S.No.	Proteases	GeneDB ID	Clan	Family	LocTree3	TMHMM	SignalP	CELLO
1	presenilin-like aspartic peptidase, putative	LdBPK_151600.1	AA	A22	ER membrane	7	no	plasma membrane
2	signal peptide peptidase, putative	LdBPK_290990.1	AD	A22	ER membrane	6	no	plasma membrane
Clans of Cysteine peptidases								
3	cysteine peptidase B (CPB)	LdBPK_070600.1	CA	C1	nucleus	1	no	nucleus
4	cathepsin L-like protease	LdBPK_080950.1	CA	C1	secreted	0	no	nucleus
5	cathepsin L-like protease	LdBPK_080960.1	CA	C1	secreted	1	yes ARA-IY 27&28	lysosome
6	cysteine peptidase A (CBA)	LdBPK_191460.1	CA	C1	secreted	1	yes GSA-LI 24&25	extra-cellular
7	cysteine peptidase C (CPC)	LdBPK_290860.1	CA	C1	vacuole	1	Yes 28-29 LYA-KP	lysosome
8	Calpain-like cysteine peptidase, putative	LdBPK_040430.1	CA	C2	cytoplasm	0	no	cytoplasm
9	calpain-like cysteine peptidase, putative	LdBPK_140910.1	CA	C2	secreted	0	no	cytoplasm
10	calpain-like cysteine peptidase, putative	LdBPK_140920.1	CA	C2	secreted	0	no	cytoplasm
11	calpain-like cysteine peptidase, putative	LdBPK_181070.1	CA	C2	cytoplasm	0	no	plasma membrane
12	calpain-like cysteine peptidase, putative	LdBPK_201210.1	CA	C2	ER	0	no	nucleus/cytoplasm
13	calpain-like cysteine peptidase, putative	LdBPK_201220.1	CA	C2	secreted	0	no	nucleus
14	calpain-like cysteine peptidase, putative	LdBPK_201230.1	CA	C2	cytoplasm	0	no	cytoplasm
15	calpain-like cysteine peptidase, putative	LdBPK_201240.1	CA	C2	cytoplasm	0	no	nucleus
16	calpain-like cysteine peptidase, putative	LdBPK_201250.1	CA	C2	cytoplasm	0	no	plasma membrane

TH-1832_126106036

17	calpain-like cysteine peptidase, putative	LdBPK_201320.1	CA	C2	secreted	0	no	nucleus/cytoplasm
18	calpain-like cysteine peptidase, putative	LdBPK_201340.1	CA	C2	secreted	0	no	nucleus/mitochondria
19	calpain-like cysteine peptidase, putative	LdBPK_201350.1	CA	C2	secreted	0	no	cytoplasm/nucleus
20	calpain, putative	LdBPK_210160.1	CA	C2	nucleus	0	no	plasma membrane/nucleus
21	calpain, putative	LdBPK_210170.1	CA	C2	cytoplasm	0	no	Mitochondria/membrane
22	calpain family cysteine protease-like protein	LdBPK_251540.1	CA	C2	nucleus	0	no	mitochondria/nucleus
23	calpain-like cysteine peptidase, putative	LdBPK_270500.1	CA	C2	secreted	0	no	cytoplasm/extra-cellular
24	calpain-like cysteine peptidase, putative	LdBPK_270510.1	CA	C2	cytoplasm	0	no	nucleus/cytoplasm
24	cysteine peptidase, Clan CA, family C2, putative	LdBPK_270520.1	CA	C2	cytoplasm	0	no	nucleus
25	calpain-like cysteine peptidase, putative	LdBPK_302040.1	CA	C2	cytoplasm	0	no	nucleus/plasma membrane
26	calpain-like cysteine peptidase, putative	LdBPK_310410.1	CA	C2	cytoplasm	0	no	cytoplasm
27	calpain-like protein, putative	LdBPK_310420.1	CA	C2	cytoplasm	0	no	chloroplast/nucleus
28	calpain-like cysteine peptidase, putative	LdBPK_310430.1	CA	C2	cytoplasm	0	no	plasma membrane
29	calpain-like cysteine peptidase, putative	LdBPK_310440.1	CA	C2	cytoplasm	0	no	nucleus/extra-cellular
30	calpain-like cysteine peptidase, putative	LdBPK_310450.1	CA	C2	cytoplasm	0	no	chloroplast/cytoplasm
31	calpain-like cysteine peptidase, putative	LdBPK_310480.1	CA	C2	cytoplasm	1	no	mitochondria
32	calpain-like cysteine peptidase, putative	LdBPK_321020.1	CA	C2	nucleus	0	no	nucleus
33	calpain-like cysteine peptidase, putative	LdBPK_322140.1	CA	C2	cytoplasm	0	no	cytoplasm/nucleus
34	calpain protease-like protein	LdBPK_332130.1	CA	C2	nucleus	0	no	nucleus/chloropla

TH-1832_126106036

								st
35	calpain-like cysteine peptidase, putative	LdBPK_340300.1	CA	C2	nucleus	0	no	nucleus
36	Ubiquitin carboxyl-terminal hydrolase, putative cysteine peptidase	LdBPK_250190.1	CA	C12	cytoplasm	0	no	cytoplasm
37	Ubiquitin carboxyl-terminal hydrolase, putative	LdBPK_240420.1	CA	C12	nucleus	0	no	cytoplasm
38	Ubiquitin hydrolase, putative	LdBPK_120170.1	CA	C19	ER membrane	0	no	nucleus
39	Ubiquitin hydrolase, putative	LdBPK_151320.1	CA	C19	nucleus	0	no	nucleus
40	Ubiquitin hydrolase, putative	LdBPK_160730.1	CA	C19	nucleus	0	no	nucleus
41	Ubiquitin hydrolase, putative	LdBPK_292410.1	CA	C19	cytoplasm	0	no	extra-cellular
42	Ubiquitin hydrolase, putative	LdBPK_300250.1	CA	C19	cytoplasm	0	no	cytoplasm/nucleus
43	Ubiquitin hydrolase, putative (fragment)	LdBPK_301260.1	CA	C19	secreted		no	mitochondria
44	Ubiquitin hydrolase, putative	LdBPK_321310.1	CA	C19	ER membrane	0	no	nucleus
45	Ubiquitin hydrolase, putative	LdBPK_323060.1	CA	C19	ER membrane	0	no	plasma membrane
46	Ubiquitin hydrolase, putative	LdBPK_343890.1	CA	C19	nucleus	0	no	cytoplasm/nucleus
47	Ubiquitin hydrolase, putative	LdBPK_351730.1	CA	C19	nucleus	0	no	nucleus
48	Ubiquitin hydrolase, putative	LdBPK_352460.1	CA	C19	nucleus	0	no	nucleus/mitochondrial
49	Ubiquitin carboxyl-terminal hydrolase, putative cysteine peptidase	LdBPK_090390.1	CA	C19	nucleus	0	no	nucleus
50	Ubiquitin carboxyl-terminal hydrolase, putative cysteine peptidase	LdBPK_171190.1	CA	C19	nucleus	0	no	nucleus
51	Ubiquitin carboxyl-terminal hydrolase, putative	LdBPK_210460.1	CA	C19	nucleus	0	no	nucleus
52	Ubiquitin hydrolase	LdBPK_240630.1	CA	C19	nucleus	0	no	nucleus
53	Ubiquitin carboxyl-terminal hydrolase, putative cysteine peptidase	LdBPK_271170.1	CA	C19	ER membrane	0	no	nucleus
54	Ubiquitin carboxyl-terminal hydrolase, putative	LdBPK_310150.1	CA	C19	nucleus	0	no	cytoplasm

TH-1832_126106036

55	AUT2/APG4/ATG4 cysteine peptidase, putative	LdBPK_300270.1	CA	C54	cytoplasm	0	no	extracellular
56	AUT2/APG4/ATG4 cysteine peptidase, putative	LdBPK_324040.1	CA	C54	cytoplasm	0	no	mitochondria
57	Otubain cysteine peptidase, putative	LdBPK_171520.1	CA	C65	cytoplasm	0	no	cytoplasm
58	GPI-anchor transamidase subunit 8 (GPI8), putative	LdBPK_180360.1	CD	C13	ER membrane	1	yes AYA-AV 30-31	extra-cellular
59	Metacaspase, putative	LdBPK_351580.1	CD	C14	Secreted	0	no	nucleus/plasma membrane
60	Separin, putative	LdBPK_201650.1	CD	C50	nucleus	0	no	pl. membrane/nucleus/extra cellular
61	Pyroglutamyl-peptidase I (PGP), putative	LdBPK_341750.1	CF	C15	secreted	0	no	cytoplasm
Clans of Metallopeptidases								
62	Puromycin-sensitive aminopeptidase-like protein	LdBPK_120830.1	MA	M1	ER membrane	0	no	plasma membrane
63	Aminopeptidase-like protein	LdBPK_260290.1	MA	M1	secreted	0	no	plasma membrane
64	Aminopeptidase M1, putative metallo-peptidase	LdBPK_292350.1	MA (E)	M1	ER	0	no	plasma membrane/peroxisome
65	Aminopeptidase, putative	LdBPK_312330.1	MA(E)	M1	cytoplasm	0	no	chloroplast
66	Thimet oligopeptidase, putative	LdBPK_261550.1	MA	M3	cytoplasm	0	no	cytoplasm
67	Mitochondrial intermediate peptidase, putative	LdBPK_364670.1	MA	M3	mitochondria	0	no	cytoplasm/mitochondria/nucleus
68	GP63, leishmanolysin (fragment)	LdBPK_100510.1	MA	M8	secreted	1	no	nucleus/mitochondria
69	GP63, leishmanolysin	LdBPK_100520.1	MA	M8	secreted	0	no	nucleus/extra-cellular
70	GP63-like protein, leishmanolysin-like protein	LdBPK_312040.1	MA	M8	cytoplasm	0	yes VAA-PS 29-30	extra-cellular/plasma membrane
71	Peptidyl dipeptidase, putative	LdBPK_010850.1	MA	M13	cytoplasm	0	no	nucleus/mitochondria
72	Peptidyl-dipeptidase, putative	LdBPK_020710.1	MA	M13	cytoplasm	0	no	cytoplasm
73	Carboxypeptidase, putative	LdBPK_130090.1	MA	M32	cytoplasm	0	no	cytoplasm
74	Carboxypeptidase, putative	LdBPK_140180.1	MA	M32	cytoplasm	0	no	cytoplasm

TH-1832_126106036

75	Carboxypeptidase, putative metallo-peptidase	LdBPK_332670.1	MA (E)	M32	cytoplasm	0	no	cytoplasm
76	Carboxypeptidase, putative	LdBPK_366520.1	MA	M32	cytoplasm	0	no	mitochondria
77	ATP-dependent zinc metallopeptidase, putative	LdBPK_180620.1	MA	M41	mitochondria membrane	1	no	mitochondria/chloroplast
78	ATP-dependent zinc metallopeptidase, putative	LdBPK_310730.1	MA	M41	mitochondria membrane	2	no	mitochondria
79	ATP-dependent zinc metallopeptidase, putative	LdBPK_321570.1	MA	M41	mitochondrial membrane	1	no	mitochondria/cytoplasm/nucleus
80	Mitochondrial ATP-dependent zinc metallopeptidase, putative	LdBPK_341130.1	MA(E)	M41	nucleus	2	no	mitochondria
81	Mitochondrial ATP-dependent zinc metallopeptidase, putative	LdBPK_362850.1	MA(E)	M41	mitochondria membrane	1	no	cytoplasm/chloroplast
82	CAAX prenyl protease 1, putative	LdBPK_270040.1	MA	M48	ER membrane	3	no	plasma membrane
83	Dipeptidyl-peptidase III, putative	LdBPK_050960.1	MA	M49	cytoplasm	0	no	cytoplasm/peroxisome
84	Metalloprotease-like protein, putative	LdBPK_040820.1	MA	M67	mitochondria	0	no	Mito
85	Zinc carboxypeptidase, putative	LdBPK_342670.1	MC	M14	cytoplasm	0	no	plasma membrane/nuclear
86	Zinc carboxypeptidase, putative metallo-peptidase	LdBPK_364230.1	MC	M14	cytoplasm	0	no	nucleus
87	Metallo-peptidase, putative	LdBPK_330210.1	MC	M14	cytoplasm	0	no	plasma membrane
88	Metallo-peptidase, Mitochondrial-processing peptidase subunit beta, putative	LdBPK_010670.1	ME	M16	mitochondria	0	no	mitochondria
89	Pitrilysin-like metalloprotease	LdBPK_070250.1	ME	M16	mitochondria	0	no	nuclear
90	mitochondrial processing peptidase alpha subunit, putative	LdBPK_332750.1	ME	M16	mitochondria	0	no	mitochondria
91	Metallopeptidase, mitochondrial processing peptidase beta subunit,	LdBPK_351390.1	ME	M16	mitochondria	0	no	mitochondria

TH-1832_126106036

	putative							
92	mitochondrial processing peptidase alpha subunit, putative	LdBPK_130760.1	ME	M16	mitochondria	0	no	mitochondria
93	Aminopeptidase, putative (fragment) metallopeptidase	LdBPK_110640.1	MF	M17	cytoplasm	0	no	chloroplast
94	Aminopeptidase, putative	LdBPK_190150.1	MF	M17	cytoplasm	0	no	cytoplasm
95	Cytosolic leucyl aminopeptidase	LdBPK_231120.1	MF	M17	cytoplasm	0	no	mitochondria
96	Aminopeptidase, putative (fragment) metallo-peptidase,	LdBPK_110630.1	MF	M17	cytoplasm	0	no	cytoplasm
97	Aminopeptidase, putative	LdBPK_332700.1	MF	M17	mitochondria	0	no	chloroplast
98	Metallo-peptidase (methionine aminopeptidase, putative)	LdBPK_190150.1	MG	M24	cytoplasm	0	no	cytoplasm
99	methionine aminopeptidase, putative	LdBPK_190540.1	MG	M24	cytoplasm	0	no	cytoplasm
100	methionine aminopeptidase 2, putative	LdBPK_210960.1	MG	M24	cytoplasm	0	no	cytoplasm
101	Aminopeptidase P1, putative	LdBPK_020010.1	MG	M24	secreted	0	no	mitochondria/chloroplast/nucleus
102	Aminopeptidase P1, putative	LdBPK_252540.1	MG	M24	cytoplasm	0	no	chlroplast/nucleus/mitochondria
103	Aminopeptidase P, putative	LdBPK_352400.1	MG	M24	mitochondria	0	no	cytoplasm
104	Aminopeptidase P1, putative	LdBPK_365800.1	MG	M24	mitochondria	0	no	plasma membrane/mitochondria
105	Aspartyl aminopeptidase, putative	LdBPK_292470.1	MH	M18	cytoplasm	0	no	cytoplasm
106	Peptidase t, putative	LdBPK_170250.1	MH	M20	cytoplasm	0	no	cytoplasm
107	Glutamyl carboxypeptidase, putative	LdBPK_291680.1	MH	M20	cytoplasm	0	no	cytoplasm/chloroplast
108	ATP-dependent zinc metallopeptidase, putative	LdBPK_191620.1	MH	M41	mitochondria membrane	1	no	cytoplasm/mitochondria
109	O-sialoglycoprotein endopeptidase, putative	LdBPK_310110.1	MK	M67	mitochondria	0	no	cytoplasm
110	Proteasome regulatory non-	LdBPK_340670.1	MP	M67	nucleus	0	no	mitochondria/cytopla

TH-1832_126106036

	ATPase subunit 11, putative							sm
111	Glutaminyl cyclase, putative	LdBPK_050950.1	M-	M28	secreted	1	no	mitochondria
112	Cytosolic nonspecific dipeptidase, putative	LdBPK_331710.1	M-	M20/M25/ M40	cytoplasm	0	no	cytoplasm
113	CAAX prenyl protease 2, putative	LdBPK_262720.1	M-	U48	ER membrane	2	no	plasma membrane
Clans of Serine peptidases								
114	Serine peptidase, Membrane-bound transcription factor site-1 protease, putative subtilisin-like serine peptidase	LdBPK_130940.1	SB	S8	cytoplasm	2	yes 28&29 PLA-EG	nuclear/plasma membrane
115	Subtilisin-like serine peptidase	LdBPK_282540.1	SC	S8	secreted	13	no	plasma membrane
116	Oligopeptidase B-like protein	LdBPK_060340.1	SC	S9	cytoplasm	0	no	cytoplasm
117	Oligopeptidase B Serine peptidase, putative	LdBPK_090820.1	SC	S9	cytoplasm	0	no	cytoplasm
118	Dipeptidyl-peptidase 8-like serine peptidase serine peptidase,	LdBPK_362550.1	SC	S9	cytoplasm	0	no	plasma membrane
119	Prolyl oligopeptidase, putative	LdBPK_367060.1	SC	S9	cytoplasm	0	no	cytoplasm
120	Serine carboxypeptidase (CBP1), putative	LdBPK_180450.1	SC	S10	vacuole	1	yes VYA-ST 29-30	lysosome
121	Serine peptidase, putative	LdBPK_120920.1	SC	S10	secreted	0	no	plasma membrane
122	Serine peptidase, putative	LdBPK_330410.1	SC	S10	cytoplasm	0	no	mitochondria
123	Bem46-like serine peptidase	LdBPK_354070.1	SC	S10	ER membrane	1	no	plasma membrane
124	X-pro, dipeptidyl-peptidase,serine peptidase, Clan SC, family S15, putative	LdBPK_282080.1	SC	S15	cytoplasm	0	no	extra cellular/lysosome
125	Signal peptidase type I, putative	LdBPK_080460.1	SF	S26	endoplasmic reticulum membrane	0	no	plasma membrane
126	Mitochondrial inner membrane signal peptidase, putative	LdBPK_360220.1	SF	S26	Mito memb	0	no	extra-cellular
127	Rhomboid-like protein	LdBPK_040850.1	S-	S54	golgi apparatus membrane	4	no	plasma membrane

TH-1832_126106036

128	Rhomboid-like protein	LdBPK_020400.1	S-	S54	secreted	2	yes SSG-RW 27-28	plasma membrane
Clans of Threonine peptidases								
129	Proteasome beta 6 subunit, putative	LdBPK_060140.1	PB	T1	cytoplasm	0	no	cytoplasm/nuclear
130	Proteasome alpha 7 subunit, putative	LdBPK_110240.1	PB	T1	nucleus	0	no	cytoplasm
131	Proteasome beta-1 subunit, putative	LdBPK_120030.1	PB	T1	cytoplasm	0	no	extra-cellular
132	Proteasome alpha 2 subunit, putative	LdBPK_212070.1	PB	T1	nucleus	0	no	cytoplasm/chloroplast
133	Proteasome subunit alpha type-5, putative	LdBPK_212200.1	PB	T1	nucleus	0	no	cytoplasm
134	Proteasome alpha 7 subunit, putative	LdBPK_270190.1	PB	T1	nucleus	0	no	cytoplasm/chloroplast
135	Proteasome beta 3 subunit, putative	LdBPK_280110.1	PB	T1	cytoplasm	0	no	cytoplasm
136	Proteasome beta 2 subunit, putative	LdBPK_353880.1	PB	T1	cytoplasm	0	no	cytoplasm
137	20S proteasome subunit proteasome subunit beta type-2, putative	LdBPK_360340.1	PB	T1	cytoplasm	0	no	extra-cellular
138	20s proteasome subunit, putative proteasome subunit alpha type-1, putative	LdBPK_361670.1	PB	T1	nucleus	0	no	cytoplasm
139	Proteasome subunit beta type-5, putative	LdBPK_361730.1	PB	T1	cytoplasm	0	no	extra-cellular
140	Proteasome alpha 3 subunit, putative	LdBPK_140310.1	PB	T1	nucleus	0	no	cytoplasm
141	Proteasome alpha 1 subunit, putative	LdBPK_354910.1	PB	T1	nucleus	0	no	cytoplasm/chloroplast/mitochondrial

TH-1832_126106036

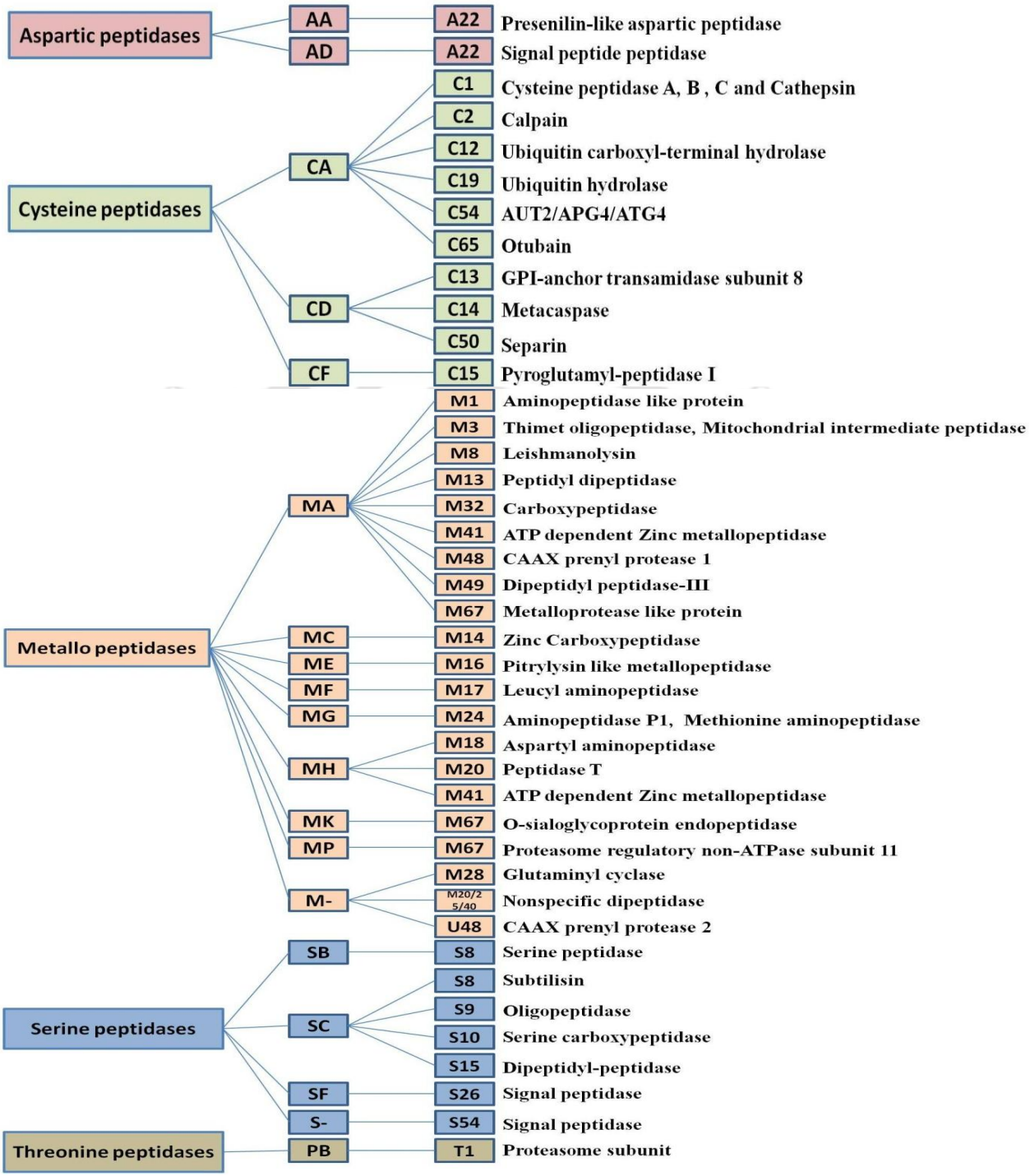

Figure 2.1: All *L. donovani* peptidases are classified in their respective clan and family. Nomenclature of estimated peptidases is done on the basis of MEROPS database, SVMProt, ProtoNet and SUPERFAMILY. Examples of each clan and family are also shown.

TH-1832_126106036

2.4.2 Sub-cellular localization: Function of proteins is mainly related to its sub-cellular localization. It is important to predict the sub-cellular localization to get the insight of protein. For membrane topology prediction, TMHMM server is run which is based on hidden Markov model (HMM). Statistical reports suggest that accuracy of TMHMM is 84% for prediction of transmembrane helices but it drops when signal peptide sequences are present. Moreover, TMHMM can differentiate between soluble and membrane protein with sensitivity and specificity greater than 99 % (Krogh et al., 2001). To check whether presence of signal peptides in amino acid sequences, SignalP 4.1 server are used which predicts signal peptide/non signal peptide using a combination of several artificial neural networks *(Emanuelsson et al., 2007).* Out of total 141 predicted *L. donovani* peptidases, 24 peptidases having trans-membrane helices and 8 peptidases having signal peptide sequences which counts for 23 % of total peptidases. Results of TMHMM and Signal P prediction are shown in Figure 2.2A and Table 4. If experimental data of sub-cellular localization are not available, LocTree3 server and CELLO are used to predict the localization. In eukaryotes, LocTree3 can predict 18 classes of sub-cellular localization with overall accuracy of 80 % whereas; its accuracy for extracellular protein and nuclear protein is 88 % and 81 %, respectively. LocTree3 mainly uses homology based localization annotation using PSI-BLAST, UniProt, PDB and SWISS-PROT databases. In addition to homology based annotation, it also utilizes support vector machine system. The result displayed by LocTree3 prediction shows a score ranging between 0-100 in which 100 is the most reliable prediction. Moreover, the result also shows the expected accuracy in percentage, predicted single localization class, gene ontology terms and type of annotation used *(Goldberg et al., 2014).* In our studies, the threshold set for predicted accuracy was > 80 % and prediction score was >80 on 0 - 100 scale. Based on the result of LocTree3 prediction, the maximum percentage of peptidases present in cytoplasm is 60 % followed by nuclear fraction 19 %, secreted 15 %, mitochondria 8 %, mitochondrial membrane 4 %, endoplasmic reticulum membrane 6 %, endoplasmic reticulum 4 %, vacuole and Golgi apparatus membrane fraction accounts for 1 % of peptidases. The result of LocTree3 prediction is shown in Figure 2.2B. When the sub-cellular localization of peptidases was checked in experimental database *i.e.* BRENDA enzyme database, we observed that many of the peptidases are localized at multiple sub-cellular locations. LocTree3 does not predict the multiple sub-cellular localization of signal peptidase; hence it

TH-1832_126106036

became important to use another sub-cellular localization prediction tools which may predict multiple localization sites with better accuracy. CELLO v 2.5: sub cellular localization predictor server developed by Molecular Bioinformatics Centre, NCTU; uses two level support vector machine systems to predict the sub cellular localization in which the first level contain the support vector machine classifiers whereas second level comprises of probability distribution for possible localizations. Overall accuracy for CELLO prediction is 94.9 % if sequence identity is >30%. In case of sequence identity < 30 %, most of the sub cellular localization predictor tools shows fairly bad result with low accuracy, whereas CELLO predicts the overall accuracy of 82.6 % *(Yu et al., 2006).* The result for CELLO prediction is shown in Figure 2.2C.

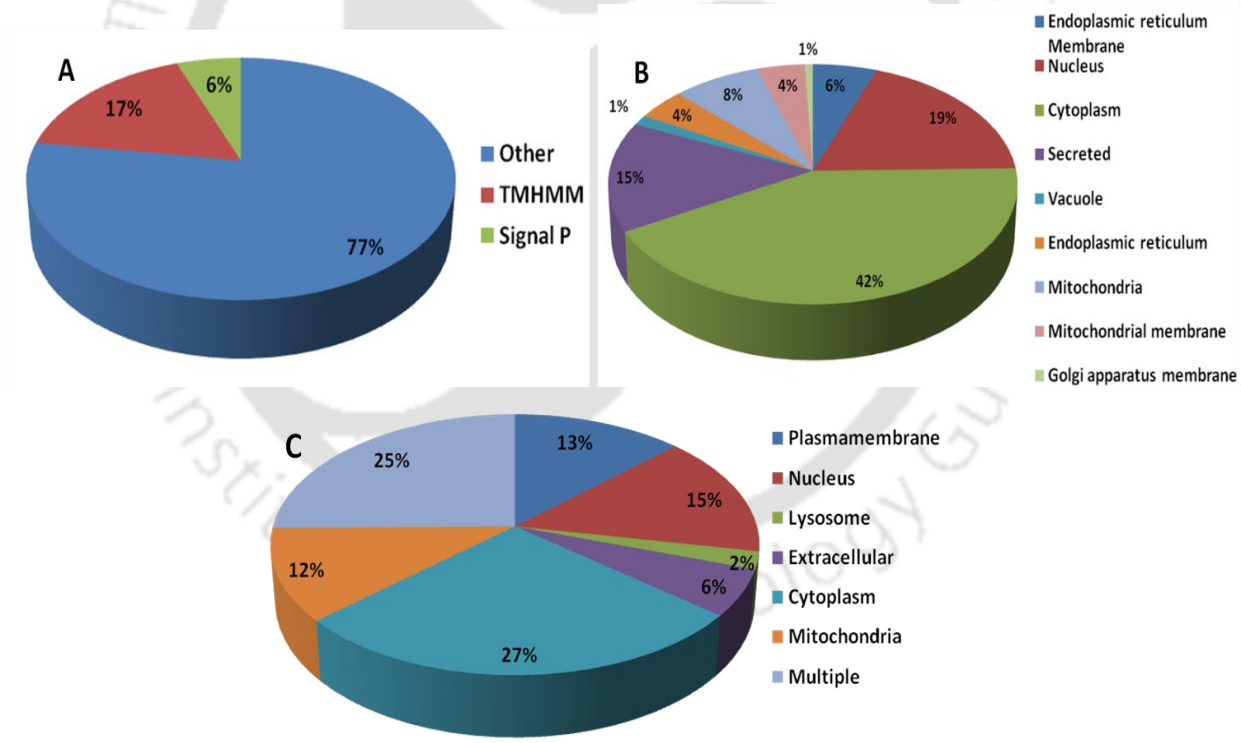

Figure 2.2: Subcellular localization of 141 peptidases of *L.donovani* utilizing the prediction result of various bioinformatics tools. The chart shows the (A) transmembrane helices and secretory peptides predicted by TMHMM and SignalP server. (B) subcellular localization prediction by LocTree3 server. (C) subcellular localization prediction by CELLOv2.0 server.

TH-1832_126106036

2.4.3 Apoptosis detection: *L. donovani* promastigotes cells treated with 50 µM of miltefosine for 24 hr were stained with Annexin V-FITC and PI, and data were analyzed by flow cytometry. As also reported in literature *(Paris et al., 2004; Verma and Dey, 2004)*, the condition provided us significant fraction of parasite in apoptotic condition as shown in Figure 2.3. The parasite after treatment with miltefosine as mentioned earlier was used for analysis of protease genes in apoptotic conditions.

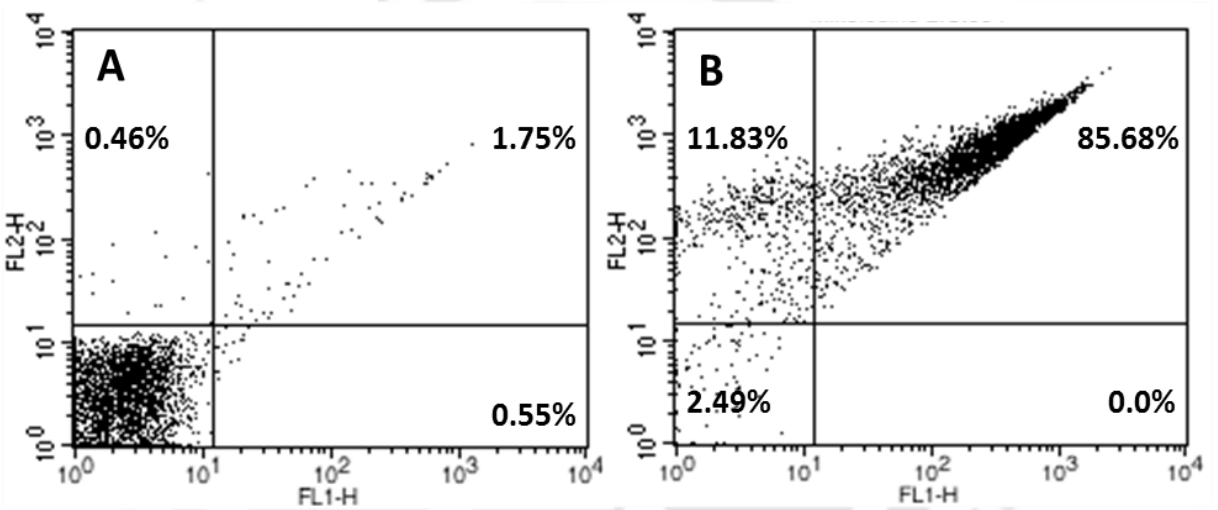

Figure 2.3: Externalization of phosphatidyl serine on plasma membrane analyzed by Annexin V-FITC and PI staining. Apoptotic cells are Annexin V positive, whereas necrotic cells are PI positive, FL1 represents green channel whereas FL2 represents red channel. (A) Control promastigotes treated with 0.2 % DMSO. (B) Promastigotes treated with 50 µM of miltefosine for 24 hrs. After treatment with miltefosine for 24 hrs, 85.68 % cells were in late apoptotic stage and 11.83 % cells were in necrotic stage. Data are representative image of three independent experiments.

2.4.4 Expression analysis of L. donovani protease genes by Real time-qPCR: In an initial attempt to identify the involvement of various peptidases in apoptotic cell death (Program Cell Death) pathway of parasite, the mRNA level of 24 protease genes of *L. donovani* was analyzed by Real time-qPCR in control cells and apoptotic cells under miltefosine treated. Alpha tubulin was used as an endogenous control. Minimum one peptidase was preferred from each clan and primer was designed for respective peptidase gene of *L. donovani* to

TH-1832_126106036

compare the mRNA level in control and treated cells. Our gene expression analysis of *Leishmania* peptidases in apoptotic condition shows altered expression of several proteases hinting involvement of these peptidases in the process, directly or indirectly. The results of m-RNA expression analysis are shown in Figure 2.4 and Figure 2.5. The previous report has shown that the activities of metacaspases are increased in H_2O_2 induced apoptosis of parasite *(Lee et al., 2007).* In our studies, we have also reported that the mRNA expression level of metacaspases is increased by two fold in treated cells. Moreover, the mRNA expression level of other cysteine peptidases involved in autophagy processes of parasite is increased more than metacaspases. Two cysteine peptidases namely ATG4.1 and ATG4.2 are reported in the autophagic processes of parasite in which ATG4.2 is more important than ATG4.1 (*Besteiro et al., 2006).* Multiple orthologues of single ATG4 are reported in case of mammals. Orthologues of ATG4 in mammals, mainly ATG4D is involved in apoptotic processes and mitophagy *(Betin and Lane, 2009a; Betin and Lane, 2009b).* As increased mRNA expression level of ATG4.1 and ATG4.2 in treated cells suggest that there may be the possible role of ATG4 in apoptotic processes of parasite. In addition to this, expression level of several other peptidases genes are increased many folds indicating that the involvement of peptidases directly or indirectly in apoptosis of parasite. Many of the peptidases, whose mRNA expression level is found to be increased in our data, are predicted by bioinformatics tools to be localized at common sub cellular compartment. There is very high possibility that some of the peptidases which may evolved in such a way to help in PCD processes of parasite, may act as an caspase like activity or act as an effector molecule to activate other peptidases for PCD. As very few experimental data available and limitations of bioinformatics tools, it is difficult to predict the cleavage site position (if present in peptidases) with significant accuracy.

TH-1832_126106036

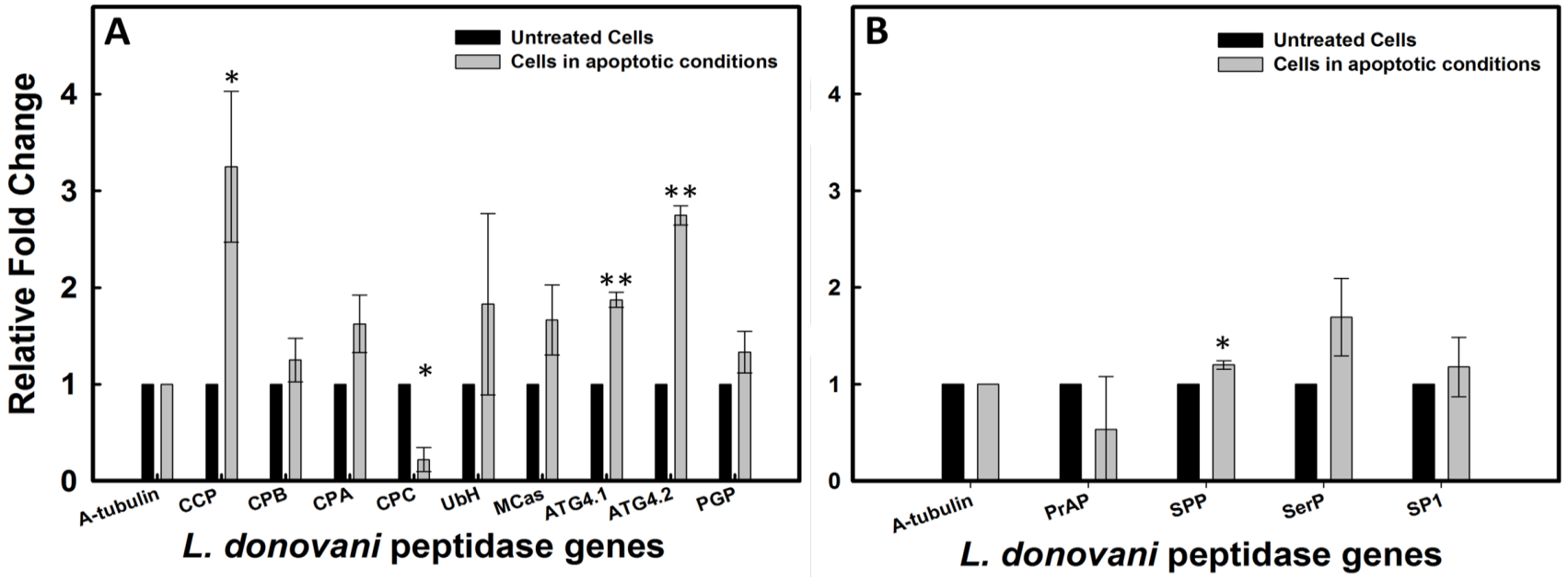

Figure 2.4: Real time-qPCR analysis of various protease genes. Expression level of (A) Cysteine protease and (B) Aspartic protease genes of *L.donovani* in apoptotic conditions. Cells were treated with 50 µM of miltefosine for 24 hrs to induce apoptosis. Equal amount of cDNA was taken for real time-qPCR analysis. Alpha-tubulin was used as an endogenous control. Results are mean ± SD of three independent experiments. Statistical analysis was done using Student's unpaired t-test in SigmaPlot software (*denotes p value ≤ 0.05 and **denotes p value ≤ 0.01). Abbreviations: CCP - Calpain-like cysteine peptidase; CPB - Cysteine peptidase B; CPA- Cysteine peptidase A; CPC - Cysteine peptidase C; UbH- Ubiquitin hydrolase; MCas- Metacaspase; ATG4.1-AUT2/APG4/ATG4 cysteine peptidase; ATG4.2 AUT2/APG4/ATG4 cysteine peptidase; PGP - Pyroglutamyl-peptidase; PrAP – Presenilin like aminopeptidase; SPP - Signal peptide peptidase; SerP- Serine peptidase; SP1 - Signal peptidase type I; PAP – Puromycin sensitive aminopeptidase.

TH-1832_126106036

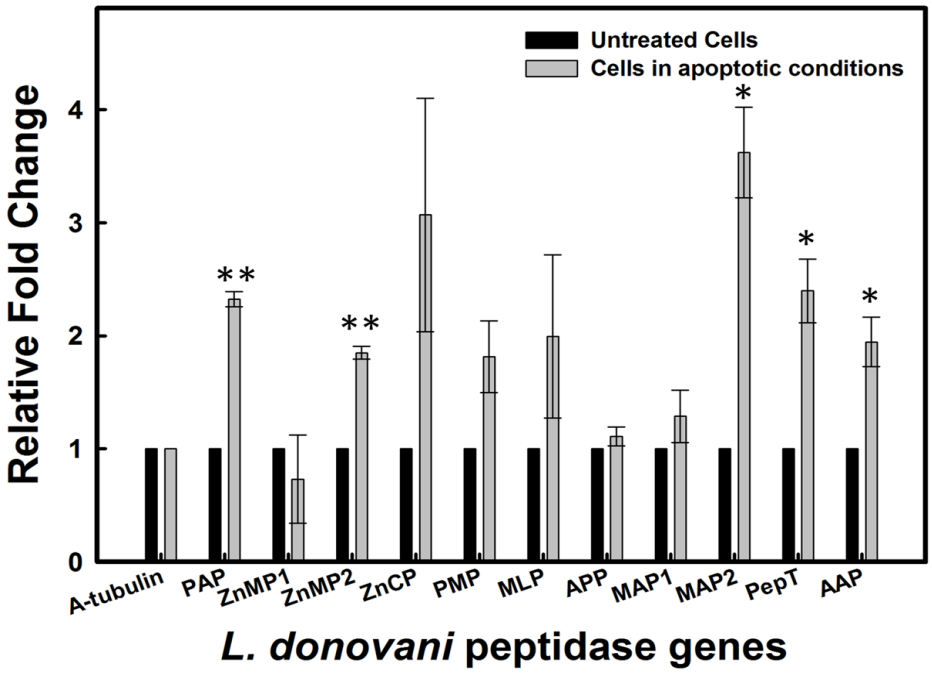

Figure 2.5: Expression level of Metalloprotease genes of *L. donovani* in apoptotic conditions. Cells were treated with 50 µM of miltefosine for 24 hrs to induce apoptosis. Equal amount of cDNA was taken for real time-qPCR anlaysis. Results are mean ± SD of three independent experiments. Statistical analysis was done using Student's unpaired t-test in SigmaPlot software (*denotes p value ≤ 0.05 and **denotes p value ≤ 0.01). Abbreviations: PAP – Puromycin sensitive aminopeptidase; ZnMP1 - Mitochondrial ATP-dependent zinc metallopeptidase; ZnMP2- ATP-dependent zinc metallopeptidase, putative; ZnCP- Zinc carboxypeptidase; PMP- Pitrilysin-like metalloprotease; MLP- Metalloprotease like protein; APP - Aminopeptidase P; MAP1 - Methionine aminopeptidase; MAP2 - Methionine aminopeptidase 2; PepT- Peptidase t; AAP – Aspartylaminopeptidase

2.4.5 Prediction of BH3-like domain and Caspase 3 cleavage site: BH3-like domain is known as pro-apoptotic protein which binds to the hydrophobic pocket of multi domain Bcl-2 family, a well-known anti-apoptotic protein and triggers apoptosis via caspase mediated pathway *(Betin et al., 2012).* As BH3 – like domain having low conservation and shorter peptide length, it is difficult to annotate this domain by common bioinformatics tools. Several studies have reported that human ATG4D (hATG4D) contains Caspase-3 cleavage site on its N-terminal and BH3-domain like protein on its C-terminal whereas BH3 – domain like protein contains conserved LXXXXD region *(Broustas et al., 2004; Betin et al., 2012; Day et al., 2008).* The amino acid sequences of ATG4.1 protease of *L. donovani* was physically verified and run the ESPript 3.o with already known BH3-domain like protein whose results are shown in Figure 2.6. All protein sequences were retrieved from Uniprot

TH-1832_126106036

database and accession numbers are written in the legend of Figure 2.6. The highly conserved region LXXXXD was observed in *L. donovani* ATG4.1 protease using ESPript 3.o alignment. Based on this result, we have proposed the presence of BH3-domain like protein in *L. donovani* ATG4.1 protease. Moreover, Caspase 3 cleavage site DEVD*T are also identified at C-terminus of *L. donovani* ATG4.1 protease and shown in Figure 2.6.

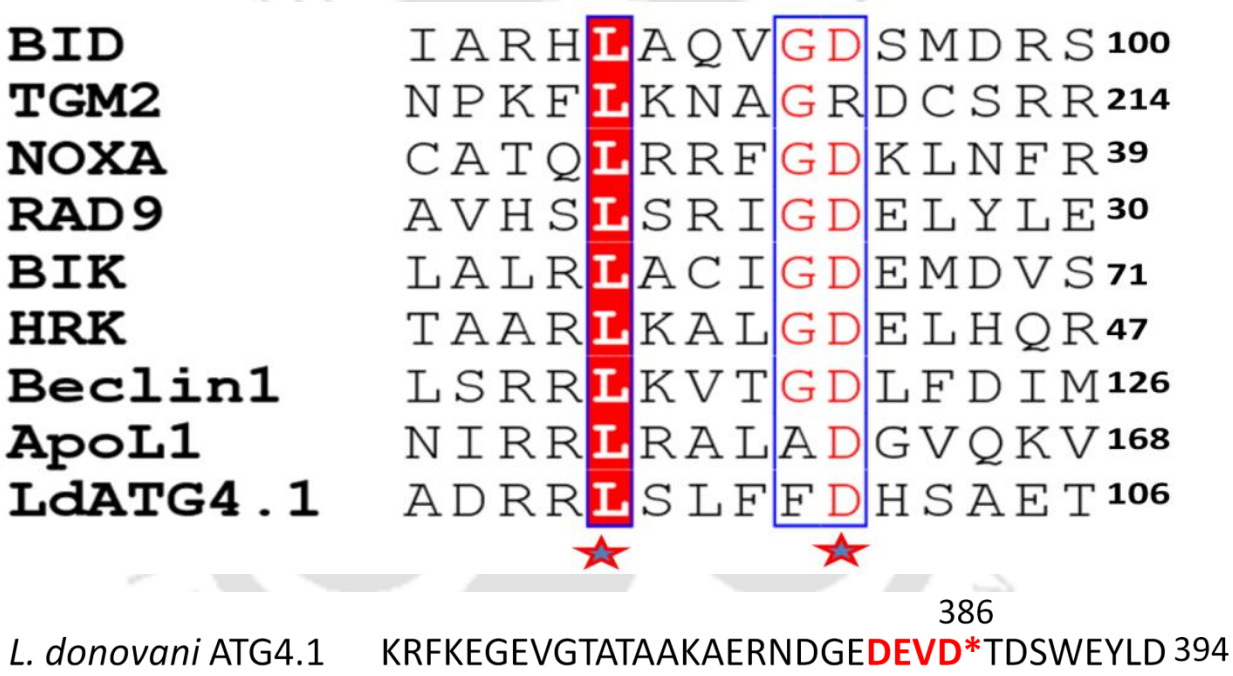

Figure 2.6: Sequence alignment *L. donovani* ATG4.1 protease with known BH3-like domain protein. C-terminal sequence positions are indicated on right. *in red shows highly conserved LXXXXD region. Known BH3 – like protein and their Uniprot IDs are: BID-55957; TGM2- P21980; NOXA- Q13794; RAD9- Q99638; BIK- Q13323; HRK- O00198; Beclin1- Q14457; ApoL1- O14791. Caspase-3 cleavage sequence of *L. donovani* ATG4.1 protease (GeneDB ID: LdBPK_300270.1) C-terminal sequence position is also shown.

TH-1832_126106036

2.5 Discussion

Mainly five types of peptidases are found in *Leishmania* – Aspartic, Cysteine, Serine, Threonine and Metallo peptidases. In *L. donovani*, two aspartic peptidases are present and their predicted sub-cellular localization is in plasma membrane/endoplasmic reticulum membrane. Sequence homology reveals that these proteases are similar to presenilin like aspartic peptidase (PrAP) and signal peptide peptidase. In humans, PrAP are abundantly present in endoplasmic reticulum and helps in the processing of amyloid precursor protein (APP) *(Xia and Wolfe, 2003).* Moreover, PrAP are also reported to have role in macroautophagy as PrAP gene knockout mice do not show macroautophagic process *(Gamliel et al., 2013).* In our mRNA expression analysis, no significant increase in transcription level of aspartic peptidases was found in apoptotic conditions of parasite. As role of PrAP was reported in macroautophagy, hence it is important to establish the role of *L. donovani* PrAP in autophagic processes and the molecular mechanism behind it.

Classification of peptidases of *L. donovani* revealed that 61 cysteine peptidases are present which are mainly belongs to clan CA. This clan mainly contains cysteine peptidase A, B, C, cathepsins, calpains, Ubiquitin hydrolases and ATG4 peptidases. In addition to this, two more clan of cysteine peptidases are present- Clan CD and CF. Metacaspases, an important peptidase which are initially considered to have caspase like activities in parasite, are important member of clan CD and pyroglutamyl peptidases are member of clan CF. In higher organisms, calpain helps in Ca^{2+} regulated signaling pathway, cell differentiation and apoptotic mediated cell death. It has been reported that Ca^{2+} activates the calpain which in turn cleaves the Bcl2-family protein *i.e.* anti-apoptotic protein eventually increasing the apoptotic cascade *(Sharma and Rohrer, 2004).* Moreover, activation of calpain also requires in macroautophagic process. Activated calpain cleaves ATG5 protein and in turn truncated ATG5 induces the release of cytochrome c from mitochondria leading to apoptotic cell death *(Yousefi et al., 2006).* We have observed that in apoptotic condition, transcription of calpain gene has increased more than three folds compared to control. ATG5 gene (LmjF.30.0980) is present in *L. major* but till now it is not annotated in *L. donovani* genome. Annotation of ATG5 gene in *L. donovani* and experimental validation is crucial to understand the increased transcription level of calpain in autophagy and apoptotic conditions. In addition to this, we

TH-1832_126106036

have observed the increased transcription of Ubiquitin hydrolase gene suggesting higher protein turn over in apoptosis.

Interplay of autophagy and apoptosis has been reported in the literature *(Mariño et al., 2014).* However, most of these studies are reported in higher organism. Existence of autophagy and apoptosis modes of cell death in *Leishmania* is already established *(Williams et al., 2013).* Reports suggesting that protozoan parasites evade host cell defense system using autophagy and has important role in infection process *(Williams et al., 2013; Picazarri et al., 2008; Romano et al., 2008; Pinheiro et al., 2009).* However, not much detailed investigation has been done about correlation between apoptosis and autophagy. Over-expression of ATG4.1 and ATG4.2 under apoptotic condition of *Leishmania* parasite points out toward correlation in there two cell death mechanism in the protozoan parasite. ATG4 proteins, cysteine proteases, reported to have important function in autophagy process as they are involved in formation of autophagosomes and their subsequent targeting to lysosomes *(Mitzushima et al., 2011).* Very significant over-expression of ATG4.1 and ATG4.2 under apoptotic condition of Leishmania parasite suggests some correlation between these two processes in protozoan parasites as well. The link between autophagy and apoptosis is poorly understood and remains matter of controversy (*Gump et al., 2011; Yonekawa and Thorburn, 2013).* Some proteins are involved in both the processes and the cross talk between autophagy and apoptosis needs further extensive investigation.

Two ATG4 cysteine proteases namely ATG4.1 and ATG4.2 of clan CA, family C54 are present in *L. donovani* and their role in macroautophagy is well documented in *L. major (Williams et al., 2013).* In case of mammals, four orthologs of ATG4 (ATG4A-D) proteases are present, having various roles in autophagosome formation (Mariño et al., 2014). Human ATG4D (hATG4D) is reported to have distinct role in mitophagy and apoptosis [29]. It contains Caspase 3 cleavage site DEVD*K at position 63 from N-terminus [29]. After cleavage by Caspase 3, hATG4D localizes to mitochondria where it increases the permeabilization of outer mitochondrial membrane which leads to release of pro apoptotic factor from mitochondria and eventually induction of apoptosis *(Boya et al., 2003; Betin et al., 2012).* BH3-like domain present at the C-terminus of hATG4D which are exposed after proteolysis by Caspase-3. These are known to bind with Bcl2-family, an anti-apoptotic protein. Binding of BH3-like domains to Bcl2-family inhibits their binding with pro

TH-1832_126106036

apoptotic proteins and thus induces apoptosis *(Maiuri et al., 2007).* Moreover, during oxidative stress, ATG4D also involves in mitophagy (selective removal of damaged mitochondria) and decreases the release of pro apoptotic factors eventually limit the apoptosis *(Betin and Lane. 2009a; Betin and Lane. 2009b; Betin et al., 2012).* Interestingly, we have observed that *L. donovani* ATG4.1 protease also contains Caspase 3 cleavage site DEVD*T at position 386 of C-terminus but till now no Caspase 3 gene is identified in parasite. So it remains elusive to know the importance of Caspase 3 cleavage site in ATG4.1 proteases of parasite. We have also reported the presence of BH3-like domain at N-terminus of ATG4.1 protease. Several reports have suggested that after induction of apoptotic condition, cell lysates of parasite is able to cleave caspase3/7 substrates *(Saudagar and Dubey, 2014; Saudagar et al., 2013).* So, there may be possibility that some of the proteases which are cleaving caspase 3 substrates; may cleave ATG4.1 at DEVD*T site and after cleavage it may expose proposed BH3-like domain to mitochondria and increases the apoptotic demise. Experimental studies are important to validate the significance of BH3-like domain present at the N-terminus of ATG4.1 protease. In our mRNA expression data, we have found increased transcription of ATG4 gene in apoptotic conditions suggesting its role in generation of apoptotic proteins from mitochondria or increasing permeability of outer mitochondrial membrane and escalating PCD.

Eight clans of metallo-peptidases are identified in *L. donovani* and mainly consist of aminopeptidases, leishmanolysin, carboxypeptidases and dipeptidases. We have reported the increased transcription level of AAP, PepT, MLP, ZnMP2, PAP in apoptotic conditions by >2 times and in MAP2, ZnCP by >3.5 times. Some of the metallo-peptidases like PMP, APP and MAP1 do not show any significant altered expression level in our experiment. Very few of the metallo-peptidases are characterized in *Leishmania*. So, detailed experimental analysis is required to understand the role of metallo-peptidases in PCD of parasite.

Total 15 Serine peptidases are identified in *L. donovani*, belongs to clan SB, SC and SF. Several studies have reported that Serine peptidases are involved in host cell invasion *(Burleigh et al., 2002; da Silva-Lopez et al., 2004).* In plasmodium, serine peptidases are involved in proteolytic cleavage of proteins present in cytoplasmic membrane of RBC thereby allowing the parasite to infect the host *(Braun and Pereira, 1993).* In trypanosomes, oligopeptidase B, a serine protease belong to clan SC helps in the invasion of parasite to

TH-1832_126106036

mammalian host *(Williams et al., 2013).* Real time-qPCR data of our experiment reveals that no significant altered expression level of SP1 gene in apoptotic condition while there is increased transcription level in SerP gene of *L. donovani.* Various studies have suggested the role of non caspase proteases which includes metacaspases, calpains, cathepsins etc in PCD of parasite. Based on that, it is essential to recognize the non caspase proteases and establish the molecular mechanism of apoptosis in parasite.

We have earlier reported studies on redox metabolism of the parasite *(Saudagar et al., 2013; Saudagar and Dubey, 2014).* We have focused our research on understanding involvement of various *Leishmania* proteases in apoptotic processes. The data shows altered expression of various protease m-RNA in apoptotic condition of *Leishmania*. This indicates possible role of various proteases in apoptotic process, directly or indirectly. Further, the data suggests some crosstalk between autophagy and apoptosis modes of cell death of *Leishmania* parasite.

TH-1832_126106036

Chapter III

Methionine aminopeptidase 2 is a key regulator of apoptotic like cell death in *Leishmania donovani*[*]

3.1 Abstract

The treatment of *L. donovani* promastigote cells with miltefosine induced the over-expression of methionine aminopeptidase 2 (*MAP2)* by 3.5 times compared to control cells as reported in chapter II. This prompted us to investigate the role of methionine aminopeptidase 2 (MAP2) in miltefosine induced programmed cell death (PCD) in promastigote form of *L. donovani*. We report that TNP-470, an inhibitor of MAP2, inhibits programmed cell death in miltefosine treated promastigotes. It inhibits the biochemical features of metazoan apoptosis, including caspase3/7 protease like activity, oligonucleosomal DNA fragmentation, collapse of mitochondrial transmembrane potential, and increase in cytosolic pool of calcium ions but did not prevent the cell death and phosphatidyl serine externalization. The data suggests that the MAP2 is involved in the regulation of PCD in parasite. Moreover, TNP-470 shows the leishmanicidal activity (IC_{50} =15 µM) and *in vitro* inhibition of *Ld*MAP2 activity (K_i =13.5 nM). Further studies on MAP2 and identification of death signaling pathways provide valuable information that could be exploited to understand the role of non caspase proteases in PCD of *L. donovani.*

***Part of this work is published in *Scientific Reports*, 2017;7:95**

TH-1832_126106036

3.2 Introduction

Apoptotic like cell death in *Leishmania* and other unicellular organisms after drug treatment or under stress conditions is well characterized *(Das et al., 2001; Zangger et al., 2002; Das et al., 2008; Saudagar et al., 2013; Saudagar and Dubey, 2014)*. The major biochemical features of apoptosis include the proteolytic activation of caspase3/7 like proteases *(Hengartner, 2000; Thornberry and Lazebnik, 1998)*, permeabilization of mitochondrial membrane resulting in changes in transmembrane potential, release of cytochrome C from mitochondria *(Zamzami and Kroemer, 2001)*, oligonucleosomal DNA fragmentation *(Nagata, 2000)* and increase in Annexin-V positive cells *(Savill and Fadok, 2000)*. *Leishmania* parasite shows all these characteristics under apoptotic conditions *(Das et al., 2008; Saudagar et al., 2013; Saudagar and Dubey, 2014).* Caspase3/7 protease like activities associated with apoptotic cell death in *Leishmania* is also very well documented *(Zangger et al., 2002; Das et al., 2008; Saudagar et al., 2013; Saudagar and Dubey, 2014)*. However, no caspase gene or caspase homologue has been identified in *Leishmania* genome *(Downing et al., 2011).* The genes encoding metacaspases which belongs to an ancestral matacaspase, paracaspase and caspase superfamily have been identified in several lower eukaryotes including *Leishmania (Downing et al., 2011; Uren et al., 2000; Aravind et al., 2001)*. Very few reports have been published on the role of metacaspases in programmed cell death (PCD) in *Leishmania*. There are certain reports that point towards the role of metacaspases in the regulation of apoptotic like cell death in *L. major (Lee et al., 2007; González et al., 2007; Castanys-Muñoz et al., 2012).* A detailed biochemical characterization of metacaspases in *Trypanosoma* and *Leishmania* signifies that it prefers the substrate specificity with an Arginine and Lysine residue at P1 position and are unable to cleave caspase specific substrates as well as insensitive to caspase specific inhibitors *(Moss et al., 2007; Machado et al., 2013).* Thus, the source of caspase like activity in apoptotic stage *L. donovani* promastigotes cell lysates remains elusive. Further, role of other proteases in apoptotic like cell death in *Leishmania* is also not yet extensively studied. Miltefosine, the only available oral drug against the parasite, is known to induce apoptosis in *L. donovani* promastigotes *(Zuo et al., 2011).* The treatment of *L. donovani* promastigote cells with miltefosine induced the over-expression of methionine aminopeptidase 2 (*MAP2)* by 3.5 times compared to control cells (*Kumar et al., 2016).* This finding suggests the involvement

TH-1832_126106036

of MAP2 in apoptosis like cell death of the parasite and prompted us to study the role of MAP2 in the apoptotic processes of *Leishmania* parasite.

Methionine aminopeptidase (MAP) catalyzes the removal of N-terminal methionine residue during translation of protein *(Bradshaw et al., 1998).* Removal of methionine residue from newly synthesized protein is important for proper translocation of protein. Two types of methionine aminopeptidases are reported in eukaryotes, methionine aminopeptidase 1 (MAP1) and methionine aminopeptidase 2 (MAP2). MAP2 is also involved in the protection of eukaryotic initiation factor 2 alpha (eIF2-α) from inhibitory *phosphorylation (Datta, 2000; Datta et al., 2001; Datta et al., 2003a; Datta et al., 2003b)*. Several publications have suggested the role of MAP2 in the angiogenesis *i.e.* the formation of new blood vessels in higher eukaryotes which is necessary for tumor growth and metastasis *(Folkman, 1996; Hanahan and Folkman, 1996).* Increased expression of MAP2 is reported in mesothelioma cells and several other cancer cells *(Catalano et al., 2001).* Compounds belonging to fumagillin family are potent inhibitors of angiogenesis, and are reported to bind MAP2 and inhibit its activity *(Ingber et al., 1990).* An analog of fumagillin, TNP-470, is reported to inhibit MAP2 selectively without inhibiting closely related isoenzyme MAP1 (*Turk et al., 1999*). However, the functional role(s) of MAP2 in protozoan parasite *Leishmania* is not very well explored.

In the present study, we cloned, expressed, purified and characterized MAP2. Further, we confirmed inhibition of MAP2 from *L. donovani* (*Ld*MAP2) by TNP-470 and derived biochemical parameters of inhibition. We have successfully demonstrated that a specific MAP2 inhibitor prevents miltefosine induced apoptotic features like increased caspase3/7 protease like activity, DNA degradation, disruption in transmembrane potential of mitochondria, and increase in cytosolic calcium.

3.3 Methods

3.3.1 Parasites, cell lines and chemicals: The *Leishmania donovani* (MHOM/IN/2010/BHU1081) strain was generously donated by Prof. Shyam Sundar, Banaras Hindu University. TNP-470 was obtained from Sigma. Caspase 3/7 Assay kit was procured from Promega. Annexin V-FITC Apoptosis detection kit and MitoCapture™

TH-1832_126106036

Apoptosis detection kit was purchased from Calbiochem. *E. coli* strain DH5α, BL21 (DE3) and restriction enzymes were obtained from Life Technologies. All the chemicals used in the experiments were of the highest grade procured from Sigma-Aldrich or Merck.

3.3.2 Parasite culture and Genomic DNA isolation: *Leishmania donovani* promastigotes were grown at 25˚ C in M199 media supplemented with 15 % heat-inactivated fetal bovine serum (FBS) and Penicillin streptomycin (1 %), and Genomic DNA was isolated as reported earlier *(Saudagar et al., 2013; Sambrook et al., 1989).* The lysis buffer contains 10mM Tris-HCl pH 8.0, 100 mM EDTA pH 8.0, 0.5% SDS and 20 µg/ml RNase A. Proteinase K was added at a final concentration of 100 µg/ml.

3.3.3 PCR Amplification of LdMAP2 and construction of expression vector: A putative sequence was identified for *Ld*MAP2 from the GeneDB database with accession number LdBPK_210960.1. The coding region of full length *Ld*MAP2 was amplified from *L. donovoni* genomic DNA by PCR using the forward primer (*Ld*MAP2 F: AA*GAATTC*ATGCCACCAAAGATGTCTGC), containing an *Eco*RI restriction site and start codon, and the reverse primer (*Ld*MAP2 R: AA*CTCGAG*CTAGTAGTCGCTTCCCTTG), containing *Xho*I restriction site and stop codon. The conditions used for PCR are as follows: initial denaturation at 95 ˚C for 5 min, followed by 30 cycles of denaturation at 95 ˚C for 30 s, annealing at 59 ˚C for 1 min, extension at 72 ˚C for 2 min and final extension step at 72 ˚C for 10 min. 1.39 kb fragment was amplified by PCR and amplification was checked on 1% agarose gel stained with approximately 0.5 µg/ml EtBr. Amplified PCR product was purified by QIA quick gel extraction kit (Qiagen, USA) following manufacturer protocols. The purified PCR fragment and pET-28a(+) were digested with *Eco*RI and *Xho*I to generate complementary sticky ends and further ligated with T4 DNA ligase to generate pET-28a-*Ld*MAP2 plasmid. The resultant plasmids were transformed into *E.coli* DH5α competent cells for the amplification of plasmid. The transformed colonies were initially identified by PCR using gene specific primers and restriction digestion reactions. The clones were further confirmed by sequencing.

TH-1832_126106036

3.3.4 Expression and purification of LdMAP2: pET-28a- *Ld*MAP2 construct was transformed into BL21 (DE3) competent *E. coli* expression cells and transformed cells were grown overnight at 37˚C at 180 rpm in Luria Broth (LB) media containing 50 µg/mL kanamycin. The overnight grown culture (1 %) was sub-cultured in 200 ml of LB media containing 50 µg/mL kanamycin at 37˚C and 180 rpm. The absorbance of culture was measured at 600 nm and at absorbance value of 0.6, the culture was cooled to 25 ˚C and 250 µM final concentration of IPTG was added. The bacterial culture was grown for 8 hrs at 25 ˚C, 180 rpm and then the induced culture was harvested by centrifugation at 6000 rpm for 10 min at 4 ˚C. The cell-pellet was re-suspended into 20 mL lysis buffer (50 mM Tris-HCl buffer pH 8.0 containing 250 mM NaCl and 5% glycerol) and further subjected to sonication. After sonication, the cell lysates were centrifuged at 10000 rpm for 20 min at 4 ˚C. The pellet containing inclusion bodies was collected and washed twice with wash buffer-01 (20 mM Tris-HCl, 0.5 M NaCl, 10 mM EDTA, 1% Triton X-100, pH 7.5), wash buffer-02 (20 mM Tris-HCl, 0.5 M NaCl, 10 mM EDTA, 0.1% Triton X-100, pH 7.5) and wash buffer-03 (20 mM Tris-HCl, pH 7.5, 10 mM EDTA, pH 7.5), simultaneously. After washing, the pellet was dissolved in solubilization buffer (20 mM Tris-HCl, 0.5 M NaCl, 8M urea, pH 7.5) at 4˚C by continuous stirring and then centrifuged at 10,000 rpm for 30 min at 4˚C to remove the insoluble traces. The clear supernatant obtained after centrifugation, was filtered by 0.4 µm filter and applied to Nickel-NTA affinity column, pre-equilibrated with equilibration buffer (50mM Tris-HCl buffer pH 8.0 containing 500 mM NaCl, 10mM imidazole and 8 M urea). Then column was further washed by ten column volume of wash buffer (50 mM Tris-HCl buffer pH 8.0 containing 500 mM NaCl, 20 mM imidazole and 8 M urea) to remove unbound contaminants. Bound protein was eluted in 10 ml of elution buffer (50 mM Tris-HCl buffer pH 8.0 containing 500 mM NaCl and 200 mM imidazole and 8M urea). Dialysis of eluted fraction was done against 20 mM Tris-HCl buffer, pH 7.5 containing 200 mM NaCl and size of the recombinant protein was analyzed on 12 % SDS-PAGE.

3.3.5 Refolding of LdMAP2: The dialyzed recombinant protein was subjected to refolding for active conformation. The protein was diluted ten times (50µg protein / ml refolding buffer) followed by drop wise addition of protein in refolding buffer (20 mM Tris-HCl, 300 mM arginine, 20 mM cysteine,150 mM NaCl, 5% (v/v) glycerol, pH 7.5) at 4˚C. The

TH-1832_126106036

solution was left overnight at 4˚C with constant slow stirring *(Singh et al., 2013*). Size of the recombinant protein was analyzed on 12 % SDS-PAGE.

3.3.6 Western blot analysis: Purified recombinant *Ld*MAP2 was run on 12 % SDS-PAGE, and then transferred on Polyvinylidene fluoride (PVDF) membrane. The PVDF membrane was then incubated overnight at 4˚C in 5 % skimmed milk solution for blocking. After that, the membrane was incubated overnight at 4˚C with antibodies against mouse anti-His (1:1000), and further treated with anti-mouse horse radish peroxidase conjugated secondary antibodies (1:1000). The membrane was further subjected to 3,3'-Diaminobenzidine (DAB) and 1 % H_2O_2 for immunodetection *(Krajewski et al., 1996).*

3.3.7 Determination of LdMAP2 enzyme activity: The flurogenic substrate L-Methionine 7-amido-4-methylcoumarin (Met-AMC) was used for enzymatic assay. Met-AMC was dissolved in DMSO at final concentration of 200 mM. The *Ld*MAP2 enzymatic activity was determined by measuring the release of 7-AMC by fluorescence (λ_{Ex} = 360 nm and λ_{Em} = 440 nm) *(Yang et al., 2001; Li et al., 2003). Ld*MAP2 enzymatic assay was carried out at 37 ˚C with 1 ml reaction volume containing 50 mM Tris-HCl pH 7.5, 5 mM $NiSO_4$, 10 µM-150 µM Met-AMC and 15 µg recombinant *Ld*MAP2. The release of 7-AMC was measured after 2 h incubation at 37 ˚C. The *Km* (Michaelis constant) was determined by an end point assay.

3.3.8 Optimum pH and Temperature analysis: Total 1 ml reaction volume with 50 µM Met-AMC as a substrate and 10 µg recombinant *Ld*MAP2 was used to perform optimum pH analysis. The buffer systems used were 50 mM Sodium acetate for pH 4.0 to 5.5, 50 mM Sodium phosphate buffer for pH 6.0 – 6.5 and 50 mM Tris-HCl buffer for pH 7.0 – 11.0. 5 mM $NiSO_4$ was also added in each buffer system. The reaction was incubated at 37 ˚C for 2 h. The amount of released 7-AMC was measured by fluorescence. For optimum temperature studies different sets of temperature (20˚C – 60˚C) were used in 1 ml reaction mixture containing 50 mM Tris-HCl pH 7.5, 5 mM $NiSO_4$, 10 µg recombinant *Ld*MAP2 and 50 µM Met-AMC as a substrate.

TH-1832_126106036

3.3.9 Effect of divalent metal ions on LdMAP2 activity: The flurogenic assay with Met-AMC substrate was used to determine the effect of divalent metal ions on *Ld*MAP2 activity. $NiSO_4$, $NiCl_2$, $CuCl_2$, $CaCl_2$, $MgCl_2$, $ZnCl_2$, $MnCl_2$ and EDTA were added at a final concentration of 5 mM in assay mixture containing 50 mM Tris-HCl pH 7.5, 50 µM Met-AMC and 10 µg recombinant *Ld*MAP2. Assay mixture was incubated at 37˚C for 2 h and released 7-AMC was measured by fluorescence.

3.3.10 LdMAP2 inhibition studies: The known inhibitor of MAP2, TNP-470 was assessed against the recombinant *Ld*MAP2. Single point inhibition assay was carried out in 1 ml reaction volume containing 100 µM inhibitor TNP-470, pre-incubated in 50 mM Tris-HCl buffer pH 7.5, 5 mM $NiSO_4$ for 30 min. Varying concentration of substrate Met-AMC and 15 µg recombinant *Ld*MAP2 was added in pre-incubated reaction mixture and further incubated at 37˚C for 2 h. The data were plotted in double-reciprocal plot to examine the mode of inhibition and to calculate the inhibitory constant (K_i).

3.3.11 In vitro Cell cytotoxicity assay: MTT [3-(4,5-dimethylthiazol-2-yl)-2,5-diphenyltetrazolium bromide] cell proliferation assay was performed as reported earlier with minor modifications *(Mosmann, 1983; Shukla et al., 2012).* Briefly, 2.5 X 10^6 cells/ml logarithmic phase *L. donovani* promastigote were grown in 96 well culture microplate. The cells were treated with various concentrations (0.25 µM – 75 µM) of TNP-470 for 24 h at 25˚C. After incubation, plate was centrifuged to remove the media. 200 µl of MTT (0.5 mg/ml) solution was added to each well and incubated for 4 h at 25˚C. Cells were centrifuged and pellet containing formazan products were dissolved in 100 µl of DMSO. The absorbance was measured with microplate reader (BIOTEK Synergy HT) at 570 nm. The color formed is directly proportional to viable cells. Promastigote cells treated with 0.2 % DMSO were used as a negative control, whereas $2IC_{50}$ value of miltefosine (50 µM) served as positive control. The IC_{50} value of TNP-470 was calculated by plotting percent cell viability vs. concentration.

3.3.12 Determination of caspase-3/7 protease like activity: Intracellular caspase-3/7 like protease activity in *L. donovani* promastigote cells was measured flurometrically using Apo-1 homogenous caspase 3/7 activity assay kit (Promega). The assays were performed

TH-1832_126106036

according to manufacturer's instructions and as reported earlier *(Saudagar et al., 2013).* Briefly, 1 x 10^6 promastigote cells were treated with 20 µM of TNP-470 and incubated for 18 h at 25˚C. 0.2 % DMSO treated promastigotes were taken as negative control, whereas 25 µM of miltefosine treated cells were used as a positive control. The cells were centrifuged at 1000 X g for 5 min. The cell pellets were dissolved in 100 µl of reaction buffer containing caspase substrate Z-DEVD-R110 and incubated in dark at room temperature. The release of R110 was measured by fluorescence at an excitation and emission wavelengths of 485 nm and 530 nm, respectively. In parallel set of reactions, caspase3/7 inhibitor was added in reaction mixture prior to the addition of treated cells.

3.3.13 DNA fragmentation Assay by agarose gel electrophoresis: DNA fragmentation was analyzed by agarose gel electrophoresis of total genomic DNA, which was isolated as reported earlier with minor modifications *(Sambrook et al., 1989; Saudagar and Dubey, 2014).* In brief, 1 x 10^8 *L. donovani* promastigotes were cultured and treated with 20 µM of TNP-470 for 18 h at 25˚C. Cells treated with 0.2 % DMSO were used as a negative control and 25 µM of miltefosine as a positive control. Briefly, cell pellets of 1 x 10^8 promastigotes were lysed in 500 µl of lysis buffer (50 mM Tris-HCl, 10 mM EDTA, 0.5% SDS; pH 7.5) containing proteinase K (100 µg/ml), vortexed and kept overnight to digest at 50 ˚C. RNase A (0.3 mg/ ml) was added and then incubated at 37˚C for 1 h. The lysates were extracted using phenol-chloroform-isoamylalcohol (25:24:1) and centrifuged at 15000 X g for 10 min. The upper aqueous phase was collected, treated with 1/10^{th} volume of 3M sodium acetate and 2 volume of 100 % ethanol overnight at -20˚C. The sample was centrifuged at 15000 X g for 15 min and washed with 500 µl of 70 % ethanol. The DNA pellet was dissolved in TE buffer (10 mM Tris-HCl, 1 mM EDTA; pH 8.0) and quantified spectrophotometrically at 260/280 nm. A total of 10 µg of genomic DNA was run on 1.5 % agarose gel containing ethidium bromide for 2 h at 50 V and visualized under UV illuminator (Bio-Rad).

3.3.14 Flow cytometric analysis of DNA content: Flow cytometric analysis of DNA content was done by the methods described in our earlier publications with minor modifications (*Saudagar et al., 2013).* In brief, 2 x 10^7 *L. donovani* promastigote cells were treated with 20 µM of TNP-470 in presence or absence of miltefosine (25 µM) for 12 hrs at 25˚C. Cells were

TH-1832_126106036

then centrifuged at 1000 X g for 5 min and washed twice with cold PBS to remove the traces of media, fixed in pre chilled 70 % methanol (added drop wise) and incubated overnight at -20˚C. The fixed cells were centrifuged at 3000 X g, washed twice with cold PBS and then treated with RNase A (200 µg/ml) and incubated at 37˚C for 30 min. Cells were then treated with 20 µg/ml of PI (propidium iodide), incubated at room temperature for 30 min in the dark and acquired by CytoFLEX Flow Cytometer-Beckman Coulter, Inc. The percentage of hypodiploidy was calculated by CytExpert software.

3.3.15 Laser Scanning Confocal Microscopy analysis to check the transmembrane potential of mitochondria (ΔΨm): $\Delta\Psi m$ was estimated by using the MitoCapture™ apoptosis detection kit (Calbiochem) according to the earlier reports (*Das et al., 2013).* MitoCapture™ dye aggregates in mitochondria at higher transmembrane potential and give red fluorescence, whereas mitocapture cannot accumulate in mitochondria at lower $\Delta\Psi m$ and remains as monomer in cytosol giving green fluorescence. Briefly, 1 x 10^7 promastigote cells after different treatment were centrifuged at 1000 X g for 5 min, washed twice by PBS and resuspended in 1 ml incubation buffer containing MitoCapture™ dye. The cells were incubated for 30 min at 37 ˚C, washed twice and resuspended into 500 µl of incubation buffer. Stained promastigotes were mounted on a glass slide and were observed by Leica DMi8 Confocal Microscopy under magnification of 63 X (1.4 NA). The fluorescence signal was observed sequentially, exciting first at 488 nm (Ar-Kr laser beam) and then at 543 nm (He-Ne laser beam). The green fluorescence was measured at 488 nm excitation and red fluorescence was monitored at 543 nm.

3.3.16 Detection of phosphatidyl serine exposure on plasma membrane: Analysis of phosphatidyl serine exposure on plasma membrane of promastigote cells was done by using Annexin-V-FITC apoptosis detection kit (Calbiochem) according to our earlier publications *(Das et al., 2013; Singh et al., 2015).* Briefly, 1 x 10^6 untreated or treated cells were centrifuged at 1000 X g for 5 min, washed twice with cold PBS and stained with Annexin-V-FITC and PI as per manufacturer's instructions with minor modifications. Promastigote cells treated with 25 µM of miltefosine for 18 h were used as positive control. The fluorescence

TH-1832_126106036

intensity was detected by FACSCalibur flow cytometer (Becton Dickinson) and analyzed by CellQuest software.

3.3.17 Measurement of intracellular Ca^{2+} concentrations: Changes in intracellular Ca^{2+} concentrations were estimated by fluorescent probe, FURA 2AM as described earlier with minor changes *(Das et al., 2013*). In brief, 1 x 10^6 promastigote cells were treated with 20 µM of TNP-470 and incubated for 18 h at 25 ˚C. 0.2 % DMSO treated promastigotes were taken as negative control, whereas 25 µM of miltefosine treated cells were used as positive control. After incubation, the cells were centrifuged at 1000 X g for 5 min and washed twice with wash buffer (5.5 mM glucose, 116 mM NaCl, 0.8 mM $MgCl_2$, 5.4 mM KCl, and 50 mM MOPS; pH 7.4). The cell pellet was re-suspended into 500 µl of reaction buffer (wash buffer containing 8 mM FURA 2AM and 15% sucrose) and incubated for 6 h at 25 ˚C. Promastigote cells were then centrifuged at 1000 X g for 5 min, washed twice in wash buffer and re-suspended in same buffer. Fluorescence intensity was measured at an excitation and emission wavelength of 340 nm and 510 nm, respectively.

3.4 Results

3.4.1 Cloning of LdMAP2 in pET-28a(+) vector: The genomic DNA of *L. donovani* was amplified using gene specific primers of *Ld*MAP2. The amplified band of 1.39 kb was cloned in pET-28a(+) vector as described in materials and method section. The pET-28a(+)-*Ld*MAP2 construct was confirmed by PCR and restriction digestion. The PCR amplification of 1.39 kb band and release of 1.39 kb band by double digestion with *Eco*RI and *Xho*I, confirmed the insertion of *Ld*MAP2 in pET-28a(+) vector (Figure 3.1). The clone was further confirmed by sequencing using primers for T7 promoter and T7 terminator.

TH-1832_126106036

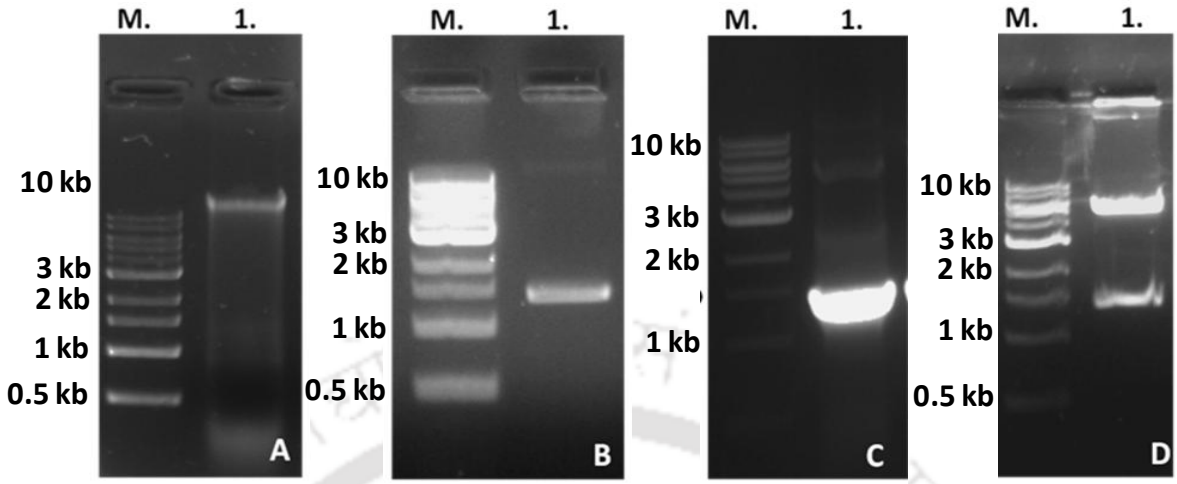

Figure 3.1: Sub cloning of *Ld*MAP2 in expression vector pET-28a(+) and expression in BL21 (DE3) *E. coli*. (**A**) Genomic DNA was isolated from *Leishmania donovani*. (**B**) Lane M. 1 kb DNA ladder, Lane 2. PCR amplification of *Ld*MAP2 from genomic DNA of *L. donovani*. **(C)** Clone confirmation of *Ld*MAP2 in pET-28a(+) by PCR. Lane M: 1 kb DNA ladder, lane 1: positive clones. **(D)** Lane M. 1 kb DNA ladder, lane 1. pET-28a-*Ld*MAP2 construct digested with *Eco*RI and *Xho*I.

3.4.2 Expression and Purification of LdMAP2: The pET-28a(+)-*Ld*MAP2 construct was transformed into BL21 (DE3) expression strain of *E. coli*, induced by 0.25 mM final concentration of IPTG (25˚C, 8 hrs) for the overexpression of protein and produced an insoluble and enzymatically inactive protein in inclusion bodies as shown in Figure 3.2. The recombinant protein from inclusion bodies was solubilized in 8 M urea and purified by Ni-NTA affinity chromatography. The purified protein was dialyzed, refolded using the refolding buffer system as described above, and run on SDS-PAGE gel. Migration of *Ld*MAP2 on SDS-PAGE showed an apparent molecular mass of 55.1 kDa (Figure 3.3A). Western blot analysis using mouse anti-His antibodies recognized the recombinant *Ld*MAP2 containing His-tag at its N-terminal (Figure 3.3B). The approximate yield of recombinant *Ld*MAP2 protein was 5 to 7 mg/L. The proper refolding of protein was checked by enzymatic assay using the substarte Met-AMC. Standard graph was plotted to measure the released 7-AMC after hydrolysis of Met-AMC and data was shown in Figure 3.6.

TH-1832_126106036

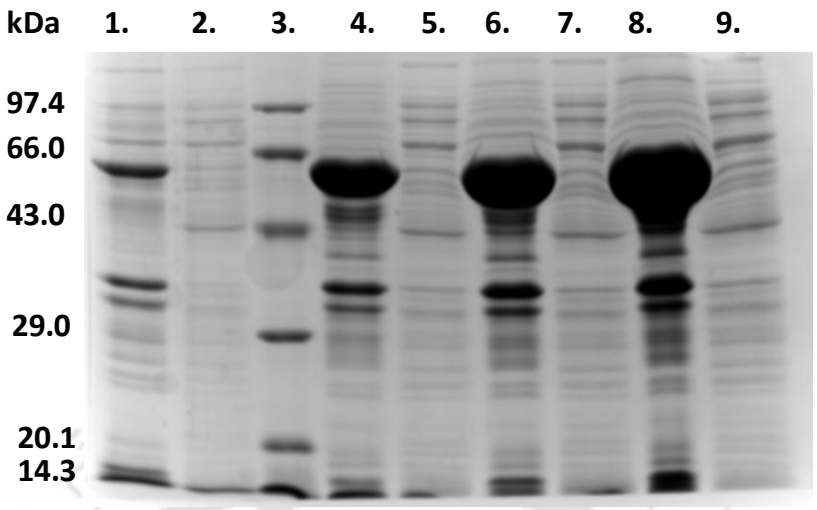

Figure 3.2: SDS-PAGE showing expression of Recombinant *Ld*MAP2; Lane 1. Insoluble fraction of un-induced BL21 (pET-28a-*Ld*MAP2); Lane 2. Soluble fraction of un-induced BL 21 (pET-28a-*Ld*MAP2); Lane 3. Medium Range Protein Marker; Lane 4. Insoluble fraction at 25˚C, 4 hrs; Lane 5. Soluble fraction at 25˚C, 4 hrs; Lane 6: Insoluble fraction at 25˚C, 6 hrs; Lane 7: Soluble fraction at 25˚C, 6 hrs; Lane 8: Insoluble fraction at 25˚C, 8 hrs; Lane 9: Soluble fraction at 25˚C, 8hrs; 0.25 mM IPTG Concentration was used in each experiment to induce the expression of protein.

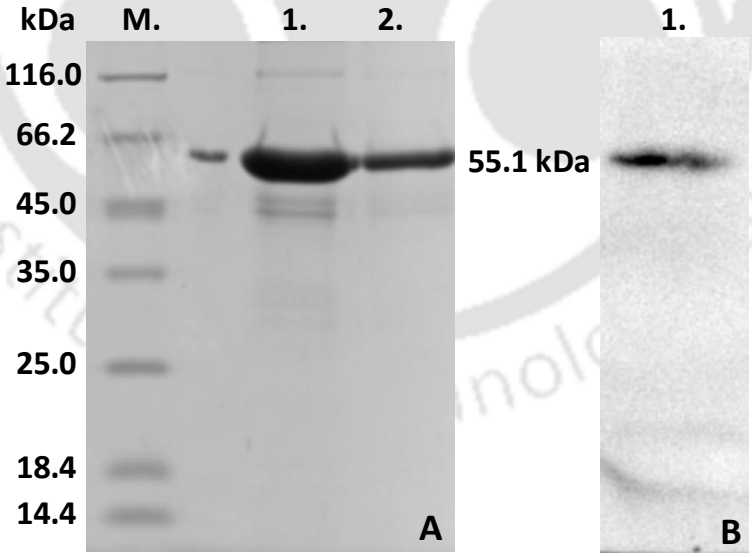

Figure 3.3: Expression of recombinant *Ld*MAP2 in BL21 (DE3) *E. coli*. (A) SDS-PAGE analysis of purified His-tagged r*Ld*MAP2, Lane M. medium range protein marker, lane 1 and 2. *Ld*MAP2 after Ni-NTA affinity purification. (B) Western blot image of Purified His-tagged *Ld*MAP2, mouse anti-His antibodies were used for immunodetection.

TH-1832_126106036

3.4.3 Enzymatic characterization of LdMAP2: The *Ld*MAP2 enzymatic assay was carried out by measuring the release of 7-AMC by fluorescence at an excitation and emission wavelength of 360 nm and 440 nm, respectively. A pH range (pH 4.0 to 10.0) in mixed buffer system as mentioned in method section was used to determine the optimum pH for the enzyme activity against the fluorogenic substrate Methionine-7-amido-4-methyl coumarin (Met-AMC). The temperature range (20°C to 60°C) was used to check the optimum temperature. The pH and temperature optima studies showed an optimum pH of 7.5 and temperature optima at 37°C for the substrate Met-AMC (Figure 3.4). The activity of purified *Ld*MAP2 was reduced to ~5 % after incubating with 5 mM EDTA, signifying that metal ions are required for enzyme activity. The activity was found to be maximum in the presence of Ni(II), followed by Cu(II), Ca(II), Mg(II), Zn(II) and Mn(II). Furthermore, no *Ld*MAP2 activity was observed in the absence of divalent metal ions (Figure 3.5). The enzyme kinetic studies showed the *Km* and *Vmax* values of 0.2 mM and 5.71 nM/min, respectively (Figure 3.7). The *Km* and *Vmax* values were calculated by varying the substrate concentration of Met-AMC (10 µM to 100 µM).

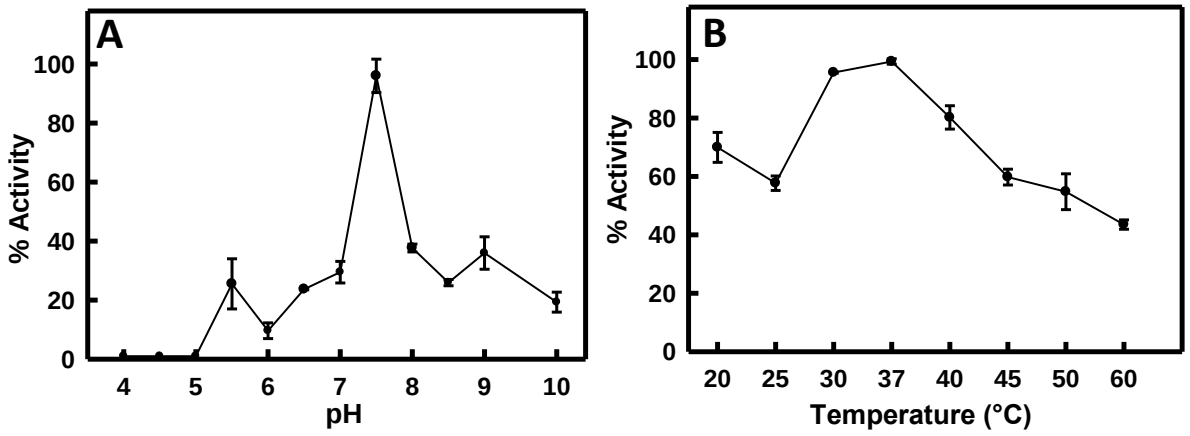

Figure 3.4: pH optima, temperature optima on enzymatic activity of *Ld*MAP2 (A) pH- profile. The pH optima studies giving a pH optimum of 7.5. (B) Optimum temperature studies. Assays were carried out in different temperature conditions ranging from 20- 60˚C. *Ld*MAP2 has an optimum activity at 37˚C. Data represents the mean ± SD of three independent experiments.

TH-1832_126106036

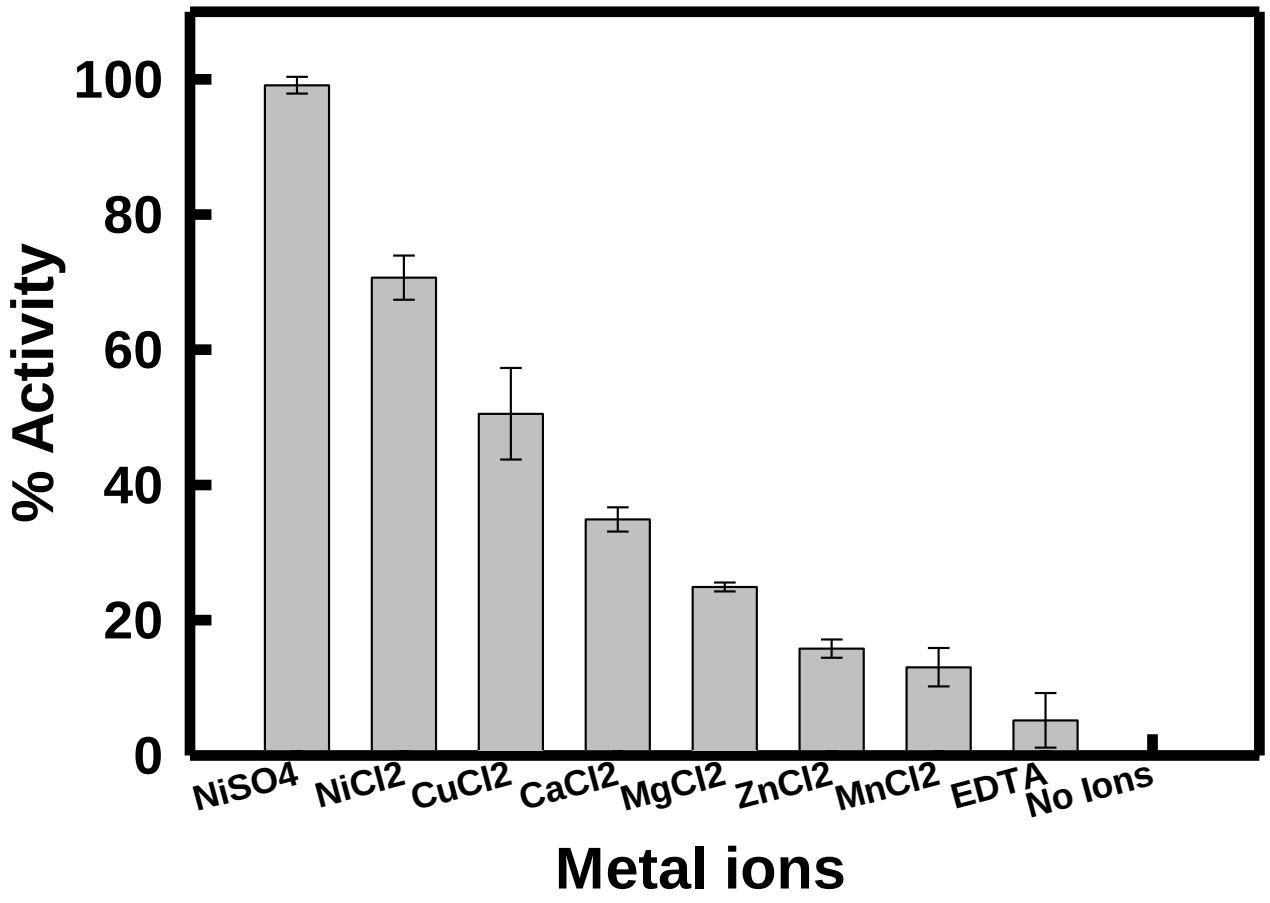

Figure 3.5: Effect of metal ions on enzyme activity of *Ld*MAP2; maximum activity was found in presence of Ni(II) and very less activity was found in presence of EDTA. Data represents the mean ± SD of three independent experiments.

TH-1832_126106036

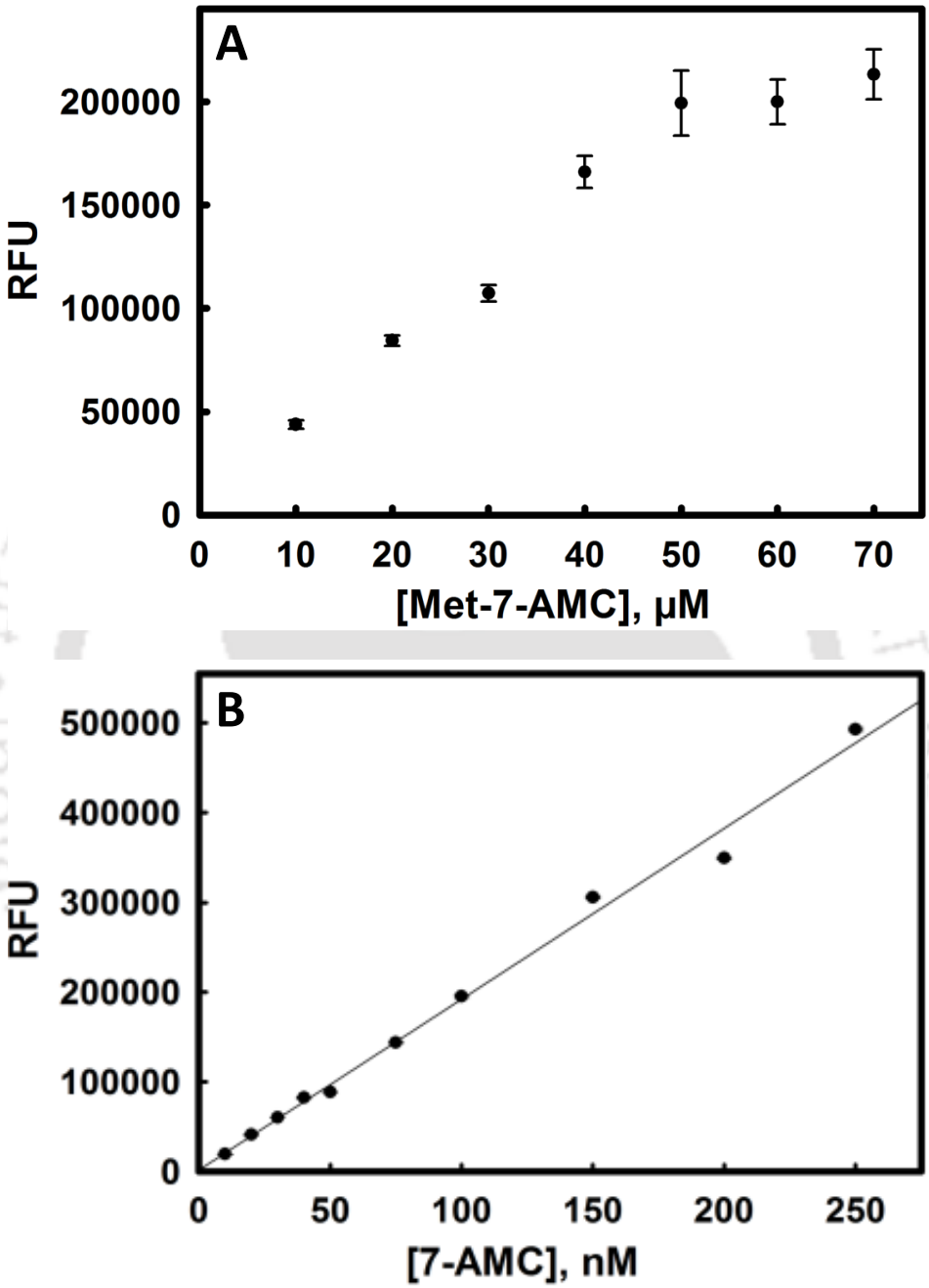

Figure 3.6: Enzyme activity and standard graph to measure the release of 7-AMC after hydrolysis of Met-AMC. *Ld*MAP2 enzymatic assay was carried out by measuring the release of 7-AMC by fluorescence at an excitation and emission wavelength of 360 nm and 440 nm, respectively. (A) *Ld*MAP2 activity with substrate Met-AMC to check the correct refolding of recombinant protein, purified from inclusion bodies. Total 15 µg of refolded recombinant *Ld*MAP2 was mixed in reaction buffer to check the activity. (B) Standard graph was plotted by measuring the known concentration of 7-AMC by fluorescence at an excitation and emission wavelength of 360 nm and 440 nm.

TH-1832_126106036

3.4.4 Inhibition studies of functionally active LdMAP2 by TNP-470 and leishmanicidal activity of the inhibitor on L. donovani promastigotes: The inhibitor TNP-470 was found to inhibit *Ld*MAP2 activity, which was assessed by Lineweaver-Burk plots (Figure 3.7A). TNP-470 showed a competitive mode of inhibition at a final concentration of 100 µM with respect to varied concentration of Met-AMC as *Vmax* did not change but there was an increase in *Km* value in the presence of inhibitor. The inhibitory constant (*Ki*) value was found to be 13.5 nM as the substrate concentration was varied.

L. donovani promastigote cells ($2.5x10^6$cells/mL) were treated with varying concentrations (0.25 µM to 50 µM) of TNP-470 for 24 h to check the antileishmanial activity. TNP-470 showed significant leishmanicidal activity with IC_{50} values of 15.01 ± 0.73 µM (Figure 3.7B). Promastigote cells treated with 0.2 % DMSO were used as negative control whereas cells treated with 25 µM of miltefosine served as positive control.

3.4.5 TNP-470 causes inhibition of Caspase3/7 protease like activity and oligonucleosomal-DNA fragmentation in L. donovani: Treatment of *L. donovani* promastigotes with miltefosine strongly revealed the apoptosis like mode of cell death with activation of Cas3/7 protease like activity which is well documented by various groups *(Paris et al., 2004; Verma and Dey, 2004).* In control studies, promastigote cells treated with miltefosine (25 µM for 18 h incubation at 25 ºC) also showed an increased Cas3/7 protease like activity whereas the promastigote cells treated with TNP-470 (20 µM for 18 h incubation at 25 ºC) did not show activation of Cas3/7 protease like activity. Unlike miltefosine treated cells, no significant increase in activity of Cas3/7 like protease was observed in case of promastigotes treated with both miltefosine (25 µM, 18 h) and TNP-470 (20 µM, 18 h). Cas3/7 protease like activity in cell lysates of miltefosine (25 µM) treated cells in presence of 100 µM of caspase-3 inhibitor (N-Acetyl-Asp-Glu-Val-Asp-al) or in presence of TNP-470 (20 µM) was even lesser than control cells (Figure 3.8). Control cells treated with 0.2% DMSO did not show significant increase in Cas3/7 protease like activity. Flow cytometric analysis of promastigotes population was used to calculate the percentage of sub-G_1cells (hypo-diploid cells) after cell permeabilization and staining with propidium–iodide (PI).

TH-1832_126106036

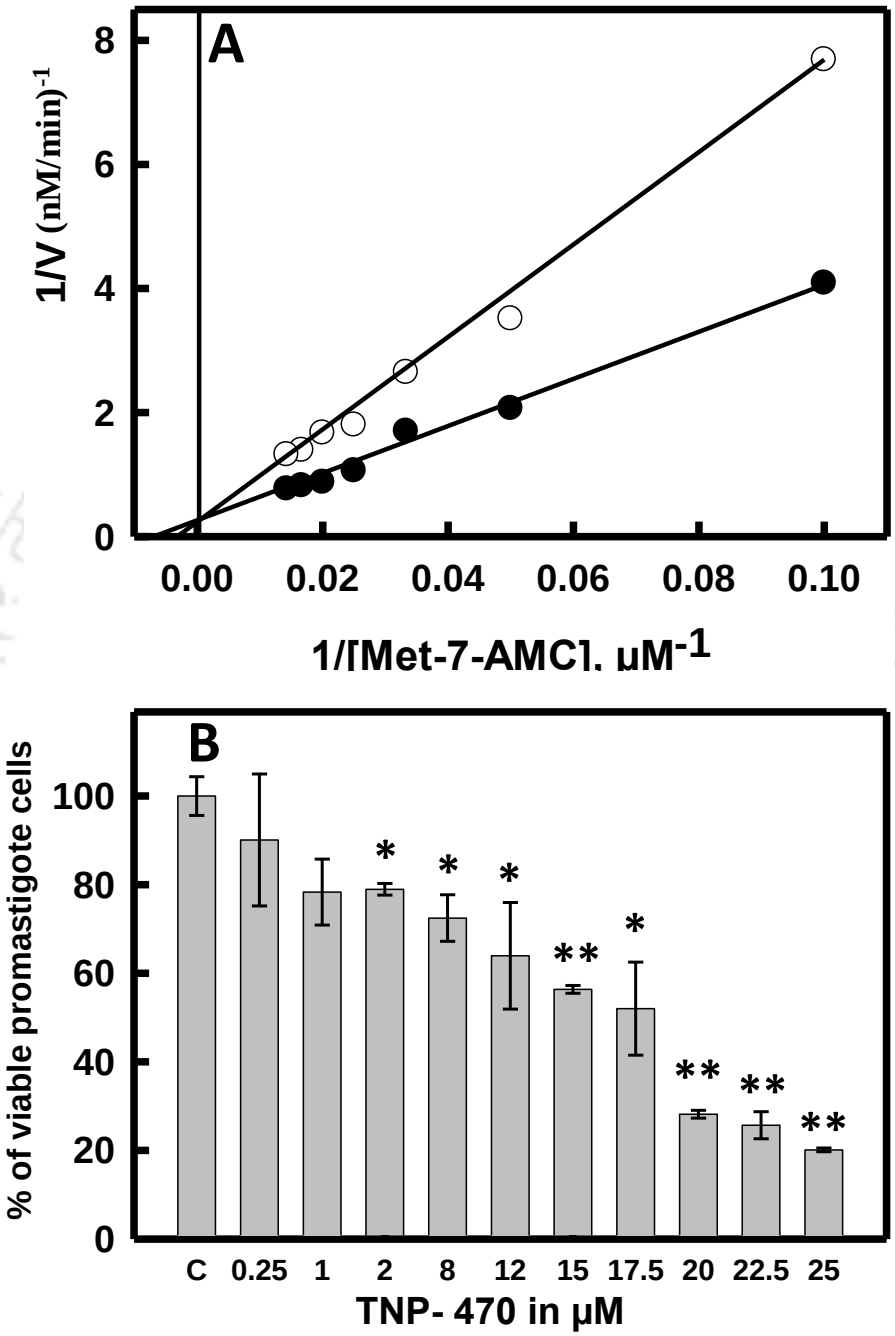

Figure 3.7: Lineweaver-Burk plot and Cell proliferation assay in presence of MAP2 inhibitor, TNP-470 (A) Inhibition studies for TNP-470 (100 µM), Competitive inhibition with respect to Met-AMC as a substrate. *Ki* value was found to be 13.5 nM. (B) MTT Assay; Effect of TNP-470 on *L. donovani* promastigotes, IC_{50} value against *L. donovani* promastigotes were found to be 15.01±0.73 µM. Data represents the mean ± SD of three independent experiments. Statistical analysis was done using Student's unpaired t-test in SigmaPlot software (*denotes p value ≤ 0.05 and **denotes p value ≤ 0.01).

TH-1832_126106036

The fluorescence intensity of bound PI correlates the amount of DNA in which the percentage of sub-G_1 peak shows the amount of DNA degradation in apoptotic like cells. Only 1.72 % of the control cells (promastigote cells treated with 0.2 % DMSO) were found in the sub-G_1 region (Figure 3A) whereas leishmanial cells treated with 25 µM of miltefosine for 12 h resulted in 21.48 % cells in apoptotic region (sub-G_1 peak region)(Figure 3.9B). In contrast, no sub-G_1 peak region was found in TNP-470 (20 µM for 12 h) treated promastigote cells (Figure 3.9C). Promastigote cells treated with both miltefosine and TNP-470 for 12 h resulted in only 4.85 % cells in sub-G_1 peak region (Figure 3.9D), thus suggesting that MAP2 inhibitors prevents the induction of nuclear apoptosis like features in *L. donovani.* Acquistion settings to collect the data and gating the population for analysis are shown in Figure 3.10.

Fragmentation of genomic DNA into nucleosomal units is considered as the characteristic feature of apoptotic cell death (*Compton, 1992*). DNA fragmentation analysis of promastigotes treated with miltefosine (25 µM), showed fragmentation of genomic DNA on agarose gel electrophoresis as reported earlier *(Paris et al., 2004; Verma and Dey, 2004).* No significant fragmentation of genomic DNA on agarose gel electrophoresis was observed in promastigote cells treated with TNP-470 (20 µM) and in control cells treated with 0.2 % DMSO. Interestingly, the promastigote cells treated with both miltefosine (25 µM) and TNP-470 (20 µM) for 18 h did not show fragmentation of genomic DNA into oligonucleosomal fragments, suggesting the inhibition of DNA fragmentation in miltefosine mediated PCD (Figure 3.11).

TH-1832_126106036

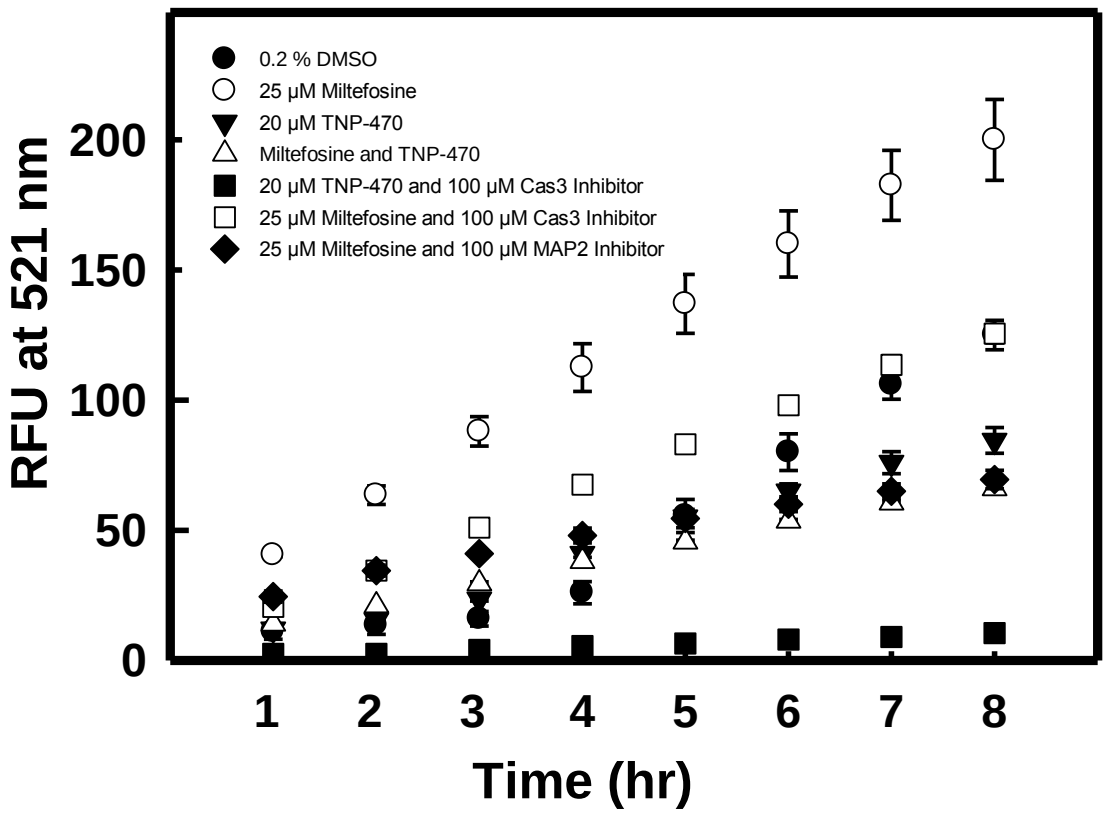

Figure 3.8: Activation of Caspase-3/7 like proteases inside *L. donovani* promastigote cells. Control cells (0.2 % DMSO), promastigotes induced with 25 µM of miltefosine, and by 20 µM TNP-470, alone or both. TNP-470 induced and miltefosine induced cell lysates were incubated with 100 µM of Cas3 inhibitor for 30 min, Miltefosine treated cell lysates were also incubated with 100 µM of MAP2 inhibitor. Data represents the mean ± SD of three independent experiments.

TH-1832_126106036

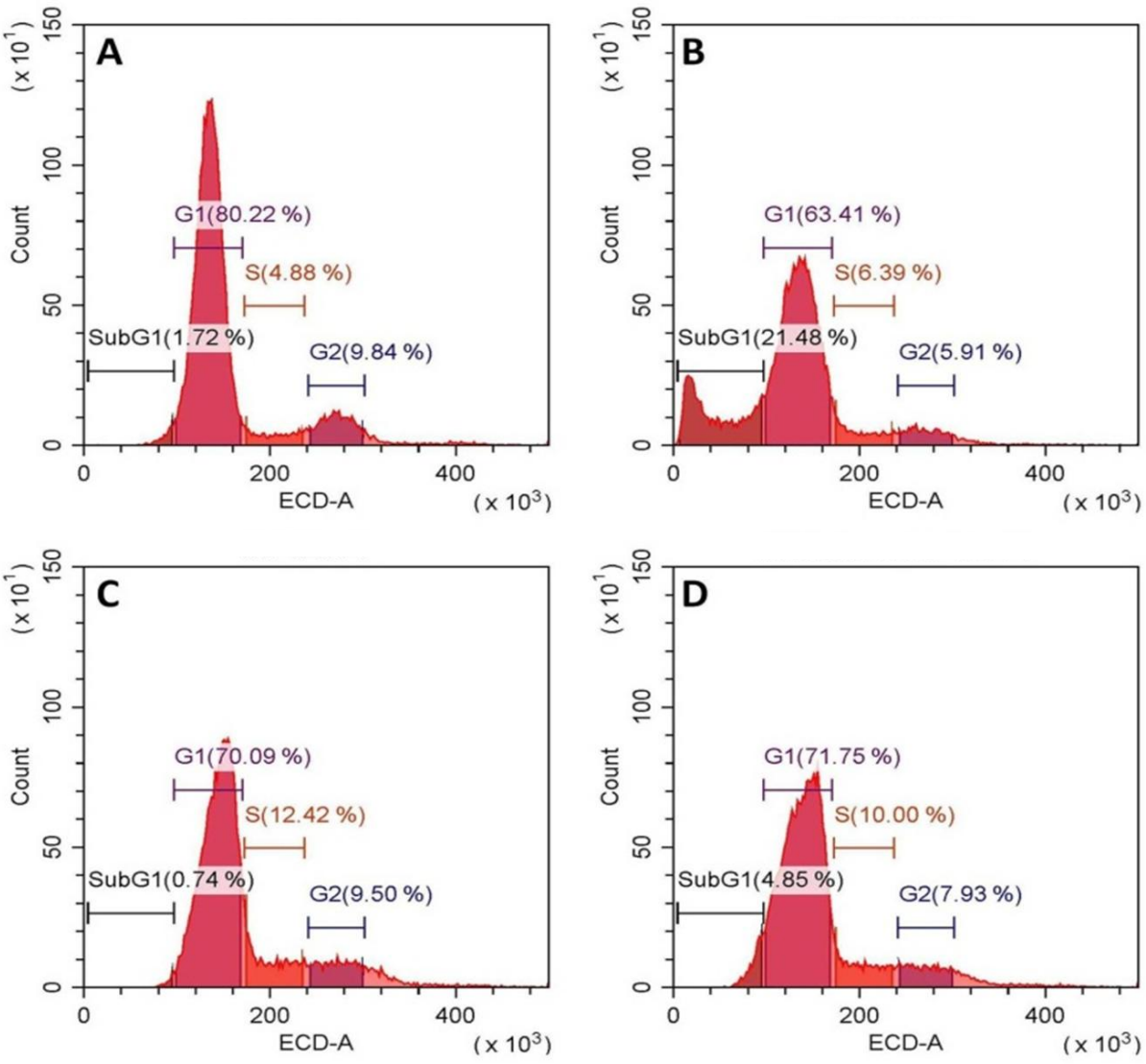

Figure 3.9: Cell cycle and DNA fragmentation analysis of *L. donovani* promastigotes. ECD represents red channel. (A) Control promastigotes treated with 0.2 % DMSO (B) Promastigotes induced with 25 µM of miltefosine (C) Cells treated with 20 µM of TNP -470 (D) Miltefosine induced promastigotes treated by TNP-470.

TH-1832_126106036

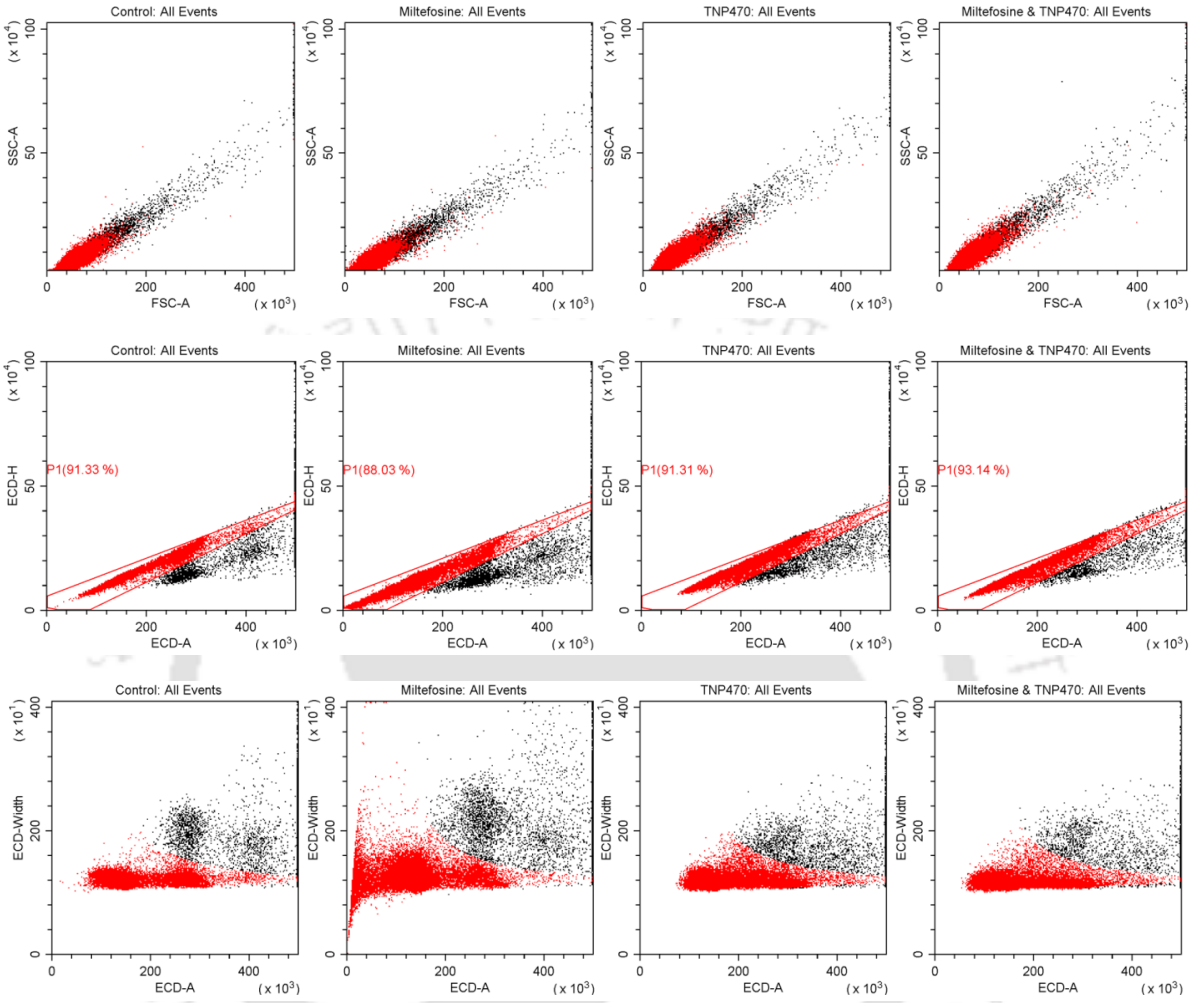

Figure 3.10: Acquisition Settings for Cell cycle and DNA fragmentation analysis of *L. donovani* promastigotes: Instrument: CytoFLEX Flow Cytometer-Beckman Coulter, Inc; Analysis by CytExpert software. Sample flow rate- 10 µl/min; Events to display- 30,000; The value of Gain for FSC-A was 120 and for SSC-A was 100; Threshold was set to default (automatic); Channel ECD was used for width. ECD-H vs ECD –A was plotted using SSC vs FSC data and gate was fixed for all the experiments. ECD-w vs ECD-A was plotted for gated cells and total no. of cells (count) vs ECD-A was plotted for analysis (ECD: Electron Coupled Dye).

TH-1832_126106036

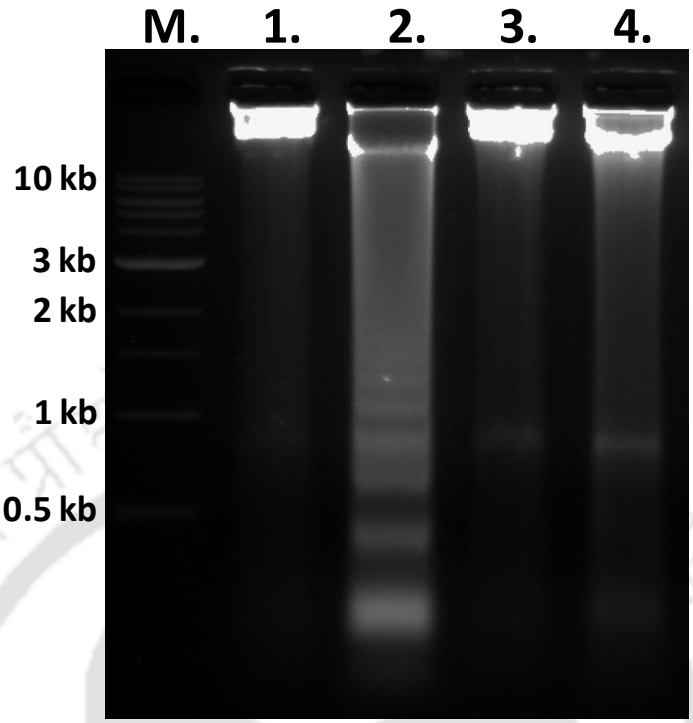

Figure 3.11: *L. donovani* genomic DNA fragmentation assay. Lane M. 1 kb ladder, Lane 1. Control cells (0.2% DMSO), Lane 2. Miltefosine induced promastigotes showing fragmentation of genomic DNA, Lane 3. TNP-470 treated, showing no fragmentation of genomic DNA, Lane 4. Both miltefosine and TNP-470 treated cells (showing inhibition of genomic DNA fragmentation)

3.4.6 TNP-470 treatment of L. donovani promastigotes does not inhibit the phosphatidyl serine externalization: In higher eukaryotes, cells undergoing apoptosis are characterized by translocation of phosphatidyl serine from the inner side to outer layer of plasma membrane, which can be analyzed by flow cytometry using annexin V-FITC and PI *(Jiménez-Ruiz et al., 2010).* Miltefosine is well known antileishmanial compound which causes translocation of phosphatidyl serine on outer plasma membrane in case of *Leishmania* promastigotes *(Paris et al., 2004; Verma and Dey, 2004).* A combined use of annexin V-FITC and PI was done to distinguish the apoptotic and necrotic cell death. Annexin V-FITC binds to exposed phosphatidyl serine with high affinity whereas PI selectively enters inside the necrotic cells and binds to DNA which allows the detection of both apoptotic and necrotic cells. Promastigotes treated with 25 µM of miltefosine for 18 h resulted in 51.71 % of Annexin-V positive (Figure 3.12B), whereas cells treated with 20 µM TNP-470 for 18 h resulted in 21.9 % of Annexin-V positive (Figure 3.12C). Only 1.06 % annexin-V positive cells were present

TH-1832_126106036

in control promastigotes treated with 0.2 % DMSO for 18 h. When the cells were treated with both miltefosine (25 µM) and TNP-470 (20 µM), the Annexin-V positive cells were 76.3 % (Figure 3.12). Thus, the MAP2 inhibitor along with miltefosine shows cumulative effect for the externalization of phosphatidyl serine on plasma membrane in *L. donovani* promastigotes.

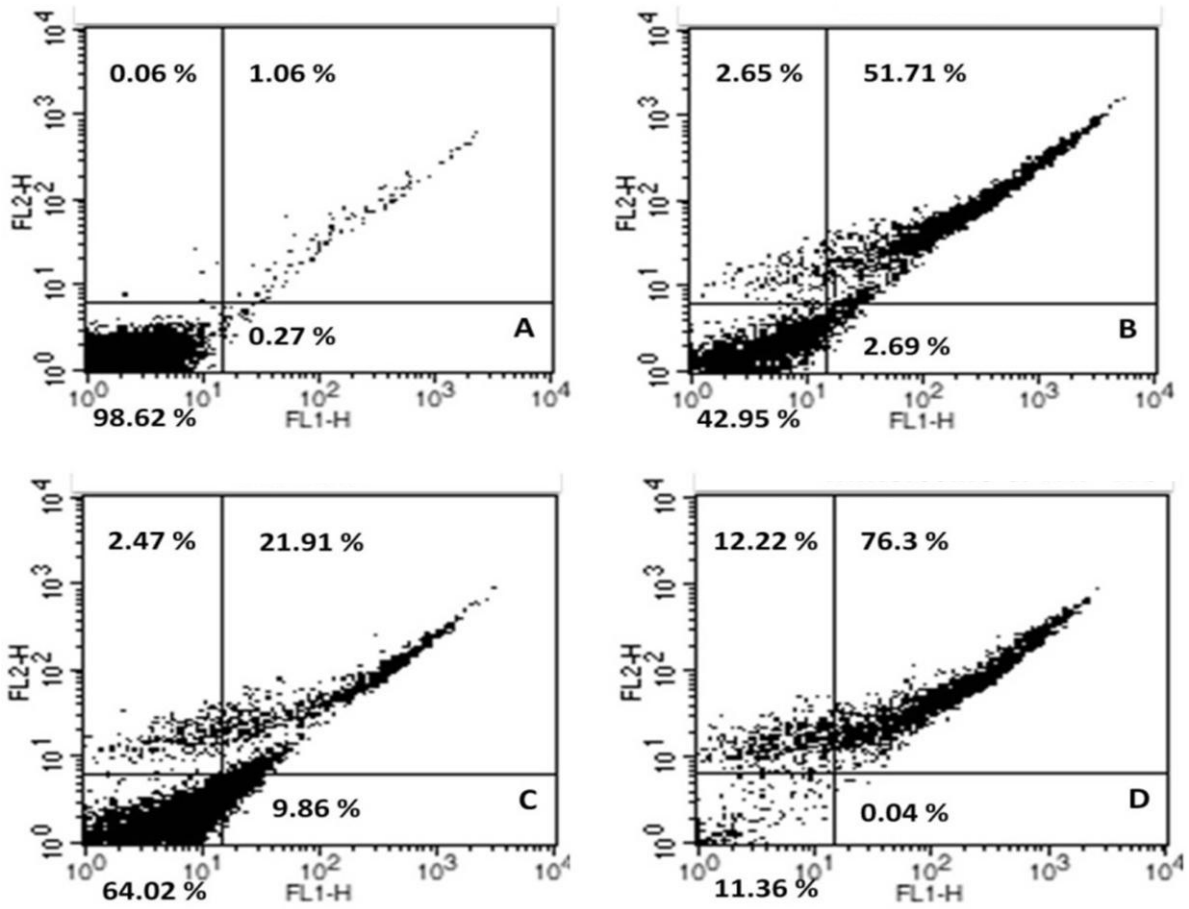

Figure 3.12: Externalization of phosphatidyl serine on plasma membrane, analysed by annexin V-FITC and PI staining (A) Control promastigotes treated with 0.2 % DMSO. (B) Promastigotes induced with 25 µM of miltefosine. (C) Cells treated with 20 µM of TNP -470. (D) Miltefosine induced promastigotes treated with TNP-470.

TH-1832_126106036

3.4.7 TNP-470 prevents alteration of transmembrane potential of mitochondria (ΔΨm) caused by miltefosine: The depolarization of $\Delta\Psi m$ is the characteristic feature of apoptosis, observed in eukaryotic cells *(Compton, 1992).* Change in mitochondrial membrane potential was detected by MitoCapture™ apoptosis detection kit, which is a cationic dye that aggregates in healthy mitochondria giving bright red fluorescence, but at lower membrane potential the dye remains in cytoplasm as monomers that fluoresce green. The mitochondrial membrane potential of promastigotes was examined by confocal microscopy stained by MitoCapture™ dye. Cells were treated with miltefosine and TNP-470, alone or both for 6 hr, mounted on glass-slides and images were captured. As shown in Figure 3.13, miltefosine treated cells showed an increase in green fluorescence (Figure 3.13B) whereas the TNP-470 treated cells showed an increase in red fluorescence (Figure 3.13C). The promastigote cells treated with both miltefosine and TNP-470, showed a significant increase in red fluorescence indicating the role of TNP-470 in the prevention of mitochondrial membrane damage in apoptotic like conditions. Leishmanial cells treated with both miltefosine (25 µM) and TNP-470 (20 µM) for 18 hr incubation at 25ºC, showed maximum debris on glass slides and were not suitable for imaging. Moreover, 6 h time point for mitochondrial membrane potential assay was chosen after optimization and based on earlier report *(Das et al., 2013).*

TH-1832_126106036

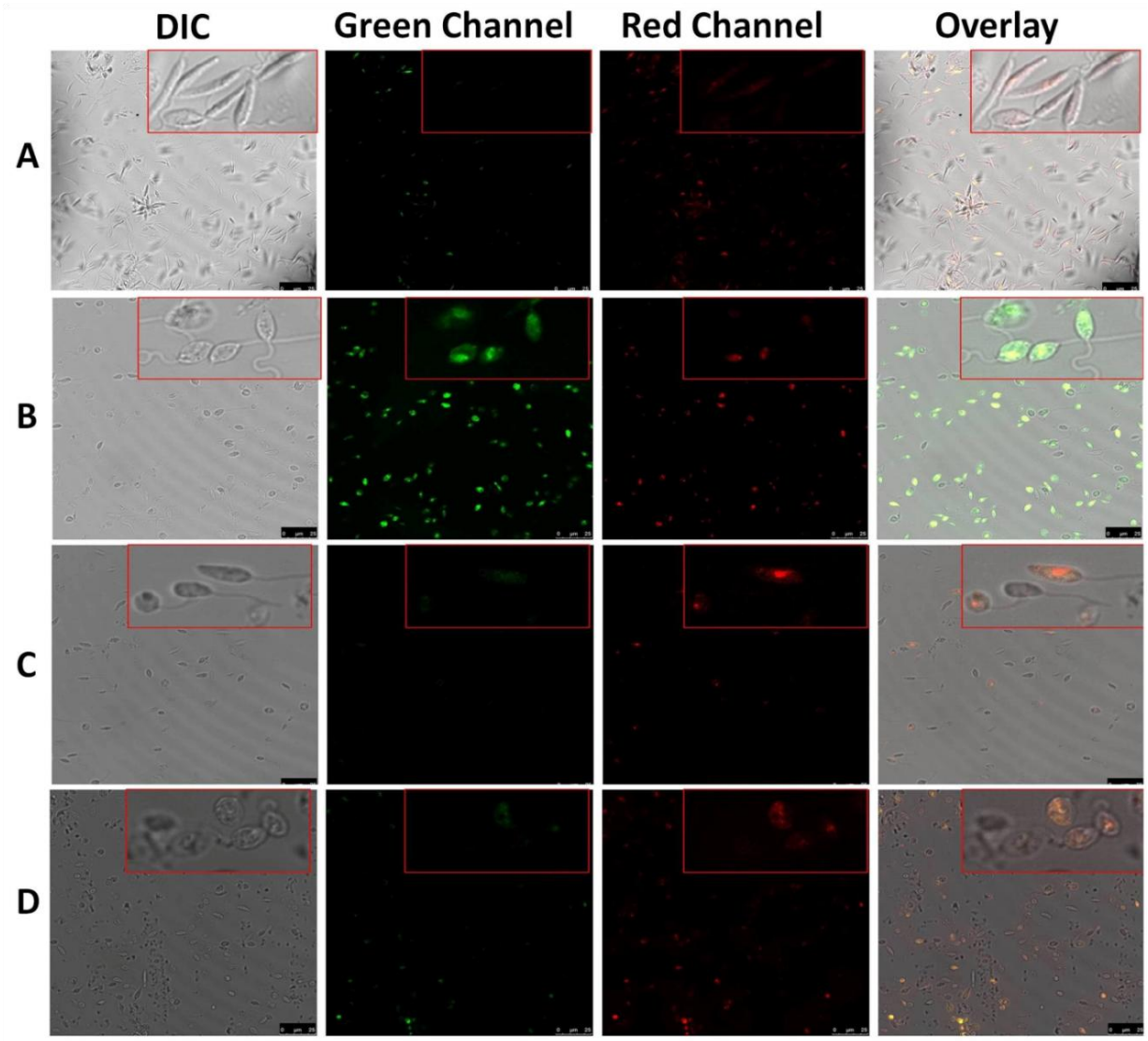

Figure 3.13: Laser Scanning Confocal Microscopy images of *L. donovani* promastigotes showing the aggregation and monomer forms of Mitocapture™ dye. *L. donovani* promastigotes were treated for 6 hr, stained with Mitocapture™ dye and image was captured by Confocal Microscopy (63X magnification). Increase in red fluorescence indicated the normal mitochondrial membrane whereas increase in green fluorescence showed the alteration in transmembrane potential of mitochondria. (A) Control promastigotes treated with 0.2 % DMSO. (B) Promastigotes induced with 25 µM of miltefosine. (C) Cells treated with 20 µM of TNP -470 and (D) Miltefosine induced promastigotes treated by TNP-470 for 6 hr. (DIC represents differential interference contrast microscopy).

TH-1832_126106036

3.4.8 TNP-470 prevents increase in cytosolic calcium caused by miltefosine: Change in $\Delta\Psi m$ in apoptotic like cell death of parasite results in release of cytochrome C from the mitochondria which in turn enhances the release of calcium from the endoplasmic reticulum, and causes a global increase in cytoplasmic calcium concentration inside the parasite. The increase in cytosolic calcium concentration in miltefosine treated cells was reported by several groups (*Kulkarni et al., 2009; Dolai et al., 2011*). In our studies, the measured fluorescence intensity at 510 nm was found to be maximum in promastigote cells treated with 25 µM of miltefosine for 18 h (Figure 3.14). When cells were treated with both miltefosine (25 µM) and TNP-470 (20 µM) for 18 h, the total cytoplasmic calcium concentration was decreased compared to miltefosine treated cells. The diminished calcium concentration pool after treatment of TNP-470 signifies the retention of $\Delta\Psi m$ as mentioned in above section.

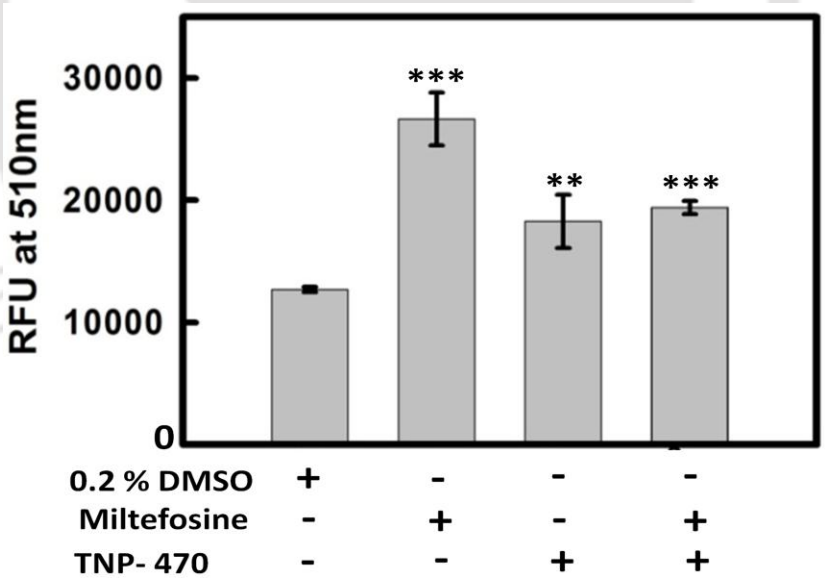

Figure 3.14: Measurement of Cytosolic concentration of Calcium using FURA2-AM dye, control cells (0.2% DMSO), miltefosine (25 µM) treated promastigotes, TNP-470 (20 µM) treated cells, and promastigote cells treated with both miltefosine and TNP-470 and stained with FURA2-AM dye. Statistical analysis was done using Student's unpaired t-test in SigmaPlot software (*denotes p value ≤0.05, **denotes p value ≤ 0.01 and *** denotes p value ≤ 0.001).

TH-1832_126106036

3.5 Discussion

Miltefosine treated *L. donovani* promastigotes shows the characteristic feature of metazoan apoptosis as reported earlier *(Paris et al., 2004; Verma and Dey, 2004).* Several other molecules *i.e* H_2O_2 *(Das et al., 2001),* heat shock *(Moreira et al., 1996),* staurosporine *(Foucher et al., 2013)* etc. are also known to induce PCD in *Leishmania* promastigotes *(Arnoult et al., 2002).* However, the biochemical pathways responsible for apoptosis like mode of cell death in *Leishmania* are still not fully deciphered. In mammalian cells, the proteolytic activation of caspases is essential for the induction of apoptosis *(Hengartner, 2000; Thornberry and Lazebnik, 1998; Green, 2000).* The activation of caspases is also required for the execution of apoptosis in the invertebrates such as *D. melanogaster (Meier et al., 2000)* and *C. elegans (Horvitz, 1999).* Even though the PCD was initially considered in multicellular organisms only, several reports suggested the similar biochemical features of PCD in unicellular eukaryotes such as *T. thermophylia (Christensen et al., 1995), D. discoideum (Cornillon et al., 1994), T. brucei (Welburn et al., 1996), T. cruzi (Ameisen et al., 1995), L. major (Arnoult et al., 2002), L. amazonensis (Moreira et al., 1996)* and *L. donovani (Paris et al., 2004; Saudagar and Dubey, 2014).*

It is reported that broad caspase inhibitors (BAF) or calpain/cysteine protease inhibitors (E64) prevent the staurosporine induced PCD of *Leishmania* parasite but does not prevent the cell death (*Arnoult et al., 2002*). Recently, it was reported that the cathepsin B like proteases are involved in PCD of parasite, and are capable to cleave caspase specific substrates (*El-Fadili et al., 2010*). Moreover, calpain inhibitor I was reported to prevent DNA fragmentation more efficiently which can inhibit calpain, cathepsins, cysteine proteases and proteasomes *(Johnson, 2000).* In contrast, a recent study suggested that the broad spectrum calpain and cysteine protease inhibitor E64 are not able to prevent the miltefosine induced DNA fragmentation. Whereas broad spectrum caspase inhibitor Z-VAD-FMK and Boc-D-FMK prevent the miltefosine induced DNA fragmentation, but have no preventive effect on externalization of phosphatidyl serine (*Paris et al., 2004*). Although the involvements of other cysteine proteases and caspase like activities are reported in PCD of *Leishmania (Arnoult et al., 2002),* caspase independent cell death pathways are also recognized *(Shibata et al., 1998).*

TH-1832_126106036

We observed higher level of gene expression of *MAP2* under apoptotic condition, suggesting the importance of *MAP2* protease in PCD of parasite *(Kumar et al., 2016).* In the present study, we examined the biochemical effect of TNP-470, a well known MAP2 inhibitor, on the miltefosine induced PCD of parasite. While control *Leishmania* promastigote cells treated with miltefosine showed all characteristics features of apoptosis whereas the *Leishmania* cells treated with both miltefosine and TNP-470 did not show the increased caspase3/7 protease like activity and several other characteristics features of apoptosis. Furthermore, the cell lysates of miltefosine induced promastigotes after pre-incubation with TNP-470, showed the decrease in caspase3/7 protease like activity. It is evident from confocal microscopy data that TNP-470 protects the leishmanial cells from miltefosine induced membrane depolarization as well as increases the global pool of cytosolic calcium. Further, TNP-470 inhibits the oligonucleosomal DNA fragmentation in miltefosine induced cells. These data together suggests the involvement of MAP2 in PCD of leishmanial cells.

However, TNP-470 treatment of *L. donovani* promastigotes does not inhibit the phosphatidyl serine externalization induced by miltefosine and prevents cell death. Although, MAP2 inhibition can inhibit induction of apoptosis of parasite under standard apoptotic condition (miltefosine treatment), the MAP2 inhibition is also not favorable for parasite survival as it is also involved in several other key functions. It is worth mentioning that in eukaryotes, MAP2 also plays a significant role in carrying out the regulation of protein synthesis and post translational modifications by removing the N-terminal methionine residue from the nascent peptide and by protection of eIF2α phosphorylation activity. Further, inhibition of phosphatidyl serine externalization is not reported in some other conditions where miltefosine induced apoptosis was inhibited by protease inhibitors. Moreover, one study on *L. donovani* (MHOM/ET/67/HU3) suggests that the Annexin-V binding cannot be a marker of apoptosis in case of *Leishmania (Weingärtner et al., 2012).*

In conclusion, our findings provided the first evidence, to our knowledge that the treatment of *L. donovani* with TNP-470, a well-known MAP2 inhibitor prevented the induction of apoptosis in miltefosine induced promastigotes, but was not able to prevent cell death of the parasites. Based on these observations, our studies suggest the role of MAP2 in *L. donovani*, as an effector molecule in higher eukaryotes which is important for the

TH-1832_126106036

induction of apoptosis but unable to prevent the cell death. The role of MAP2 in *Leishmania* parasite deserves more attention to understand its role in apoptosis like cell death. Furthermore, studies on mechanism of action of TNP-470 and proteomic analysis may provide the detailed answer.

भारतीय प्रौद्योगिकी संस्थान गुवाहाटी • Indian Institute of Technology Guwahati •

TH-1832_126106036

Chapter IV

Understanding the role of methionine aminopeptidase 2 in programmed cell death of *Leishmania donovani* by studying the *map2* knockout mutants

4.1 Abstract

Methionine aminopeptidase 2 helps in the processing of nascent polypeptide chain to remove the N-terminal methionine residues which are required for various cellular processes. Role of MAP2 in apoptotic cell death is established in our earlier work, as MAP2 inhibitor TNP-470 was able to prevent the apoptotic features of cell death in protozoan parasites (Chapter III). The data prompted us to further validate the role of MAP2 in apoptotic processes by genetic approach. The gene knockout was done using homologous recombination approach and effects of the knock out were analyzed on knock out mutants induced with miltefosine (25 µM). The gene knock out mutants treated with miltefosine showed the inhibition of miltefosine induced apoptotic processes, as inhibited the genomic DNA fragmentation, decreased the caspase-3/7 protease like activity, and prevented the decrease in transmembrane potential of mitochondria. Further, gene knock out parasite was less responsive to miltefosine. The gene knockout parasite showed a decrease in infectivity on human macrophage cell line and survives much better in miltefosine. The cell viability assay and flow cytometry assay to check the exposure of phosphatidyl serine on plasma membrane suggests that the knock out parasite showing miltefosine unresponsive phenotype.

*** Part of the data submitted for publication**

TH-1832_126106036

4.2 Introduction

Leishmaniasis is a neglected tropical disease caused by a variety of species of *Leishmania* parasite. *Leishmania* is an obligate intracellular protozoan parasite which is transmitted through the bite of female sand flies. It is prevalent in different parts of world including Asia, Africa, South and Central America. According to the tropism of *Leishmania* parasite, leishmaniasis has been divided into three different clinical forms: visceral, cutaneous and muco-cutaneous leishmaniasis. Visceral leishmaniasis is the most dangerous form of this disease as it affects internal organs of the body like spleen, bone marrow and liver. In India, visceral leishmaniasis is the most commonly found form of the disease where it is majorly transmitted by *Leishmania donovani*. The parasite has a digenetic life cycle which comprises of extracellular flagellated promastigotes found in the midgut of female sand fly and intracellular amastigotes, devoid of flagella harbor the phagolysosomes of macrophages in the vertebrate host (*Rachidi et al., 2013*).

Apoptotic cell death in *Leishmania* is well established under various stress conditions, including oxidative stress, after treatment with various anti-leishmanial drugs or compounds such as miltefosine, betulin, PS-203 etc (*Verma and Dey, 2004; Paris et al., 2004; Saudagar et al., 2013; Saudagar and Dubey, 2014*). Role of various proteases, including caspases, is recognized in various organisms and human cell lines (*Patel et al., 1996*). However, in *Leishmania*, studies remained focused on role of caspases and metacaspase in the apoptotic process. Extensive studies about possible role of other proteases in the apoptosis are not reported. Thus, the mechanism of apoptotic death with respect to role of proteases remains elusive. Caspases are the important regulator of apoptotic cell death in higher eukaryotic organisms are absent in *Leishmania* but the increased caspase like activities have been reported consistently after treatment with various anti-leishmanial compounds (*Saudagar et al., 2013; Saudagar and Dubey, 2014*). The role of non caspase proteases of parasite such as cathepsins, calpains and other cysteine proteases are reported in PCD of parasite, as specific inhibitor prevents the apoptotic death of parasite. We have observed increased mRNA expression of *MAP2* in miltefosine induced programmed cell death of parasite (*Kumar et al., 2016*). This initial finding led us to investigate the involvement of *Ld*MAP2 in the cell death pathway of *L. donovani* as mentioned in Chapter II and Chapter III.

TH-1832_126106036

Methionine aminopeptidases (MAPs) are bifunctional enzyme that catalyzes the release of N-terminal methionine residues from nascent peptide and arylamides *(Ben-Bassat et al., 1987; Jackson and Hunter, 1970; Solbiati et al., 1999)*. In eukaryotes, two types of MAPs are reported; MAP1 and MAP2 whereas in prokaryotes only one MAP gene is present *(Giglione et al., 2004).* Studies conducted in *E. coli* have shown that knockout of *map* gene is lethal, suggesting their important role in growth and survival of bacteria *(Chang et al, 1989).* During post translational modifications, removal of methionine is vital for amino terminal modifications such as addition of myristoyl group at N-terminal glycine residue and addition of acetyl group *(Boutin, 1997; Farazi, 2002).* These modifications are important for the biological activity of proteins, sub cellular localization and cell cycle progression *(Bradshaw et al., 1998).* Several other proteins involved in signal transduction pathways and in regulatory pathways are myristoylated such as calcineurin, G-proteins, cAMP dependent protein kinases, proteins involved in ADP ribosylation and several oncoproteins *(Carr et al., 1982; Aitken et al., 1982; Schultz et al., 1987; Johnson et al., 1995)*. Initially, MAP2 were reported to associate with eukaryotic initiation factor 2α (eIF2α) and regulate the protein synthesis pathway required for cell growth and survival. MAP2 bound with eIF2α protects the inhibitory phosphorylation of eIF2α and in turn regulate the cell growth *(Li et al., 1996).*

In our previous studies (Chapter III), we have found that the TNP-470, a synthetic analog of fumagillin family inhibits recombinant *Ld*MAP2. The promastigotes cells incubated with TNP-470 prevents the miltefosine induced PCD of parasite. The inhibition of apoptosis was measured using several biochemical markers of apoptosis used in protozoan parasites. The result obtained in Chapter II and Chapter III, prompted us to validate the role in MAP2 in PCD of *Leishmania* parasite by gene knock out approach. In the present study *map2* gene knockout was done by homologous recombination approach and effect of *map2* knockout mutants were studied in miltefosine induced PCD of parasite. Further, complementation studies of *map2* gene were also done using episomal expression to validate the effect of knock out mutants.

TH-1832_126106036

4.3 Methods

4.3.1 Parasites, Cell lines and Chemicals: *L. donovani* strain was generously provided by Prof. Shyam Sunder, Banaras Hindu University Varanasi. U937 human monocyte cell line was obtained from National cell sciences, Pune. The cell line was maintained at 37ºC and 5 % CO_2 in RPMI media (pH 7.4) supplemented with 10 % fetal bovine serum and 1% penicillin-streptomycin. All restriction enzymes used in preparation of molecular constructs and T4 DNA ligase were purchased from NEB. Genomic DNA isolation kit was procured from Bioline. Plasmid isolation kit, PCR cleanup kit, MTT reagent, Phleomycin, Pen-strap, RIPA buffer was purchased from Sigma, USA. Annexin V-FITC apoptosis detection kit (Life technologies), Mitocapture™ apoptosis detection kit (Merck), G418 geneticin (Gibco), Puromycin (Himedia) and all other chemicals of highest purity grade were procured from either Sigma or Merck. The antibody against *L. donovani* MAP2 were raised in mouse and protein A purified mouse-anti- *Ld*MAP2 was commercially synthesized by Abgenex Pvt. Ltd., India. All the pXG vectors used in gene knockout studies were generously donated by Prof. Stephen Beverly, Washington University Medical School in St. Louis, USA.

***4.3.2 Leishmania* parasite culture and Cell culture:** Parasite was maintained at 25ºC in M199 media (pH 7.4) supplemented with 15 % fetal bovine serum (FBS) and 1 % penicillin-streptomycin according to the already established protocol in our laboratory (*Saudagar et al., 2013*). Single knock out (SKO) parasites were selected in Geneticin G418 at 20µg/ml and after selection maintained at 50 µg/ml of G418. Double knock out parasite (DKO) were selected in Puromycin at 10µg/ml and maintained at 20µg/ml. For complementation studies, complemented parasites (CKO) were selected in 5µg/ml of phleomycin and maintained at 10µg/ml. The concentration of antibiotic was determined by previous studies (*Beverley and Clayton, 1993; Bhardwaj et al., 2016*). For all the biochemical analyses, the parasites were transferred and kept in fresh media without any selection antibiotic for 24 hr.

4.3.3 Preparation of molecular constructs for gene knockout and complementation of LdMAP2 to study their role in apoptotic processes of parasite: Molecular constructs to delete the *map2* gene were prepared using the pXG vectors containing different selection markers. pXG B1288 NEO containing G418 as a selection marker, pXGB3325 PAC

TH-1832_126106036

containing puromycin and pXGB3324 contains phleomycin as a selection marker. *Ld*MAP2 (Gene Id # LdBPK_210960.1) gene is present on chromosome number 21 and two copies of this gene are present, as *Leishmania* is diploid in nature. One copy of this gene was removed by pXGB1288 NEO and other copy by pXGB3325 PAC vector. For complementation, pXGB3324 phleomycin vector was used in this study. 5'UTR region of *map2* gene was cloned between *Bsr*GI and *Xho*I region present at 4867/71 and 5496/00 position on the pXGB1288 NEO vector. 5'UTR region (699 bp) was amplified from genomic DNA of *L. donovani* using the primer 1 and primer 2. Similarly, 3'UTR region (600 bp) of *map2* gene was amplified using the primer 3 and primer 4. The amplified fragment was cloned between *Xma*I and *Age*I region present at 1363/67 and 1598/1602 position on the pXGB1288 NEO vector. For cloning, amplified PCR product of 5'UTR and 3'UTR were cleaned up using PCR clean up kit. The purified fragment and pXGB1288 vector were double digested with respective restriction enzymes (*Bsr*GI and *Xho*I for 5'UTR and *Xma*I and *Age*I for 3'UTR) to generate the complementary sticky ends and ligated with T4 DNA ligase to prepare pXGB1288-5'UTR-3'UTR recombinant plasmid. The recombinant plasmid was transformed into *E.coli* DH5α competent cells for the amplification of plasmid. Further clone was confirmed was PCR amplification, restriction digestion and sequencing. For preparation of pXGB3325 PAC construct containing 5'UTR and 3'UTR region of *map2* gene, pXGB3325 PAC and pXGB1288-5'UTR-3'UTR recombinant plasmid was double digested with *Xho*I (5722/26) and *Sac*I (1043/47). The released fragment of 1931 bp from pXGB3325 PAC was cloned into pXGB1288-5'UTR-3'UTR plasmid replacing neomycin region. Similarly, for the preparation of complementary vector, the coding sequence of *map2* gene was amplified (1396 bp) using the primer 5 and primer 6. The amplified fragment and pXGB3324 phleomycin vector was double digested with *Xma*I (1362/66) and *Bam*HI (1368/72). The digested fragment was further ligated with T4 DNA ligase to form pXGB3324-*map2* expression construct. The schematic representation for the preparation of molecular construct for gene knock out studies is shown in Figure 4.1.

TH-1832_126106036

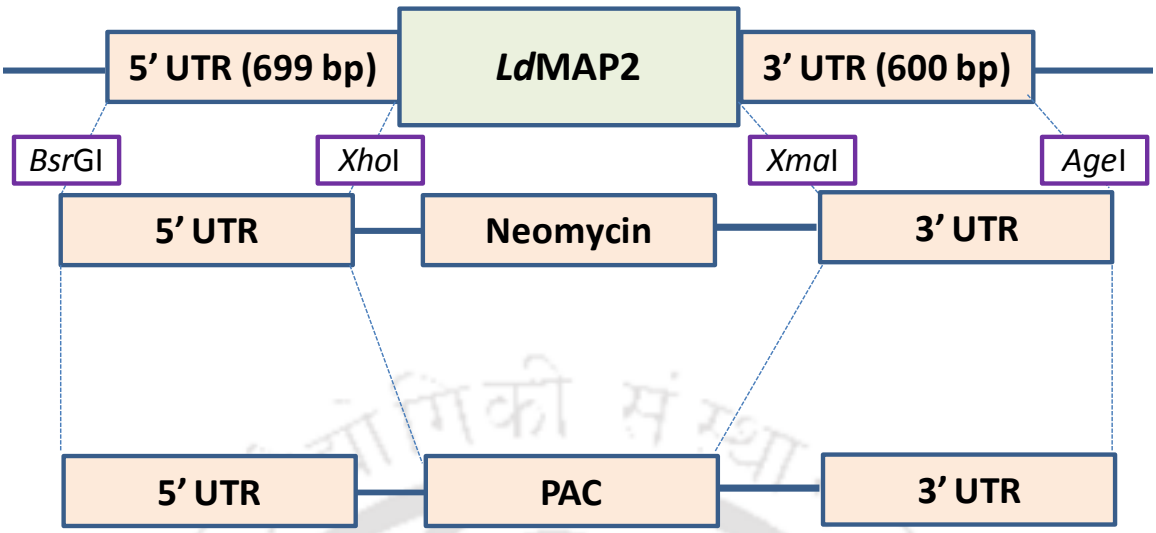

Figure 4.1: Schematic representation of molecular construct to replace the *Ld*MAP2 locus by neomycin and puromycin selection marker. 5'UTR and 3'UTR of *Ld*MAP2 was cloned in pXGB1288 Neo vector and pXGB3325 PAC vector using restriction digestion approach. Constructs were confirmed by restriction digestion and sequencing.

4.3.4 Generation of map2 knock out Leishmania parasite and preparation of map2 complemented parasite: Gene knockout studies was done using the homologous recombination method as mentioned in previous reports (*Beverley and Clayton, 1993*). For preparation of single knock out (SKO) strain, the recombinant vector pXGB1288-5'UTR-3'UTR was linearized using *Nhe*I digestion. Approximately $2.5x10^7$ cells/ml *Leishmania* parasite was taken for electroporation. Before electroporation, parasite was washed twice with cold PBSG buffer (10 mM NaH_2PO_4, 10 mM Na_2HPO_4, 145 mM NaCl and 2 % Glucose). Cells were centrifuged at 850 xg at 4ºC and pellet was washed with electroporation buffer (21 mM HEPES, 137 mM NaCl, 5 mM KCl, 0.7 mM Na_2HPO_4, 6 mM Glucose) and pellet was dissolved in 360 µl of cold electroporation buffer. After that, approximately 40 µl of 5-10 µg/µl of linearized DNA was added in the cell suspension, transferred to ice cold sterile electroporation cuvette and incubated on ice for 10 min. Electroporation was done on BioRad Gene Pulser Xcell™ Electroporation Systems with following conditions were set for electroporation (Voltage: 450 V, Capacitance: 500 µF, Resistance: 50 Ω, Path length: 2 mm and resulting time constant: 4.5 msec). Similarly, electroporation on wild type cells were done without adding DNA in cell suspension. After the electroporation, both cuvettes were

TH-1832_126106036

placed on ice for 10 min and then transferred into fresh M199 media for 24 hrs. Then, electroporated cells were transferred in M199 media containing G418 (20µg/ml) for selection of SKO cells. Once selection was confirmed, SKO cells were maintained at G418 (50µg/ml). For DKO cells, pXGB3325-5'UTR-3'UTR vector was linearized by *Nhe*I and electroporation was done as mentioned above. Selection of DKO cells were done in M199 media containing puromycin (10µg/ml) and cells were maintained at 20 µg/ml of puromycin. DKO cells were further subjected to complementation studies. Circular pXGB3324-*map2* expression construct were electroporated in DKO cells as mentioned above and selection was done in phleomycin (5µg/ml). After selection, CKO cells were maintained in 10 µg/ml phleomycin.

4.3.5 Confirmation of knockout parasite by PCR amplification: Preliminary confirmation of knockout cells were confirmed in antibiotic selection media with minimum of fifteen passages. Further, knockout parasites were confirmed by PCR using genomic DNA of respective cells as a template. Neomycin and puromycin gene specific primers were used to check the integration of the cassettes in *Leishmania* genome. UTR specific primers were also used to check the integrity at appropriate locus. Primer 1 (5'UTR FP) and primer 4 (3' UTR RP) was used to check the integration of neomycin and puromycin gene. If homologous recombination is successful, the above mentioned set of primer will show the amplification of ~3.9 kb. Another set of primer 7 (Neo FP) and primer 8 (Neo RP) was also used to check the integration of antibiotic resistance gene. Upon integration, it will show the amplification of ~ 2.9 kb. Primer 9 (Pac FP) and primer 10 (Pac RP) was used to check puromycin marker gene in DKO cells which will show the amplification of ~0.45 kb. The list of primers is mentioned in Table 4.1.

4.3.6 Confirmation of knockout parasite by western blot experiments: The knockout cells were further confirmed by western blot experiments. For western blot, wild type *Leishmania*, SKO, DKO and CKO parasites were centrifuged at 1000 x g, washed twice with cold PBS and cell pellet were lysed in RIPA buffer containing 1 mM PMSF and 1x protease inhibitor cocktail (Sigma, cat. no. P8340).

TH-1832_126106036

Table 4.1: List of primers used to prepare the molecular constructs and the primers used for confirmation of knockout by PCR amplification. *Italicized* and underlined nucleotide sequences are restriction enzyme sequences.

S.No.	Name of Primer	Sequences
01	Primer 1	CT*TGTACA*CCGCCATGTGATCATCCGCG
02	Primer 2	GC*CTCGAG*GATGGTGAGGATGGCAAC
03	Primer 3	TC*CCCGGG*AAGCGACTACTAGGCGTGG
04	Primer 4	CG*ACCGGT*CTCGGGTCACGATGACGCTC
05	Primer 5	GT*CCCCGGG*ATGCCACCAAAGATGTCTG
06	Primer 6	GT*GGATCC*CTAGTAGTCGCTTCCCTTGG
07	Primer 7	GCTTGCACCCAGGCTCGTC
08	Primer 8	GACAGGGGGAGGGCTACGG
09	Primer 9	TACAAGCCCACGGTGCGCCTCG
10	Primer 10	GAGGTCTCCAGGAAGGCGGGCA

Cell suspension was kept on ice for 10 min and lysis was done with vigorous pipetting. Cell debries was removed by centrifugation at 10000 rpm for 5 min at 4ºC and clear supernatant was quantified by Bradford assay. Equal amount of cell lysates (~40 µg) were loaded on 12 % SDS-PAGE and further transferred on polyvinylidene membrane using GE Amersham Semi-dry transfer unit. After the transfer, blot was blocked using 5 % skimmed milk in TBST solution for 2 hrs at room temperature. After successful blocking, blot was washed thrice with 1x TBST solution, incubated overnight at 4ºC with rabbit anti-MAP2 antibody (1:1500), washed thrice with 1x TBST thrice and the blot was further incubated with anti rabbit-IgG horse radish peroxidase conjugated secondary antibodies (1:3000) for 1 hr at room temperature. Blot was washed thrice with 1x TBST and chemiluminescent HRP substrate was added and incubated for 1-2 min. Image was visualized with BioRad ChemiDoc system. Primary MAP2 antibody was commercially generated in rabbit by Abgenex pvt. ltd., India.

TH-1832_126106036

Table 4.2: List of primers used for Real time-qPCR to check the differential expression of MAP2 in wild type, SKO, DKO and CKO cells.

S.No.	Name of Primer	Sequences
01	MAP2-F	CACCTCATGAACCTGAAC
02	MAP2-R	CGAGGTAGATCGTGTGTT
03	α-tubulin F	CTACGGCAAGAAGTCCAAGC
04	α-tubulin R	CAATGTCGAGAGAACGACGA

4.3.7 Confirmation of knockout parasite by Real time-qPCR experiments: To confirm the deletion of *map2* gene from parasite, Real time –qPCR was done. Total RNA was extracted from wild type, SKO, DKO and CKO parasite using RNeasy Mini Kit – QIAGEN according to the manufacturer's protocol. RNA was quantified by nanodrop at 260 nm absorbance and purity of total RNA was assessed at A260/A280 (>1.8). Equal amount of total RNA was taken to synthesize cDNA (NEB-AMV first strand cDNA synthesis kit). Equal amount of cDNA was taken to perform the SYBR Green PCR assays on Applied Biosystems 7500 Real-Time PCR System. The cycling parameter was set as default and melt curve were analyzed to check any non specific signal. Alpha-tubulin was used as an endogenous control. Data were analyzed using Applied Biosystems SDS v2.0.6 software. The primers used to check the amplification are listed in table 4.2.

4.3.8 Determination of caspase-3/7 protease like activity on knock out Leishmania parasite: Intracellular Caspase-3/7 protease like activity was measured flurometrically using Apo-1 homogenous caspase 3/7 activity assay kit (Promega). The assays were performed according to manufacturer's instruction and as reported earlier in our publication (*Saudagar et al., 2013*; *Kumar et al., 2017*). In brief, approximately $5x10^6$ cells/ml of wild type (control), SKO, DKO and CKO parasite each were taken for activity assay. In parallel set of experiments; control, SKO, DKO and CKO cells were treated with 25 µM of miltefosine for 18 hrs and taken for activity assays. After incubation, all the cells were centrifuged at 850 xg for 5 min and washed twice with 1xPBS. Cell pellets were dissolved in 100 µl of reaction buffer containing caspase substrate Z-DEVD-R110 and incubated in dark at room temperature for 4 hrs. The release of R110 was measured by fluorescence at an excitation and

TH-1832_126106036

emission wavelengths of 485 nm and 530 nm, respectively. In parallel set of reaction, Caspase-3/7 inhibitor (Ac-DEVD-CHO) was added in wild type cells treated with 25 µM miltefosine prior to addition of reaction mixture.

4.3.9 DNA fragmentation Assay by agarose gel electrophoresis on knock out Leishmania parasite: DNA fragmentation was analyzed by agarose gel electrophoresis of total genomic DNA, which was isolated as reported earlier with minor modifications *(Sambrook et al., 1989; Saudagar and Dubey, 2014).* In brief, 1 x 10^8 cells/ml of wild type (control), SKO, DKO and CKO parasite were taken for studies. In parallel set of experiments, wild type (control), SKO, DKO and CKO parasite were treated with 25 µM of miltefosine. Briefly, cell pellets of all promastigotes were lysed in 500 µl of lysis buffer (50 mM Tris-HCl, 10 mM EDTA, 0.5% SDS; pH 7.5) containing proteinase K (100 µg/ml), vortexed and kept overnight to digest at 50˚C. RNase A (0.3 mg/ ml) was added and then incubated at 37˚C for 1 h. The lysates were extracted using phenol-chloroform-isoamylalcohol (25:24:1) and centrifuged at 15000 X g for 10 min. The upper aqueous phase was collected, treated with $1/10^{th}$ volume of 3M sodium acetate and 2 volume of 100 % ethanol overnight at -20˚C. The sample was centrifuged at 15000 X g for 15 min and washed with 500 µl of 70 % ethanol. The DNA pellet was dissolved in TE buffer (10 mM Tris-HCl, 1 mM EDTA; pH 8.0) and quantified spectrophotometrically at 260/280 nm. A total of 10 µg of genomic DNA was run on 1.5 % agarose gel containing ethidium bromide for 2 h at 50 V and visualized under UV illuminator (Bio-Rad).

4.3.10 Flow Cytometry analysis to check the transmembrane potential of mitochondria (ΔΨm): Mitochondrial membrane potential was measured by MitoCapture™ apoptosis detection kit (Merck) according to manufacturer's instruction. Briefly, $5x10^6$ cells/ml of wild type, SKO, DKO and CKO cells were taken. In parallel, wild type, SKO, DKO and CKO cells were treated with 25 µM of miltefosine for 12 hr. After incubation period, cells were washed with PBS and then resuspended into incubation buffer containing mitocapture reagent. The reaction mixture was incubate for 20-25 min. Immediately, all the samples were run on flow Cytometry (FACSCalibur flow cytometer-Becton Dickinson) and data were analyzed by CellQuest software.

TH-1832_126106036

4.3.11 Flow Cytometry analysis to check the exposure of phosphatidyl serine (PS) on plasma membrane in knockout parasites: PS exposure on plasma membrane is an important biochemical marker to measure apoptotic processes in protozoan parasite. Analysis of PS exposure was done using Annexin-V-FITC apoptosis detection kit (Life technology) according to maufacturer's instruction. Briefly, $5x10^6$ cells/ml of wild type, SKO, DKO and CKO cells were taken. In parallel, wild type, SKO, DKO and CKO cells were treated with 25 µM of miltefosine for 18 hr. After incubation period, cells were washed with PBS, resuspended in incubation buffer and stained with Annexin-V-FITC and PI. The fluorescence intensity of FITC and PI was measured using flow cytometer (FACSCalibur flow cytometer Becton Dickinson) and data was analyzed by CellQuest software. Appropriate gating was done to analyze the cells.

4.3.12 Leishmanicidal effect of miltefosine on knockout mutants: Percentage of cell viability after treatment with miltefosine was analyzed by MTT [3-(4,5-dimethylthiazol-2-yl)-2,5-diphenyltetrazolium bromide] assay as mentioned earlier (*Mosman, 1983*). Briefly, $5x10^6$ cells/ml of wild type, SKO, DKO and CKO cells were taken. In parallel, wild type, SKO, DKO and CKO cells were treated with 25 µM of miltefosine for 24 hr. The cells were incubated in 96 well culture microplates at 25ºC. After incubation, cells were harvested at 4500 rpm for 45 min; cell pellet was dissolved in 200 µl of MTT (0.5 mg/ml) and incubated for 4 hr at 25ºC to form the formazan product. After incubation, cells were again harvested at 4500 rpm at 4ºC and insoluble formazan product was dissolved in 100 µl of DMSO. The absorbance was measured at 570 nm by using microplate reader (BIOTEK Synergy HT). The purple color formed is directly proportional to viable cells.

***4.3.13 Comparative analysis of infectivity of the parasite on U937 macrophage cell line after gene knockout*:** The effect of *map2* knockout on infectivity of human macrophage was checked by infectivity assay as mentioned earlier with minor modifications (*Saudagar et al., 2013; Bhardwaj et al., 2016*). Briefly, $1x10^5$ U937 human monocyte cells was seeded in 12 well plates and incubated with 100 ng/ml of phorbol-myristic acid (PMA) at 37ºC and 5 % CO_2 for 24 hr. The media was removed and fresh RPMI-1640 media was added in each well.

TH-1832_126106036

After that, $1x10^6$ *Leishmania* wild type cells, SKO, DKO and CKO cells were given infection on macrophage cell line; incubated with 24 hr at 37ºC and 5 % CO_2. The cells were washed twice with cold 1xPBS and fixation was done in methanol for 5 min. After fixation, macrophage cells were stained with Giemsa dye and incubated for 30 min. The staining solution was removed after gently washing with cold 1xPBS and kept it at room temperature for 10 min to get it dried. Approximately 60-70 macrophages were counted and infectivity index was calculated, Parasite infectivity index = percentage of infected macrophages x total number of amastigotes per macrophages.

4.4 Results

***4.4.1 Preparation of molecular constructs and confirmation of knockout by PCR amplification*:** The molecular constructs were prepared as mentioned in methods section. All molecular constructs were confirmed by restriction digestion. For confirmation of pXGB1288-5'UTR-3'UTR plasmid; recombinant plasmid was double digested with *Bsr*GI and *Xho*I to check the release of 5'UTR (699 bp) and the plasmid was double digested with *Xma*I and *Age*I to check the release of 3'UTR (600 bp) (Figure 4.2A). To confirm the replacement of Neo cassette with Pac region, the pXGB3325PAC-5'UTR-3'UTR plasmid digested with *BstE*II; and it showed the release of 1.6 kb fragment (Figure 4.2B). Similarly, pXGB3325-*map2* plasmid was double digested with *Xma*I and *Bam*HI to check the release of 1.4 kb *map2* fragment (Figure 4.2C). The clone was further confirmed by sequencing.

Knockout cells were initially confirmed in antibiotic selection media. Successful homologous recombination was confirmed by PCR using various set of primers as mentioned in methods section. Neomycin and Puromycin cassette with UTRs was confirmed by using primer 1 and primer 4. It showed an amplification of 3.9 kb fragment. Neomycin region was confirmed by using primer 7 and primer 8 which showed an amplification of 2.7 kb fragment. Puromycin region was confirmed by using primer 9 and primer 10 which showed an amplification of 479 bp. All respective amplifications are shown in Figure 4.3.

TH-1832_126106036

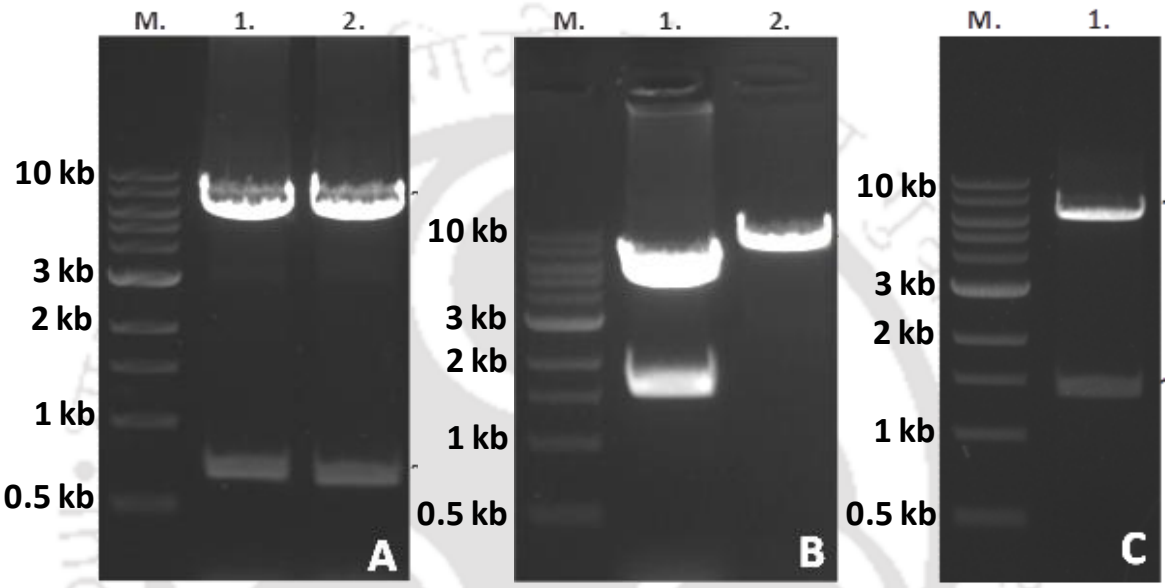

Figure 4.2: Preparation of molecular constructs for gene knockout studies as well as complementation studies. (A) Restriction digestion of pXGB1288-5'UTR-3'UTR*map2* construct. Lane M: 1 kb ladder, Lane 1: Confirmation of 5'UTR, showing release of 699 bp, Lane 2: Confirmation of 3'UTR, showing release of 600 bp (B) The Puromycin coding sequence was cloned in pXGB1288-5'UTR-3'UTR*map2* replacing neomycin gene. Confirmation of Puromycin sequence by digestion with *Bst*EII. Puromycin gene contains two recognition sites of *Bst*EII in coding frame whereas neomycin gene contains only one recognition site. Lane M: 1 kb ladder, Lane 1: digestion of pXGB3325-5'UTR-3'UTR*map2* construct by *Bst*EII, showing release of 1.6 kb fragment. Lane 2: digestion of pXGB1288-5'UTR-3'UTR*map2* construct by *Bst*EII (C) Confirmation of pXGB3325-*map2* for complementation studies. Lane M: 1 kb ladder, Lane 1: Restriction digestion showing release of 1.4 kb fragment.

TH-1832_126106036

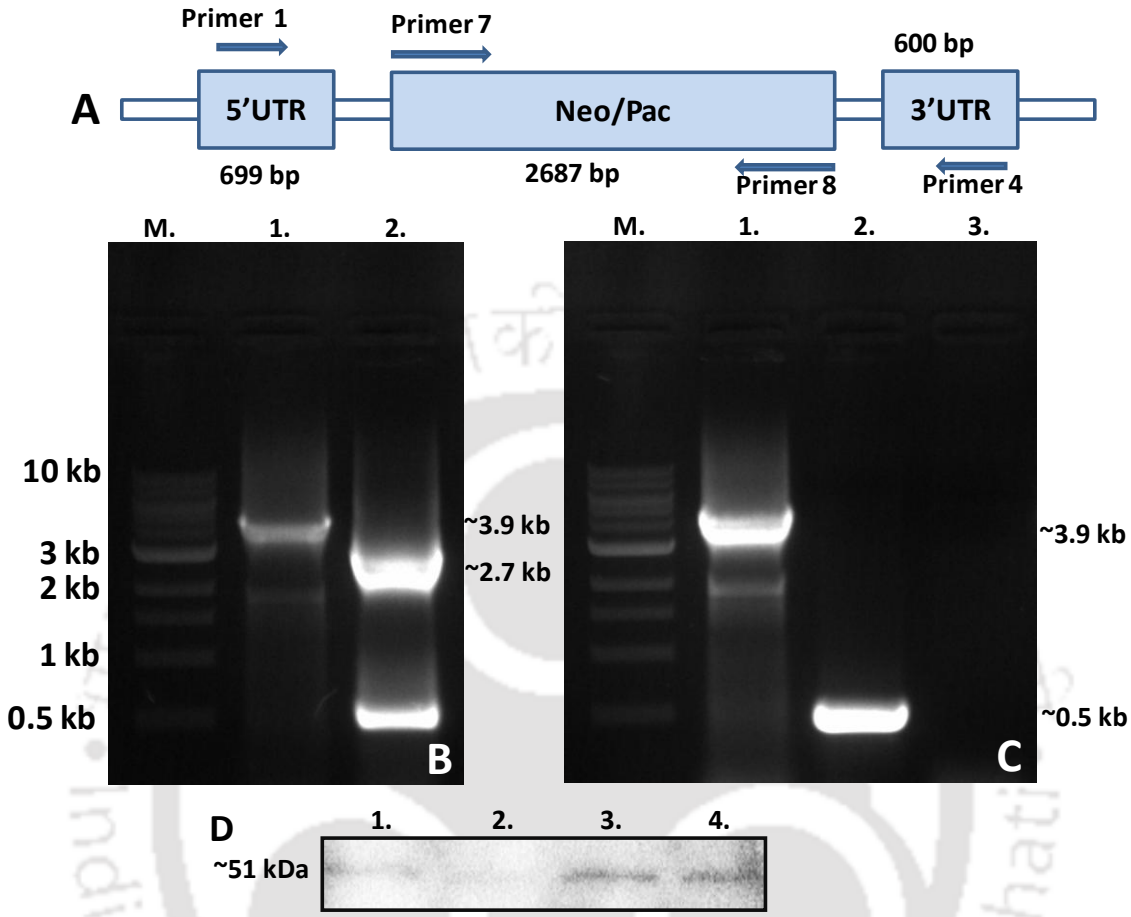

Figure 4.3: After initial confirmation of knockout in selection media, final confirmation of SKO and DKO by PCR amplification and western blot were performed. (A) Schematic representation of size of amplicon to be checked for integration. Primer 1 and primer 4 amplify the 5'UTR, Neo/Pac and 3'UTR region of the construct. The size of the amplicon will be 3986 bp. Primer 7 and primer 8 amplify the neomycin gene and size of the amplicon will be 2687 bp. Primer 9 and primer 10 amplify the Puromycin gene and size of the amplicon will be ~478 bp. (B) Confirmation of SKO, Lane M: 1 kb ladder, Lane 1: showing amplification of 3986 bp and lane 2 showing amplification of 2687 bp of neomycin region. (C) DKO confirmation, Lane M: 1 kb ladder, Lane 1: Amplification of neomycin region, Lane 2: Amplification of Puromycin gene, Lane 3: no amplification as MAP2 gene specific primer was used in PCR. (D) Western blot image showing confirmation of gene knockout. Lane 1: CKO cells, Lane 2: DKO cells, Lane 3: SKO cells and Lane 4: wild type parasite. The western blot data may not be final confirmation as house keeping protein antibody was not used as endogenous control because of limitations of availability of antibody in the laboratory. However, we have further validated the gene knock out by Real time-qPCR analysis.

TH-1832_126106036

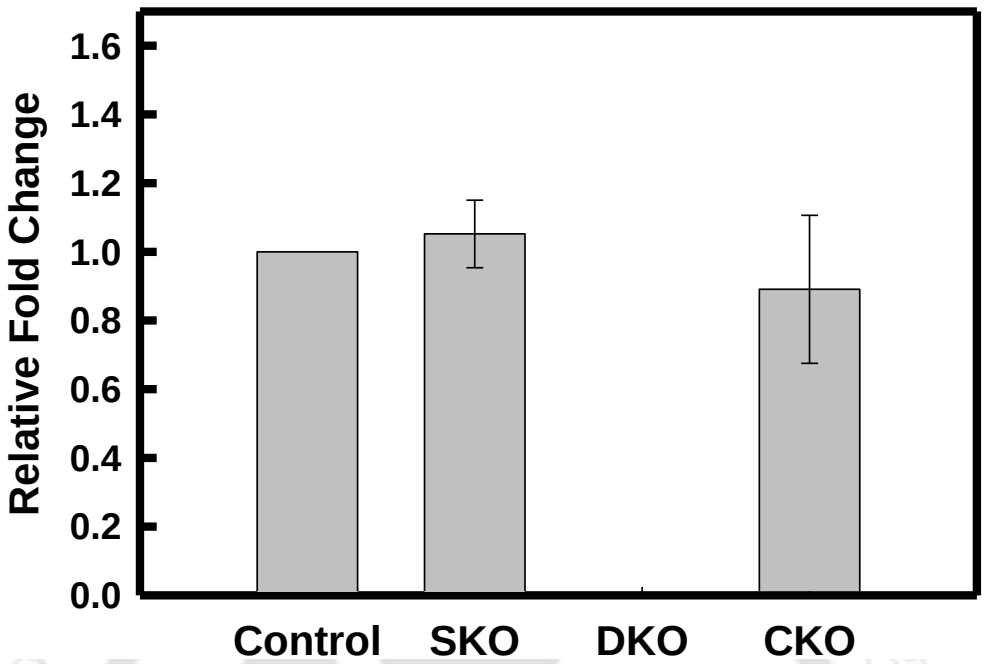

Figure 4.4: Real time-qPCR analysis of knockout cells to check the removal of *map2* gene. SKO, DKO and CKO cells were selected in appropriate selection media. mRNA expression of *map2* were checked in all cells. Alpha-tubulin was used as an endogenous control to normalize. Relative fold change was analyzed by Applied Biosystems SDS v2.0.6 software. The data clearly shows that the DKO cells do not show any mRNA expression of *map2* gene.

4.4.2 Confirmation of knockout by western blot and Real time-qPCR: Initially confirmation of knockout was done in selection marker and then homologous recombination was confirmed by PCR to verify the amplification of specific region in knockout cells. After that the comparative protein expressin of MAP2 was checked by western blot experiments and image was shown in Figure 4.4D. The western blot image clearly suggests the less expression of MAP2 protein in knock out cells, whereas no significant expression was found in DKO cells. However, the western blot data may not be final confirmation as house keeping protein antibody was not used as endogenous control because of limitations of availability of antibody in the laboratory. However, we have further validated the gene knock out by Real time-qPCR analysis. We have used alpha-tubulin as an endogenous control in Real time-qPCR and data was normalized. The DKO cells did not show any expression of *map2* gene, confirming the deletion of *map2* gene from the parasite.The data is shown in Figure 4.4.

TH-1832_126106036

4.4.3 Knockout of map2 gene shows significant decrease in caspase-3/7 protease like activity after treatment with miltefosine: Several groups have reported that after treatment with miltefosine, a well known anti-leishmanial drug; the parasite undergoes apoptotic like cell death processes with increased caspase-3/7 like protease activity. We have found in our studies that the wild type cells treated with miltefosine (25 µM for 24 hr incubation at 25ºC), showed an increased Cas3/7 protease like activity compared to untreated cells. SKO cells treated with miltefosine (25 µM, 24 hr) showed a decrease in caspase-3/7 protease like activity compared to wild type miltefosine treated parasite. Miltefosine treated DKO cells showed further decrease in caspase-3/7 protease like activity whereas miltefosine treated CKO cells showed an increase in Cas3/7 protease like activity as compared to DKO cells. In parallel set of control experiment, miltefosine induced wild type cells were incubated with caspase-3 inhibitor (N-Acetyl-Asp-Glu-Val-Asp-al) and protease activity was measured (Figure 4.5). This data clearly suggests the involvement of *Ld*MAP2 in miltefosine induced PCD of parasite as *map2* knocked out parasite showed significant decrease in caspase-3/7 protease like activity.

4.4.4 Knockout of map2 gene causes inhibition of oligonucleosomal-DNA fragmentation in miltefosine treated L. donovani: Genomic DNA fragmentation into oligonucleosomal units are considered as a hall mark of apoptotic processes. It has been reported that treatment with miltefosine (25 µM) causes the DNA fragmentation in *Leishmania* parasite. The wild type cells treated with miltefosine (25 µM, 18 hr at incubation at 25ºC) showed fragmentation of genomic DNA on agarose gel electrophoresis whereas miltefosine treated (25 µM, 18 hr) SKO and DKO cells did not show fragmentation of genomic DNA into oligonucleosomal fragments on agarose gel electrophoresis (Figure 4.6), suggesting the inhibition of oligonucleosomal DNA fragmentation after miltefosine treatment in *map2* knockout mutants.

TH-1832_126106036

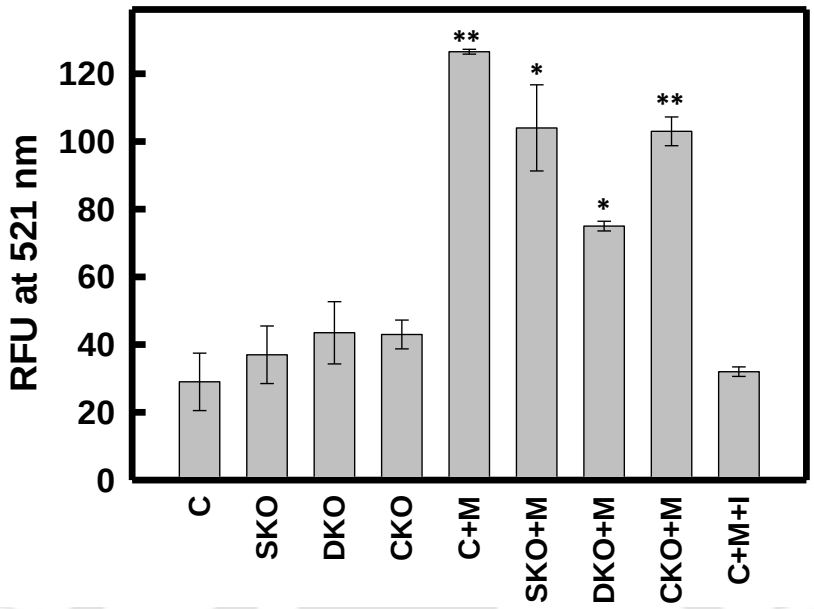

Figure 4.5: Activation of Caspase-3/7 protease like activity after induction with miltefosine. Maximum activity was observed in control promastigotes treated with miltefosine. The activity was decreased in SKO cells. In DKO cells, the cas-3/7 protease activity was further decreased. In CKO cells, the activity was increased after miltefosine treatment. Statistical analysis was done using Student's unpaired t-test in SigmaPlot software (*denotes p value ≤0.05, **denotes p value ≤ 0.01 and *** denotes p value ≤ 0.001).

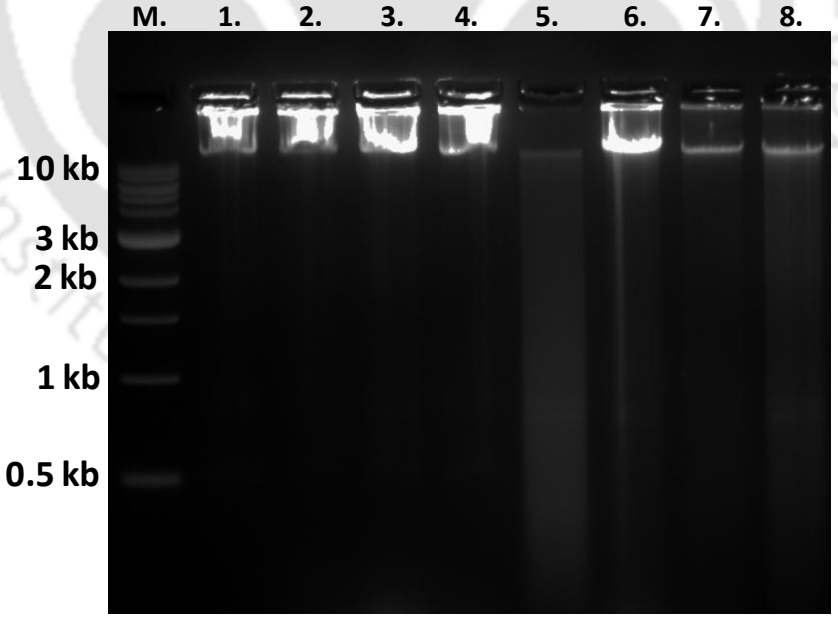

Figure 4.6: DNA fragmentation analysis of *L. donovani* promastigotes. Lane M: 1kb ladder, Lane 1: Control cells, Lane 2: SKO cells, Lane 3: DKO cells, Lane 4: CKO cells, Lane 5: Control promastigotes treated with 25 µM of miltefosine showing fragmentation of genomic DNA, Lane 6: SKO cells treated with miltefosine, Lane 7: DKO cells induced with miltefosine and Lane 8: CKO cells induced with miltefosine.

TH-1832_126106036

***4.4.5 Knockout of map2 gene prevents the collapse of mitochondrial transmembrane potential (ΔΨm) caused by miltefosine*:** The depolarization of mitochondrial membrane potential is an important biochemical marker used to analyze PCD in higher eukaryotic organisms. Several studies suggest that the mitochondrial membrane potential of protozoan parasite get collapsed after treatment with miltefosine. The change in membrane potential was measured using MitoCapture^{TM} dye. At normal mitochondrial membrane potential, dye aggregates at the mitochondria and gives red fluorescence whereas at decreased membrane potential, dye remains in the cytoplasm at monomeric form and gives green fluorescence. As expected, wild type cells showed 89.9 % cells with red fluorescence whereas wild type cells treated with miltefosine (25 µM, 12 hr), showed 60.56 % cells with green fluorescence. SKO and DKO cells treated with miltefosine (25 µM, 12 hr) did not show an increase in green fluorescence compared to the untreated cells (Figure 4.7). This data suggests that the *map2* knockout mutant prevents the collapse of mitochondrial transmembrane potential ($\Delta\Psi$m) caused by miltefosine.

***4.4.6 Knockout of map2 gene prevents the phosphatidyl serine externalization after miltefosine treatment*:** Miltefosine is well known anti-leishmanial compound which causes translocation of phosphatidyl serine on outer plasma membrane in case of *Leishmania* promastigotes and has been reported by several groups. A combined use of annexin V-FITC and PI was done to distinguish the apoptotic and necrotic cell death. Annexin V-FITC binds to exposed phosphatidyl serine with high affinity whereas PI selectively enters inside the necrotic cells and binds to DNA which allows the detection of both apoptotic and necrotic cells. Wild type promastigotes treated with 25 µM of miltefosine for 18 h resulted in 54.52 % of Annexin-V positive cells. SKO cells treated with miltefosine shows 13.09 % Annexin-V positive, DKO cells treated with miltefosine shows 14.60 % Annexin-V positive and CKO cells shows 17.09 % Annexin-V positive as shown in Figure 4.8. There is no significant cell death phenotype was observed in knockout cells treated with miltefosine, suggesting that the knockout parasite may be unresponsive to miltefosine.

TH-1832_126106036

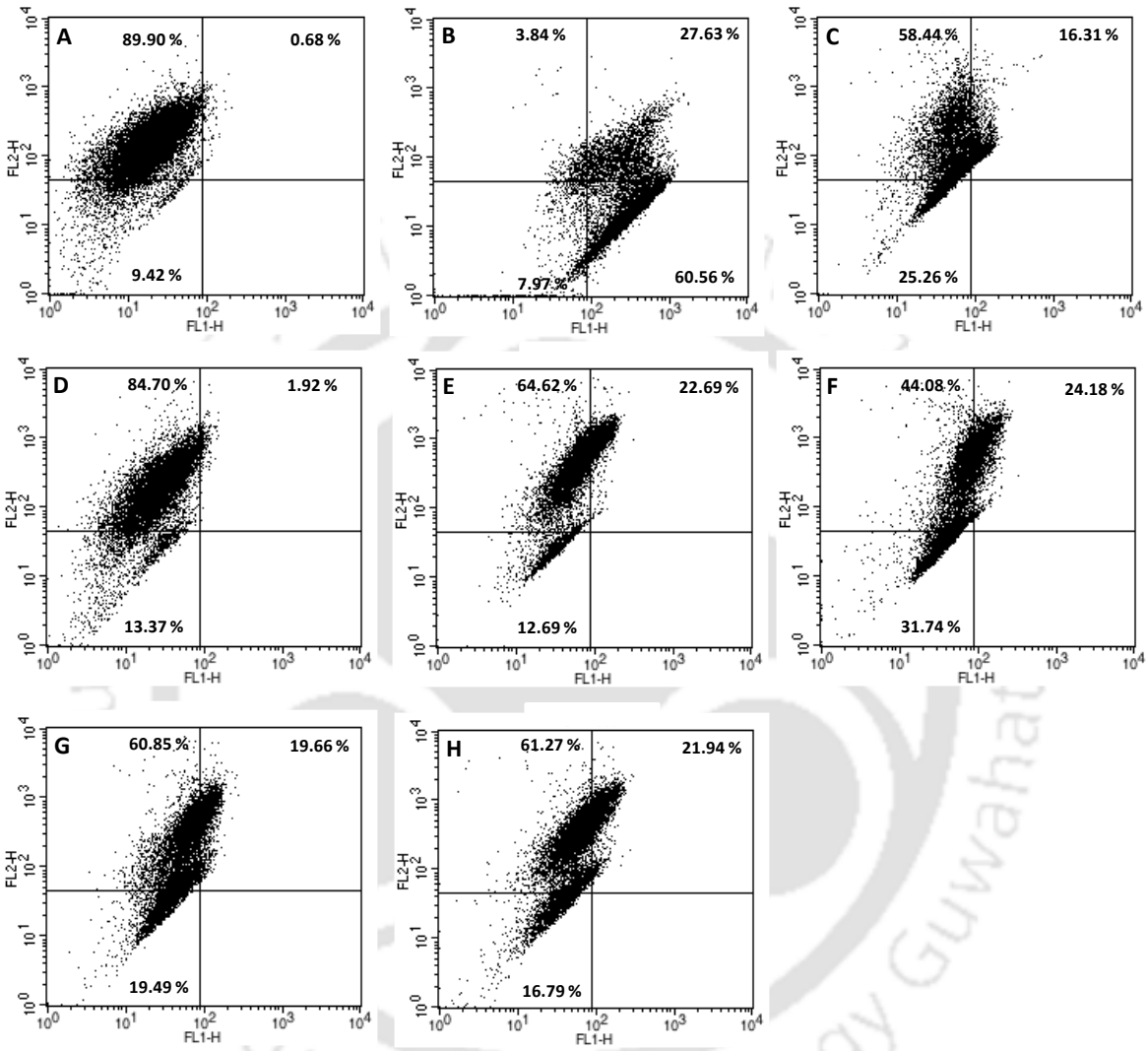

Figure 4.7: Flow Cytometry analysis to check the transmembrane potential of mitochondria. FL1 represents the green channel and FL2 represents red channel. (A) Control promastigotes, showing 89.9 % cells with red fluorescence (B) Control cell induced with 25 µM miltefosine, showing more than 60 % green fluorescence (C) CKO cells (D) SKO cells (E) SKO cells induced with miltefosine (F) CKO cells treated with miltefosine (G) DKO cells and (H) DKO cells induced with miltefosine.

TH-1832_126106036

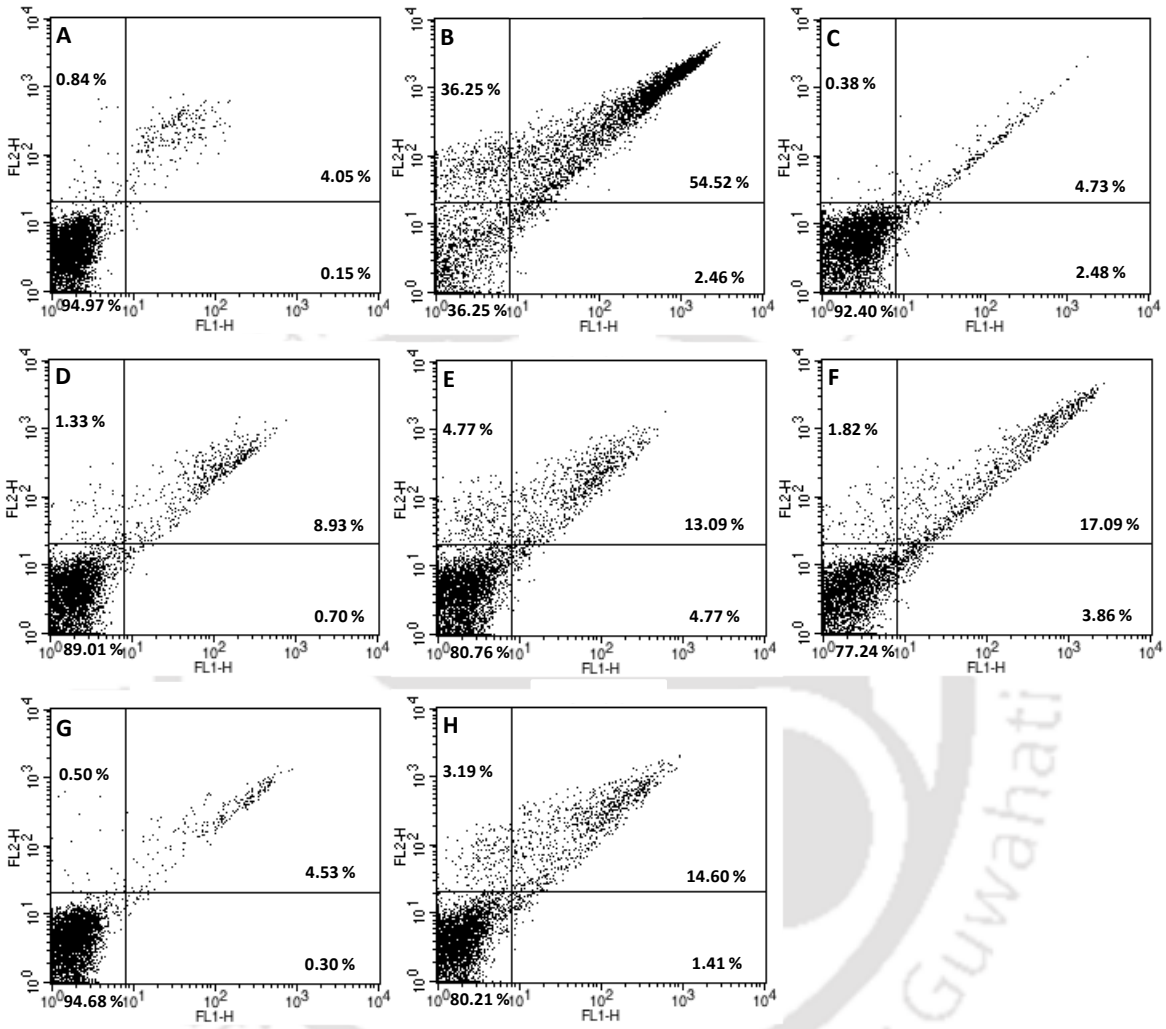

Figure 4.8: Flow Cytometry analysis to check the Externalization of phosphatidyl serine on plasma membrane, analysed by annexin V-FITC and PI staining. FL1 represents the green channel and FL2 represents red channel (A) Control promastigotes, (B) Control cell induced with 25 µM miltefosine, showing more than 50 % cells in apoptotic state (C) CKO cells (D) SKO cells (E) SKO cells induced with miltefosine (F) CKO cells treated with miltefosine (G) DKO cells and (H) DKO cells induced with miltefosine.

TH-1832_126106036

***4.4.7 Leishmanicidal effect of miltefosine on knockout mutants shows the miltefosine less responsive phenotype*:** Cell viability assay was done using MTT [3-(4,5-dimethylthiazol-2-yl)-2,5-diphenyltetrazolium bromide] assay as mentioned in methods section. Wild type cells treated with miltefosine showed significant leishmanicidal activity with IC_{50} values of 15.2 µM whereas SKO cells at 24.8 µM, DKO cells at 25 µM and CKO cells at 21 µM of miltefosine concentration (Figure 4.9). The data shows that the DKO parasites survive much better in presence of miltefosine compared to wild type cells, suggesting that the *map2* knockout parasite showing miltefosine less responsive phenotype.

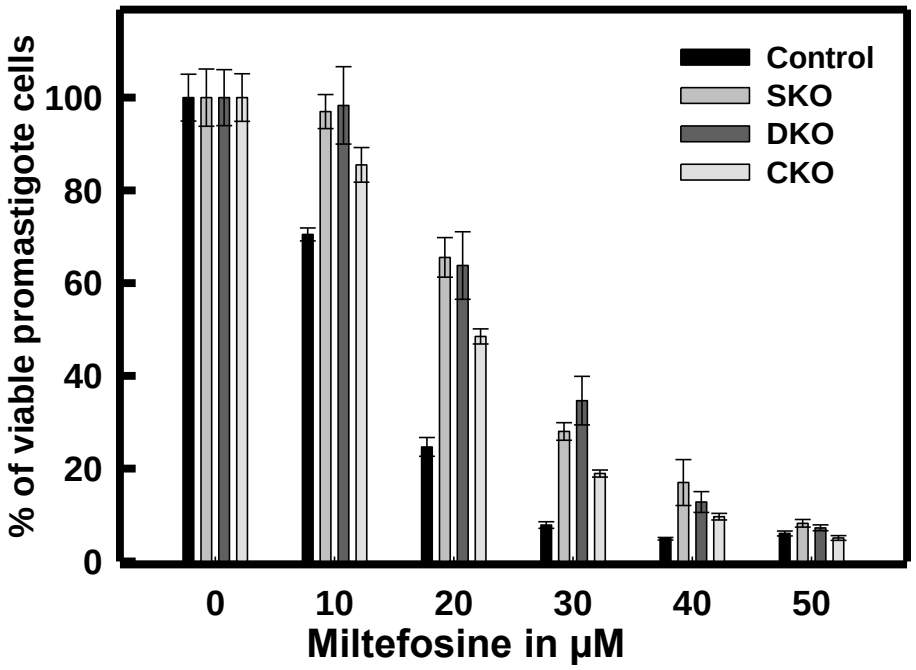

Figure 4.9: Cell proliferation assay in presence of miltefosine. Control, SKO, DKO and CKO cells were incubated with varying concentration of miltefosine. At reported IC_{50} value of miltefosine, knockout cells survive better than control cells. Data represents the mean ± SD of three experiments.

***4.4.8 Knock out parasite shows less infectivity on human macrophage cell line*:** Infectivity of the parasite was evaluated on human macrophage cell lines as mentioned in methods section. Approximately, 60-70 macrophages were counted manually after Giemsa staining using bright field microscopy at 40x resolution. The time point chosen to check the infectivity of the parasite was based on our previous reports (*Bhardwaj et al., 2016*). After 24

TH-1832_126106036

hr incubation of human macrophages with wild type, SKO, DKO and CKO parasite; the infectivity index was calculated and shown in Figure 4.10. The significant decrease in infectivity index as observed in SKO and DKO cells compared to control cells, suggesting the involvement of MAP2 in processing of important cellular proteins which are required for receptor mediated endocytosis processes.

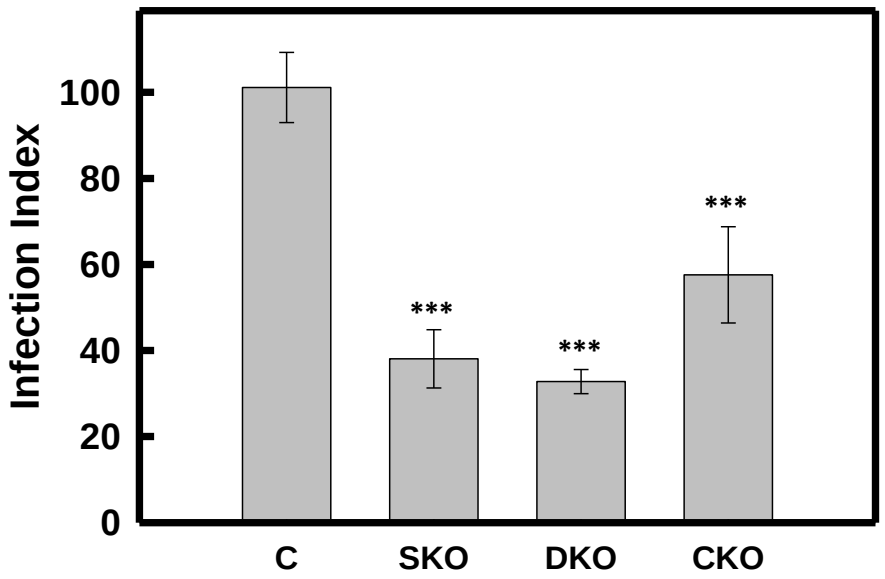

Figure 4.10: Infectivity Assay of *L. donovani* on U937 macrophage cell line. Macrophages were stained by Geimsa stain and amastigotes were counted using light microscope at 60 X. The infection index was calculated by using the formula as % of infected macrophages x total number of amastigotes per macrophages. Compared to control cells, SKO and DKO cells shows significantly lowered infection index. Data represents mean ± SD of three experiments. Statistical analysis was done using Student's unpaired t-test in SigmaPlot software (*denotes p value ≤0.05, **denotes p value ≤ 0.01 and *** denotes p value ≤ 0.001).

4.5 Discussion

Methionine aminopeptidase 2 is present on chromosome number 21 of *L. donovani* which is diploid in nature. To remove the both copy number of MAP2 from genome of *Leishmania*, two knockout cassettes containing two different antibiotic selection markers (G418 and Puromycin) was prepared. Further, *map2* gene was cloned in expression vector containing phleomycin as a selection marker to complement the effect of MAP2 in parasite.

TH-1832_126106036

In most of our experiments, the complementation of MAP2 by episomal expression is not found to be sufficient to overcome the effect of gene knock out as reports suggest that the episomal expression is lesser compared to wild type (*Taheri et al., 2014*). Moreover, the parasite shows varied expression level of proteins due to random segregation of expression vector during cell division. In all the experiments, wild type cells were also electroporated with empty vector and stabilized in fresh M199 media for minimum 24 hr before the experiment.

Methionine aminopeptidase 2 (MAP2) are known to be physiologically important enzyme which catalyzes the removal of N-terminal methionine residues from nascent polypeptide. The removal of methionine residue is an important post translational modification which required for proper machinery of cellular functions. We have found in our previous studies (Chapter III) that after using small molecule inhibitor TNP-470, the miltefosine induced parasite shows inhibition of genomic DNA fragmentation, prevents the change in transmembrane potential of mitochondria, decrease in Caspase-3/7 protease like activity, no increase in intracellular calcium pool but did not able to prevent the increase in Annexin-V positive cells and cell death. We have also observed that the miltefosine treated parasite shows an increased up-regulation of mRNA transcript of *map2* by several folds (Chapter II). Based on our previous studies, we have expected that gene knockout parasite should not show any biochemical markers of apoptotic features after induction of miltefosine as MAP2 was found to be an important regulator of miltefosine induced cell death pathways in protozoan parasites. In biochemical analysis of apoptotic markers, the knockout cells treated with miltefosine (25 μM) showed the inhibition of genomic DNA fragmentation into nucleosomal units. It further prevents the collapse of mitochondrial transmembrane potential, and decrease in caspase3/7 protease like activity. As reported in our earlier chapter, TNP-470 treated parasites shows the increase in percentage of Annexin-V positive cells after induction of apoptosis by miltefosine. It is worth mentioning here that TNP-470 is known to be specific inhibitor of MAP2. We further expected that if MAP2 is involved in PCD pathways of parasite, miltefosine treated *map2* knockout parasites will go in some other mode of cell death pathway such as necrosis other than the apoptotic pathways. In contrary to previous studies (Chapter III), *map2* gene knock out parasite prevents the externalization of phosphatidyl serine on plasma membrane as compared to wild type after induction of

TH-1832_126106036

miltefosine and approximately 70% -80% cells were Annexin-V negative and PI negative, suggesting the involvement of MAP2 to generate miltefosine less responsive phenotypic parasite. This data also points out towards the additional target(s) of TNP-470 other than MAP2 of parasite, as *map2* deleted parasite significantly decreases the total percentage of Annexin-V positive cells in presence of miltefosine. To validate this finding, the cell viability assay was done in varying concentration of miltefosine (10 µM to 50 µM) on wild type cells, SKO, DKO and CKO cells. The increase in IC_{50} value was observed in knock out parasite compared to wild type. The data imply that the *map2* knockout parasite shows a miltefosine less-responsive phenotype. Further, *map2* knockout parasite did not show any significant growth retardation effect whereas infectivity of parasite on U937 human macrophage cell line is significantly decreased compared to wild type. The overall study suggests that the MAP2 has surfaced as an important regulator of miltefosine induced PCD in the protozoan parasite which will decipher the previously unknown mechanism behind miltefosine induced cell death in *L. donovani* and which would also aid in explaining the miltefosine induced resistance in the parasite. The current work promises to uncover key molecular underpinnings of the programmed cell death pathway of *L. donovani* as well as gaining a broad understanding of the process of apoptosis as a whole in the dimorphic parasites.

TH-1832_126106036

Chapter V

Summary of Research work

5.1 Abstract

Absence of caspases**,** important regulator of PCD of parasite, in the in genome of *Leishmania donovani* and several reports of apoptotic mediated cell death processes after treatment with various anti-leishmanial drugs with increased in caspase-3/7 protease like activity made the background of the current study. Further, the role of various proteases in PCD of parasite remains unexplored. In an attempt to understand the role of proteases in PCD of parasite, up-regulation of mRNA transcript of various protease genes was analyzed by real time-quantitative PCR in apoptotic condition. The gene showing maximum increase (*Ld*MAP2) in the up-regulation of mRNA was considered for further studies to validate their role. Further, biochemical studies to check the markers of apoptosis were analyzed in presence of small molecule inhibitor TNP-470. The data revealed the role of *Ld*MAP2 in PCD of parasite as *Ld*MAP2 inhibited parasite did not show biochemical features of apoptosis after treatment with miltefosine. To further validate the role of *Ld*MAP2 in PCD of parasite, gene knockout of *map2* using homologous recombination approach was employed. The *map2* knock out parasite revealed that the *Ld*MAP2 is an important regulator of PCD of parasite. Moreover, *map2* knock out parasite shows a miltefosine less responsive phenotype. The data was validated by cell viability assay in presence of varying concentration of miltefosine.

TH-1832_126106036

5.2 Introduction to leishmaniasis and apoptotic death processes in *Leishmania:* Leishmaniasis is a vector borne disease caused by different species of *Leishmania.* The parasite is transmitted by bite of female sand fly, *Phlebotomus.* Mainly three different clinical forms of leishmaniasis are reported namely cutaneous, muco-cutaneous and visceral leishmaniasis. Visceral leishmaniasis, also known as kala-azar is the most prevalent form of disease in India. It is the most dangerous form of disease, as it affects mainly the internal organs of body such as liver, spleen and bone-marrow. There are very few drugs available for the treatment of leishmaniasis. Moreover, the parasite started showing resistance against the available drugs. Several reports suggest that after treatment with various anti-leishmanial drug the parasite undergoes apoptotic mediated cell death processes which shows all the biochemical markers to analyze the PCD processes in higher eukaryotic organisms. The genome sequencing of *L. donovani* has been completed and the available sequences reveal that the caspase genes are absent in their genome. Role of some other cysteine proteases in PCD of parasite is well documented by several groups. However, role of various other proteases in PCD of parasite are not studied in detail.

5.3 Exploring realm of proteases of *Leishmania donovani* genome and gene expression analysis of proteases under apoptotic condition: In an attempt to understand the role of proteases in PCD of parasite, the GeneDB database was explored and available proteases were identified by *in silico* approach such as BlastP, Uniprot-KB. The 141 proteases were identified and classified into their respective clan and family. The apoptosis was induced by miltefosine. Under apoptotic condition of the parasite, gene expression analyses of representative protease(s) from each clan showed altered expression levels of various proteases. Up-regulation of several cysteine proteases and metallo-proteases were observed in apoptotic processes. Moreover, *MAP2* gene showed several fold increase in the expression level in apoptotic condition. The data indicates possible role of MAP2 in apoptotic processes, directly or indirectly. Further, the up-regulation of protease genes involved in autophagic processes are also observed after treatment with miltefosine. The data clearly suggest some crosstalk between autophagy and apoptotic mode of cell death of *Leishmania* parasite.

TH-1832_126106036

5.4 Methionine aminopeptidase 2 is a key regulator of apoptotic like cell death in *Leishmania donovani:* In previous studies (Chapter II), *MAP2* gene showed several fold increase (~3.5 times) in the expression level in apoptotic conditions. This data prompted us to investigate the role of *Ld*MAP2 in PCD of parasite. A small molecule inhibitor, TNP-470 which belongs to fumagillin family and reported to bind with MAP2 was used to study the effect of *Ld*MAP2 on PCD of parasite. The protease *Ld*MAP2 was successfully cloned, protein was purified and biochemical characterization was done. The data showed that the TNP-470 inhibits the activity of recombinant *Ld*MAP2 as a competitive mode of inhibition. At 100 µM TNP-470 concentrations, the calculated *Ki* value was found to be 13.5 nM. Further, the leishmanicidal activity of TNP-470 on promastigotes was analyzed and the calculated IC_{50} value was found to be 15 µM. We further validate the role of *Ld*MAP2 in miltefosine induced apoptotic cell death. The data revealed that the TNP-470, an inhibitor of MAP2, inhibits programmed cell death in miltefosine treated promastigotes. It inhibits the biochemical features of metazoan apoptosis, including caspase3/7 protease like activity, oligonucleosomal DNA fragmentation, collapse of mitochondrial transmembrane potential, and increase in cytosolic pool of calcium ions but did not prevent the cell death and phosphatidyl serine externalization. This finding clearly points out that the MAP2 inhibitor prevented the induction of apoptosis in miltefosine treated promastigotes, but was not able to prevent cell death of the parasites. The data suggest the role of *Ld*MAP2, as an effector molecule in higher eukaryotic organisms which is important for the induction of apoptosis but unable to prevent the cell death.

5.5 Understanding the role of methionine aminopeptidase 2 in programmed cell death of *Leishmania donovani* by studying the *map2* knockout mutants: To further validate the role of *Ld*MAP2 in PCD of parasite, *map2* gene knockout strain was prepared by homologous recombination approach. The removal of *map2* gene from the parasite was confirmed by PCR amplification and western blot experiments. The complementation of *map2* gene was also confirmed by western blot as complemented vector showed an episomal expression of *Ld*MAP2. Apoptosis was induced by miltefosine as mentioned in previous sections. We have found that miltefosine treated knock out mutants did not able to show the

TH-1832_126106036

characteristic biochemical markers of apoptosis such as fragmentation of genomic DNA into oligonucleosomal units, increase in caspase-3/7 protease like activity, collapse in the transmembrane potential of mitochondria and exposure of phosphatidyl serine exposure on plasma membrane. Moreover, *map2* knock out parasite escaped the toxic effect of miltefosine, as at lower concentration of miltefosine knocked out parasite showed an increase in IC_{50} value than wild type parasite. The data points out towards the role of *Ld*MAP2 to generate the miltefosine less responsive phenotype.

TH-1832_126106036

Bibliography

Aitken A, Cohen P, Santikarn S, Williams DH, Calder AG, Smith A, Klee CB. Identification of the NH2-terminal blocking group of calcineurin B as myristic acid. *FEBS Lett.* 1982 Dec 27;150(2):314-8.

Alnemri ES, Livingston DJ, Nicholson DW, Salvesen G, Thornberry NA, Wong WW, Yuan J. Human ICE/CED-3 protease nomenclature. *Cell*. 1996 Oct 18;87(2):171.

Alvar J, Aparicio P, Aseffa A, Den Boer M, Cañavate C, Dedet JP, Gradoni L, Ter Horst R, López-Vélez R, Moreno J. The relationship between leishmaniasis and AIDS: the second 10 years. *Clin Microbiol Rev*. 2008 Apr;21(2):334-59

Alvar J, Vélez ID, Bern C, Herrero M, Desjeux P, Cano J, Jannin J, den Boer M; WHO Leishmaniasis Control Team.. Leishmaniasis worldwide and global estimates of its incidence. *PLoS One*. 2012;7(5):e35671.

Ameisen JC, Idziorek T, Billaut-Mulot O, Loyens M, Tissier JP, Potentier A, Ouaissi A. Apoptosis in a unicellular eukaryote (Trypanosoma cruzi): implications for the evolutionary origin and role of programmed cell death in the control of cell proliferation, differentiation and survival. *Cell Death Differ*. 1995 Oct;2(4):285-300.

Andrade F, Roy S, Nicholson D, Thornberry N, Rosen A, Casciola-Rosen L. Granzyme B directly and efficiently cleaves several downstream caspase substrates: implications for CTL-induced apoptosis. *Immunity*. 1998 Apr;8(4):451-60.

Aoyagi T, Takeuchi T, Matsuzaki A, Kawamura K, Kondo S. Leupeptins, new protease inhibitors from Actinomycetes. *J Antibiot (Tokyo).* 1969 Jun;22(6):283-6.

Apweiler R, Bairoch A, Wu CH, Barker WC, Boeckmann B, Ferro S, Gasteiger E, Huang H, Lopez R, Magrane M, Martin MJ, Natale DA, O'Donovan C, Redaschi N, Yeh LS. UniProt: the Universal Protein knowledgebase. *Nucleic Acids Res.* 2004 Jan 1;32(Database issue):D115-9.

Aravind L, Dixit VM, Koonin EV. Apoptotic molecular machinery: vastly increased complexity in vertebrates revealed by genome comparisons. *Science*. 2001 Feb 16;291(5507):1279-84.

Arico-Muendel CC, Belanger B, Benjamin D, Blanchette HS, Caiazzo TM, Centrella PA, DeLorey J, Doyle EG, Gradhand U, Griffin ST, Hill S, Labenski MT, Morgan BA, O'Donovan G, Prasad K, Skinner S, Taghizadeh N, Thompson CD, Wakefield J, Westlin W, White KF. Metabolites of PPI-2458, a selective, irreversible inhibitor of methionine aminopeptidase-2: structure determination and in vivo activity. *Drug Metab Dispos*. 2013 Apr;41(4):814-26

Arnoult D, Akarid K, Grodet A, Petit PX, Estaquier J, Ameisen JC. On the evolution of programmed cell death: apoptosis of the unicellular eukaryote Leishmania major

TH-1832_126106036

involves cysteine proteinase activation and mitochondrion permeabilization. *Cell Death Differ*. 2002 Jan;9(1):65-81.

Bañuls AL, Hide M, Prugnolle F. Leishmania and the leishmaniases: a parasite genetic update and advances in taxonomy, epidemiology and pathogenicity in humans. *Adv Parasitol*. 2007;64:1-109.

Barrett AJ, Kembhavi AA, Hanada K. E-64 [L-trans-epoxysuccinyl-leucyl-amido(4-guanidino)butane] and related epoxides as inhibitors of cysteine proteinases. *Acta Biol Med Ger*. 1981;40(10-11):1513-7.

Ben-Bassat A, Bauer K, Chang SY, Myambo K, Boosman A, Chang S. Processing of the initiation methionine from proteins: properties of the Escherichia coli methionine aminopeptidase and its gene structure. *J Bacteriol*. 1987 Feb;169(2):751-7.

Beresford PJ, Xia Z, Greenberg AH, Lieberman J. Granzyme A loading induces rapid cytolysis and a novel form of DNA damage independently of caspase activation. *Immunity*. 1999 May;10(5):585-94.

Bern C, Adler-Moore J, Berenguer J, Boelaert M, den Boer M, Davidson RN, Figureueras C, Gradoni L, Kafetzis DA, Ritmeijer K, Rosenthal E, Royce C, Russo R, Sundar S, Alvar J. Liposomal amphotericin B for the treatment of visceral leishmaniasis. *Clin Infect Dis*. 2006 Oct 1;43(7):917-24.

Bernier SG, Lazarus DD, Clark E, Doyle B, Labenski MT, Thompson CD, Westlin WF, Hannig G. A methionine aminopeptidase-2 inhibitor, PPI-2458, for the treatment of rheumatoid arthritis. *Proc Natl Acad Sci U S A*. 2004 Jul 20;101(29):10768-73.

Berriman M, Ghedin E, Hertz-Fowler C, Blandin G, Renauld H, Bartholomeu DC, Lennard NJ, Caler E, Hamlin NE, Haas B, Böhme U, Hannick L, Aslett MA, Shallom J, Marcello L, Hou L, Wickstead B, Alsmark UC, Arrowsmith C, Atkin RJ, Barron AJ, Bringaud F, Brooks K, Carrington M, Cherevach I, Chillingworth TJ, Churcher C, Clark LN, Corton CH, Cronin A, Davies RM, Doggett J, Djikeng A, Feldblyum T, Field MC, Fraser A, Goodhead I, Hance Z, Harper D, Harris BR, Hauser H, Hostetler J, Ivens A, Jagels K, Johnson D, Johnson J, Jones K, Kerhornou AX, Koo H, Larke N, Landfear S, Larkin C, Leech V, Line A, Lord A, Macleod A, Mooney PJ, Moule S, Martin DM, Morgan GW, Mungall K, Norbertczak H, Ormond D, Pai G, Peacock CS, Peterson J, Quail MA, Rabbinowitsch E, Rajandream MA, Reitter C, Salzberg SL, Sanders M, Schobel S, Sharp S, Simmonds M, Simpson AJ, Tallon L, Turner CM, Tait A, Tivey AR, Van Aken S, Walker D, Wanless D, Wang S, White B, White O, Whitehead S, Woodward J, Wortman J, Adams MD, Embley TM, Gull K, Ullu E, Barry JD, Fairlamb AH, Opperdoes F, Barrell BG, Donelson JE, Hall N, Fraser CM, Melville SE, El-Sayed NM. The genome of the African trypanosome Trypanosoma brucei. *Science*. 2005 Jul 15;309(5733):416-22.

Besteiro S, Williams RA, Morrison LS, Coombs GH, Mottram JC. Endosome sorting and autophagy are essential for differentiation and virulence of Leishmania major. *J Biol Chem*. 2006 Apr 21;281(16):11384-96.

TH-1832_126106036

Betin VM, Lane JD. Atg4D at the interface between autophagy and apoptosis. *Autophagy*. 2009 Oct;5(7):1057-9.

Betin VM, Lane JD. Caspase cleavage of Atg4D stimulates GABARAP-L1 processing and triggers mitochondrial targeting and apoptosis. *J Cell Sci*. 2009 Jul 15;122(Pt 14):2554-66.

Betin VM, MacVicar TD, Parsons SF, Anstee DJ, Lane JD. A cryptic mitochondrial targeting motif in Atg4D links caspase cleavage with mitochondrial import and oxidative stress. *Autophagy*. 2012 Apr;8(4):664-76.

Beverley SM, Clayton CE. Transfection of Leishmania and Trypanosoma brucei by electroporation. *Methods Mol Biol*. 1993;21:333-48.

Bhardwaj R, Kumar R, Singh SK, Selvaraj C, Dubey VK. Understanding the importance of conservative hypothetical protein LdBPK_070020 in Leishmania donovani and its role in subsistence of the parasite. Arch Biochem Biophys. 2016 Apr 15;596:10-21.

Bogitsh BJ, Middleton OL, Ribeiro-Rodrigues R. Effects of the antitubulin drug trifluralin on the proliferation and metacyclogenesis of Trypanosoma cruzi epimastigotes. *Parasitol Res*. 1999 Jun;85(6):475-80.

BoseDasgupta S, Das BB, Sengupta S, Ganguly A, Roy A, Dey S, Tripathi G, Dinda B, Majumder HK. The caspase-independent algorithm of programmed cell death in Leishmania induced by baicalein: the role of LdEndoG, LdFEN-1 and LdTatD as a DNA 'degradesome'. *Cell Death Differ*. 2008 Oct;15(10):1629-40.

Boutin JA, Myristoylation, *Cell Signal*. 1997;9:15–35.

Boya P, Andreau K, Poncet D, Zamzami N, Perfettini JL, Metivier D, Ojcius DM, Jäättelä M, Kroemer G. Lysosomal membrane permeabilization induces cell death in a mitochondrion-dependent fashion. *J Exp Med*. 2003 May 19;197(10):1323-34.

Bozhkov PV, Suarez MF, Filonova LH, Daniel G, Zamyatnin AA Jr, Rodriguez-Nieto S, Zhivotovsky B, Smertenko A. Cysteine protease mcII-Pa executes programmed cell death during plant embryogenesis. *Proc Natl Acad Sci U S A*. 2005 Oct 4;102(40):14463-8.

Bradshaw RA, Brickey WW, Walker KW. N-terminal processing: the methionine aminopeptidase and N alpha-acetyl transferase families. *Trends Biochem Sci*. 1998 Jul;23(7):263-7.

Braun Breton C, Pereira da Silva LH. Malaria proteases and red blood cell invasion. Parasitol Today. 1993 Mar;9(3):92-6.

Broustas CG, Gokhale PC, Rahman A, Dritschilo A, Ahmad I, Kasid U. BRCC2, a novel BH3-like domain-containing protein, induces apoptosis in a caspase-dependent manner. *J Biol Chem*. 2004 Jun 18;279(25):26780-8.

TH-1832_126106036

Burleigh BA, Woolsey AM. Cell signalling and Trypanosoma cruzi invasion. *Cell Microbiol*. 2002 Nov;4(11):701-11

Buss JE, Mumby SM, Casey PJ, Gilman AG, Sefton BM. Myristoylated alpha subunits of guanine nucleotide-binding regulatory proteins. *Proc Natl Acad Sci USA*. 1987 Nov;84(21):7493-7.

Caffrey P, Lynch S, Flood E, Finnan S, Oliynyk M. Amphotericin biosynthesis in Streptomyces nodosus: deductions from analysis of polyketide synthase and late genes. *Chem Biol.* 2001 Jul;8(7):713-23.

Cai CZ, Han LY, Ji ZL, Chen X, Chen YZ. SVM-Prot: Web-based support vector machine software for functional classification of a protein from its primary sequence. *Nucleic Acids Res.* 2003 Jul 1;31(13):3692-7

Capony F, Rougeot C, Montcourrier P, Cavailles V, Salazar G, Rochefort H. Increased secretion, altered processing, and glycosylation of pro-cathepsin D in human mammary cancer cells. *Cancer Res*. 1989 Jul 15;49(14):3904-9.

Carafoli E, Molinari M. Calpain: a protease in search of a function? *Biochem Biophys Res Commun*. 1998 Jun 18;247(2):193-203.

Carmona-Gutierrez D, Eisenberg T, Büttner S, Meisinger C, Kroemer G, Madeo F. Apoptosis in yeast: triggers, pathways, subroutines. *Cell Death Differ*. 2010 May;17(5):763-73.

Carr SA, Biemann K, Shoji S, Parmelee DC, Titani K. n-Tetradecanoyl is the NH2-terminal blocking group of the catalytic subunit of cyclic AMP-dependent protein kinase from bovine cardiac muscle. *Proc Natl Acad Sci U S A*. 1982 Oct;79(20):6128-31.

Carter KC, Hutchison S, Henriquez FL, Légaré D, Ouellette M, Roberts CW, Mullen AB. Resistance of Leishmania donovani to sodium stibogluconate is related to the expression of host and parasite gamma-glutamylcysteine synthetase. *Antimicrob Agents Chemother*. 2006 Jan;50(1):88-95

Castanys-Muñoz E, Brown E, Coombs GH, Mottram JC. Leishmania Mexicana metacaspase is a negative regulator of amastigote proliferation in mammalian cells. *Cell Death Dis*. 2012 Sep 6;3:e385.

Catalano A, Romano M, Robuffo I, Strizzi L, Procopio A. Methionine aminopeptidase-2 regulates human mesothelioma cell survival: role of Bcl-2 expression and telomerase activity. *Am J Pathol*. 2001 Aug;159(2):721-31.

Cerretti DP, Kozlosky CJ, Mosley B, Nelson N, Van Ness K, Greenstreet TA, March CJ, Kronheim SR, Druck T, Cannizzaro LA, et al. Molecular cloning of the interleukin-1 beta converting enzyme. *Science*. 1992 Apr 3;256(5053):97-100.

TH-1832_126106036

Chai SC, Wang WL, Ye QZ. FE(II) is the native cofactor for Escherichia coli methionine aminopeptidase. *J Biol Chem*. 2008 Oct 3;283(40):26879-85.

Chang SY, McGary EC, Chang S. Methionine aminopeptidase gene of Escherichia coli is essential for cell growth. *J Bacteriol*. 1989 Jul;171(7):4071-2

Ch'ng JH, Kotturi SR, Chong AG, Lear MJ, Tan KS. A programmed cell death pathway in the malaria parasite Plasmodium falciparum has general features of mammalian apoptosis but is mediated by clan CA cysteine proteases. *Cell Death Dis.* 2010;1:e26.

Chose O, Noël C, Gerbod D, Brenner C, Viscogliosi E, Roseto A. A form of cell death with some features resembling apoptosis in the amitochondrial unicellular organism Trichomonas vaginalis. *Exp Cell Res.* 2002 May 15;276(1):32-9

Christensen ST, Wheatley DN, Rasmussen MI, Rasmussen L. Mechanisms controlling death, survival and proliferation in a model unicellular eukaryote Tetrahymena thermophila. *Cell Death Differ.* 1995 Oct;2(4):301-8.

Claborn DM. The biology and control of leishmaniasis vectors. *J Glob Infect Dis*. 2010 May;2(2):127-34.

Compton MM. A biochemical hallmark of apoptosis: internucleosomal degradation of the genome. *Cancer Metastasis Rev*. 1992 Sep;11(2):105-19.

Cornillon S, Foa C, Davoust J, Buonavista N, Gross JD, Golstein P. Programmed cell death in Dictyostelium. *J Cell Sci*. 1994 Oct;107 (Pt 10):2691-704.

Croan DG, Morrison DA, Ellis JT. Evolution of the genus Leishmania revealed by comparison of DNA and RNA polymerase gene sequences. *Mol Biochem Parasitol*. 1997 Nov;89(2):149-59.

Croft SL, Coombs GH. Leishmaniasis--current chemotherapy and recent advances in the search for novel drugs. *Trends Parasitol*. 2003 Nov;19(11):502-8.

Croft SL, Neal RA, Pendergast W, Chan JH. The activity of alkyl phosphorylcholines and related derivatives against Leishmania donovani. *Biochem Pharmacol*. 1987 Aug 15;36(16):2633-6.

Croft SL, Sundar S, Fairlamb AH. Drug resistance in leishmaniasis. *Clin Microbiol Rev*. 2006 Jan;19(1):111-26.

da Silva-Lopez RE, Giovanni-De-Simone S. Leishmania (Leishmania) amazonensis: purification and characterization of a promastigote serine protease. *Exp Parasitol*. 2004 Jul-Aug;107(3-4):173-82.

Darmon AJ, Nicholson DW, Bleackley RC. Activation of the apoptotic protease CPP32 by cytotoxic T-cell-derived granzyme B. *Nature*. 1995 Oct 5;377(6548):446-8.

TH-1832_126106036

Das M, Mukherjee SB, Shaha C. Hydrogen peroxide induces apoptosis-like death in Leishmania donovani promastigotes. *J Cell Sci.* 2001 Jul;114(Pt 13):2461-9.

Das M, Saudagar P, Sundar S, Dubey VK. Miltefosine-unresponsive Leishmania donovani has a greater ability than miltefosine-responsive L. donovani to resist reactive oxygen species. *FEBS J.* 2013 Oct;280(19):4807-15.

Das R, Roy A, Dutta N, Majumder HK. Reactive oxygen species and imbalance of calcium homeostasis contributes to curcumin induced programmed cell death in Leishmania donovani. *Apoptosis*. 2008 Jul;13(7):867-82.

Datta B. MAPs and POEP of the roads from prokaryotic to eukaryotic kingdoms. *Biochimie.* 2000 Feb;82(2):95-107.

Datta R, Choudhury P, Bhattacharya M, Soto Leon F, Zhou Y, Datta B. Protection of translation initiation factor eIF2 phosphorylation correlates with eIF2-associated glycoprotein p67 levels and requires the lysine-rich domain I of p67. *Biochimie*. 2001 Oct;83(10):919-31.

Datta R, Choudhury P, Ghosh A, Datta B. A glycosylation site, 60SGTS63, of p67 is required for its ability to regulate the phosphorylation and activity of eukaryotic initiation factor 2alpha. *Biochemistry*. 2003 May 13;42(18):5453-60.

Datta R, Tammali R, Datta B. Negative regulation of the protection of eIF2alpha phosphorylation activity by a unique acidic domain present at the N-terminus of p67. *Exp Cell Res*. 2003 Feb 15;283(2):237-46.

Dawit G, Girma Z, Simenew K. A Review on Biology, Epidemiology and Public Health Significance of Leishmaniasis. J Bacteriol Parasitol 4:166. Dawit G, Girma Z, Simenew K. A Review on Biology, Epidemiology and Public Health Significance of Leishmaniasis. *J Bacteriol Parasitol*. 2013;4:166.

Day CL, Smits C, Fan FC, Lee EF, Fairlie WD, Hinds MG. Structure of the BH3 domains from the p53-inducible BH3-only proteins Noxa and Puma in complex with Mcl-1. *J Mol Biol*. 2008 Jul 25;380(5):958-71.

Deiss LP, Galinka H, Berissi H, Cohen O, Kimchi A. Cathepsin D protease mediates programmed cell death induced by interferon-gamma, Fas/APO-1 and TNF-alpha. *EMBO J.* 1996 Aug 1;15(15):3861-70.

Desjeux P, Alvar J. Leishmania/HIV co-infections: epidemiology in Europe. *Ann Trop Med Parasitol.* 2003 Oct;97 Suppl 1:3-15.

Dolai S, Pal S, Yadav RK, Adak S. Endoplasmic reticulum stress-induced apoptosis in Leishmania through Ca2+-dependent and caspase-independent mechanism. *J Biol Chem*. 2011 Apr 15;286(15):13638-46.

TH-1832_126106036

Donovan C. Memoranda: On the possibility of the occurrence of trypanomiasis in India. *Br Med J.* 1903; 1.2213: 1252–1254.

Donovan C. Memorandum: On the possibility of the occurrence of trypanosomiasis in India. 1903. *Natl Med J India*. 1994 Jul-Aug;7(4):196, 201-2.

Dorlo TP, Balasegaram M, Beijnen JH, de Vries PJ. Miltefosine: a review of its pharmacology and therapeutic efficacy in the treatment of leishmaniasis. *J Antimicrob Chemother*. 2012 Nov;67(11):2576-97

Dostálová A, Volf P. Leishmania development in sand flies: parasite-vector interactions overview. *Parasit Vectors*. 2012 Dec 3;5:276.

Dotiwala F, Mulik S, Polidoro RB, Ansara JA, Burleigh BA, Walch M, Gazzinelli RT, Lieberman J. Killer lymphocytes use granulysin, perforin and granzymes to kill intracellular parasites. *Nat Med*. 2016 Feb;22(2):210-6.

Downing T, Imamura H, Decuypere S, Clark TG, Coombs GH, Cotton JA, Hilley JD, de Doncker S, Maes I, Mottram JC, Quail MA, Rijal S, Sanders M, Schönian G, Stark O, Sundar S, Vanaerschot M, Hertz-Fowler C, Dujardin JC, Berriman M. Whole genome sequencing of multiple Leishmania donovani clinical isolates provides insights into population structure and mechanisms of drug resistance. *Genome Res*. 2011 Dec;21(12):2143-56.

Duan H, Orth K, Chinnaiyan AM, Poirier GG, Froelich CJ, He WW, Dixit VM. ICE-LAP6, a novel member of the ICE/Ced-3 gene family, is activated by the cytotoxic T cell protease granzyme B. *J Biol Chem*. 1996 Jul 12;271(28):16720-4.

El-Fadili AK, Zangger H, Desponds C, Gonzalez IJ, Zalila H, Schaff C, Ives A, Masina S, Mottram JC, Fasel N. Cathepsin B-like and cell death in the unicellular human pathogen Leishmania. *Cell Death Dis*. 2010 Sep 2;1:e71.

Emanuelsson O, Brunak S, von Heijne G, Nielsen H. Locating proteins in the cell using TargetP, SignalP and related tools. *Nat Protoc*. 2007;2(4):953-71.

Esseiva AC, Chanez AL, Bochud-Allemann N, Martinou JC, Hemphill A, SchneiderA. Temporal dissection of Bax-induced events leading to fission of the single mitochondrion in Trypanosoma brucei. *EMBO Rep*. 2004 Mar;5(3):268-73.

Fanos V, Cataldi L. Amphotericin B-induced nephrotoxicity: a review. *J Chemother*. 2000 Dec;12(6):463-70.

Farazi TA, Waksman G, Gordon JI. The biology and enzymology of protein N-myristoylation. *J Biol Chem.* 2001 Oct 26;276(43):39501-4.

Folkman J. Figurehting cancer by attacking its blood supply. *Sci Am*. 1996 Sep;275(3):150-4.

TH-1832_126106036

Foucher AL, Rachidi N, Gharbi S, Blisnick T, Bastin P, Pemberton IK, Späth GF. Apoptotic marker expression in the absence of cell death in staurosporine-treated Leishmania donovani. *Antimicrob Agents Chemother*. 2013 Mar;57(3):1252-61.

Froelich CJ, Metkar SS, Raja SM. Granzyme B-mediated apoptosis--the elephant and the blind men? *Cell Death Differ*. 2004 Apr;11(4):369-71.

Fujita H, Tanaka Y, Noguchi Y, Kono A, Himeno M, Kato K. Isolation and sequencing of a cDNA clone encoding rat liver lysosomal cathepsin D and the structure of three forms of mature enzymes. *Biochem Biophys Res Commun*. 1991 Aug 30;179(1):190-6.

Galluzzi L, Vitale I, Abrams JM, Alnemri ES, Baehrecke EH, Blagosklonny MV, Dawson TM, Dawson VL, El-Deiry WS, Fulda S, Gottlieb E, Green DR, Hengartner MO, Kepp O, Knight RA, Kumar S, Lipton SA, Lu X, Madeo F, Malorni W, Mehlen P, Nuñez G, Peter ME, Piacentini M, Rubinsztein DC, Shi Y, Simon HU, Vandenabeele P, White E, Yuan J, Zhivotovsky B, Melino G, Kroemer G. Molecular definitions of cell death subroutines: recommendations of the Nomenclature Committee on Cell Death 2012. *Cell Death Differ*. 2012 Jan;19(1):107-20.

Gamliel A, Teicher C, Hartmann T, Beyreuther K, Stein R. Overexpression of wild-type presenilin 2 or its familial Alzheimer's disease-associated mutant does not induce or increase susceptibility to apoptosis in different cell lines. *Neuroscience*. 2003;117(1):19-28

Gannavaram S, Debrabant A. Programmed cell death in Leishmania: biochemical evidence and role in parasite infectivity. *Front Cell Infect Microbiol*. 2012 Jul 10;2:95.

Gershenfeld HK, Weissman IL. Cloning of a cDNA for a T cell-specific serine protease from a cytotoxic T lymphocyte. *Science*. 1986 May 16;232(4752):854-8.

Ghosh E, Ghosh A, Ghosh AN, Nozaki T, Ganguly S. Oxidative stress-induced cell cycle blockage and a protease-independent programmed cell death in microaerophilic Giardia lamblia. *Drug Des Devel Ther*. 2009 Sep 21;3:103-10.

Giglione C, Boularot A, Meinnel T. Protein N-terminal methionine excision. *Cell Mol Life Sci*. 2004 Jun;61(12):1455-74.

Godbold GD, Ahn K, Yeyeodu S, Lee LF, Ting JP, Erickson AH. Biosynthesis and intracellular targeting of the lysosomal aspartic proteinase cathepsin D. *Adv Exp Med Biol*. 1998;436:153-62

Goldberg T, Hecht M, Hamp T, Karl T, Yachdav G, Ahmed N, Altermann U, Angerer P, Ansorge S, Balasz K, Bernhofer M, Betz A, Cizmadija L, Do KT, Gerke J, Greil R, Joerdens V, Hastreiter M, Hembach K, Herzog M, Kalemanov M, Kluge M, Meier A, Nasir H, Neumaier U, Prade V, Reeb J, Sorokoumov A, Troshani I, Vorberg S, Waldraff S, Zierer J, Nielsen H, Rost B. LocTree3 prediction of localization. *Nucleic Acids Res*. 2014 Jul;42(Web Server issue):W350-5.

TH-1832_126106036

González IJ, Desponds C, Schaff C, Mottram JC, Fasel N. Leishmania major metacaspase can replace yeast metacaspase in programmed cell death and has arginine-specific cysteine peptidase activity. *Int J Parasitol*. 2007 Feb;37(2):161-72.

Goodwin LG. Pentostam (sodium stibogluconate); a 50-year personal reminiscence. *Trans R Soc Trop Med Hyg*. 1995 May-Jun;89(3):339-41.

Gough J, Karplus K, Hughey R, Chothia C. Assignment of homology to genome sequences using a library of hidden Markov models that represent all proteins of known structure. *J Mol Biol.* 2001 Nov 2;313(4):903-19

Green DR. Apoptotic pathways: the roads to ruin. *Cell.* 1998 Sep18;94(6):695-8.

Green DR, Reed JC. Mitochondria and apoptosis. *Science* 1998; 281:1309-1312.

Green DR. Apoptotic pathways: paper wraps stone blunts scissors. *Cell*. 2000 Jul 7;102(1):1-4.

Griffith EC, Su Z, Turk BE, Chen S, Chang YH, Wu Z, Biemann K, Liu JO. Methionine aminopeptidase (type 2) is the common target for angiogenesis inhibitors AGM-1470 and ovalicin. *Chem Biol*. 1997 Jun;4(6):461-71.

Gu Y, Sarnecki C, Fleming MA, Lippke JA, Bleackley RC, Su MS. Processing and activation of CMH-1 by granzyme B. *J Biol Chem*. 1996 May 3;271(18):10816-20.

Guenette RS, Mooibroek M, Wong K, Wong P, Tenniswood M. Cathepsin B, a cysteine protease implicated in metastatic progression, is also expressed during regression of the rat prostate and mammary glands. *Eur J Biochem*. 1994 Dec 1;226(2):311-21.

Guicciardi ME, Deussing J, Miyoshi H, Bronk SF, Svingen PA, Peters C, Kaufmann SH, Gores GJ. Cathepsin B contributes to TNF-alpha-mediated hepatocyte apoptosis by promoting mitochondrial release of cytochrome c. *J Clin Invest.* 2000 Nov;106(9):1127-37.

Gump JM, Thorburn A. Autophagy and apoptosis: what is the connection? Trends Cell Biol. 2011 Jul;21(7):387-92.

Guroff G. A neutral, calcium-activated proteinase from the soluble fraction of rat brain. *J Biol Chem*. 1964 Jan;239:149-55.

Hamill RJ. Amphotericin B formulations: a comparative review of efficacy and toxicity. *Drugs.* 2013 Jun;73(9):919-34.

Hanahan D, Folkman J. Patterns and emerging mechanisms of the angiogenic switch during tumorigenesis. *Cell*. 1996 Aug 9;86(3):353-64.

Handman E. Leishmaniasis: current status of vaccine development. *Clin Microbiol Rev.* 2001 Apr;14(2):229-43.

TH-1832_126106036

Hayes MP, Berrebi GA, Henkart PA. Induction of target cell DNA release by the cytotoxic T lymphocyte granule protease granzyme A. *J Exp Med*. 1989 Sep 1;170(3):933-46.

Hengartner MO. The biochemistry of apoptosis. *Nature.* 2000;407:770-776.

Herwaldt BL. Leishmaniasis. *Lancet*. 1999 Oct 2;354(9185):1191-9.

Hide M, Bucheton B, Kamhawi S, Bras-Goncalves R, Sundar S, Lemesre JL, Banuls AL. Understanding Human Leishmaniasis: The need or an Integrated Approach. *Encyclopedia of Infectious Diseases: Modern Methodologies (ed. by M. Tibayrenc), Wiley-Liss Hoboken NJ*. 2007; 87.

Hoare CA. Early discoveries regarding the parasite of oriental sore. Trans R Soc Trop Med Hyg. 1938;32:67–92.

Horvitz HR. Genetic control of programmed cell death in the nematode Caenorhabditis elegans. *Cancer Res.* 1999 Apr 1;59(7 Suppl):1701s-1706s.

Howland RH. Aspergillus, angiogenesis, and obesity: the story behind beloranib. *J Psychosoc Nurs Ment Health Serv*. 2015 Mar;53(3):13-6.

Hüttemann M, Pecina P, Rainbolt M, Sanderson TH, Kagan VE, Samavati L, Doan JW, Lee I. The multiple functions of cytochrome c and their regulation in life and death decisions of the mammalian cell: From respiration to apoptosis. *Mitochondrion*. 2011 May;11(3):369-81.

Ingber D, Fujita T, Kishimoto S, Sudo K, Kanamaru T, Brem H, Folkman J. Synthetic analogues of fumagillin that inhibit angiogenesis and suppress tumour growth. *Nature*. 1990 Dec 6;348(6301):555-7.

Ivens AC, Peacock CS, Worthey EA, Murphy L, Aggarwal G, Berriman M, Sisk E, Rajandream MA, Adlem E, Aert R, Anupama A, Apostolou Z, Attipoe P, Bason N, Bauser C, Beck A, Beverley SM, Bianchettin G, Borzym K, Bothe G, Bruschi CV, Collins M, Cadag E, Ciarloni L, Clayton C, Coulson RM, Cronin A, Cruz AK, Davies RM, De Gaudenzi J, Dobson DE, Duesterhoeft A, Fazelina G, Fosker N, Frasch AC, Fraser A, Fuchs M, Gabel C, Goble A, Goffeau A, Harris D, Hertz-Fowler C, Hilbert H, Horn D, Huang Y, Klages S, Knights A, Kube M, Larke N, Litvin L, Lord A, Louie T, Marra M, Masuy D, Matthews K, Michaeli S, Mottram JC, Müller-Auer S, Munden H, Nelson S, Norbertczak H, Oliver K, O'neil S, Pentony M, Pohl TM, Price C, Purnelle B, Quail MA, Rabbinowitsch E, Reinhardt R, Rieger M, Rinta J, Robben J, Robertson L, Ruiz JC, Rutter S, Saunders D, Schäfer M, Schein J, Schwartz DC, Seeger K, Seyler A, Sharp S, Shin H, Sivam D, Squares R, Squares S, Tosato V, Vogt C, Volckaert G, Wambutt R, Warren T, Wedler H, Woodward J, Zhou S, Zimmermann W, Smith DF, Blackwell JM, Stuart KD, Barrell B, Myler PJ. The genome of the kinetoplastid parasite, Leishmania major. *Science*. 2005 Jul 15;309(5733):436-42.

Jackson R, Hunter T. Role of methionine in the initiation of haemoglobin synthesis. *Nature*. 1970 Aug 15;227(5259):672-6.

TH-1832_126106036

Jha TK, Sundar S, Thakur CP, Felton JM, Sabin AJ, Horton J. A phase II dose-ranging study of sitamaquine for the treatment of visceral leishmaniasis in India. *Am J Trop Med Hyg*. 2005 Dec;73(6):1005-11.

Jiménez-Ruiz A, Alzate JF, Macleod ET, Lüder CG, Fasel N, Hurd H. Apoptotic markers in protozoan parasites. *Parasit Vectors*. 2010 Nov 9;3:104.

Johnson DE. Noncaspase proteases in apoptosis. *Leukemia.* 2000 Sep;14(9):1695-703

Johnson DR, Bhatnagar RS, Knoll LJ, Gordon JI. Genetic and biochemical studies of protein N-myristoylation. *Annu Rev Biochem*. 1994;63:869-914.

Kamhawi S. Phlebotomine sand flies and Leishmania parasites: friends or foes? *Trends Parasitol*. 2006 Sep;22(9):439-45.

Kanno T, Endo H, Takeuchi K, Morishita Y, Fukayama M, Mori S. High expression of methionine aminopeptidase type 2 in germinal center B cells and their neoplastic counterparts. *Lab Invest*. 2002 Jul;82(7):893-901.

Kaye P, Scott P. Leishmaniasis: complexity at the host-pathogen interface. *Nat Rev Microbiol*. 2011 Jul 11;9(8):604-15.

Krajewski S, Zapata JM, Reed JC. Detection of multiple antigens on western blots. *Anal Biochem*. 1996 May 1;236(2):221-8.

Krogh A, Larsson B, von Heijne G, Sonnhammer EL. Predicting transmembrane protein topology with a hidden Markov model: application to complete genomes. *J Mol Biol*. 2001 Jan 19;305(3):567-80.

Kulkarni MM, McMaster WR, Kamysz W, McGwire BS. Antimicrobial peptide-induced apoptotic death of leishmania results from calcium-de pend ent, caspase-independent mitochondrial toxicity. *J Biol Chem*. 2009 Jun 5;284(23):15496-504.

Kumar R, Mohapatra P, Dubey VK. Exploring Realm of Proteases of Leishmania donovani Genome and Gene Expression Analysis of Proteases under Apoptotic Condition. *J. Proteomics. Bioinform*. 2016;9:200-8.

Kusaka M, Sudo K, Fujita T, Marui S, Itoh F, Ingber D, Folkman J. Potent anti-angiogenic action of AGM-1470: comparison to the fumagillin parent. *Biochem Biophys Res Commun*. 1991 Feb 14;174(3):1070-6.

Lachaud L, Bourgeois N, Plourde M, Leprohon P, Bastien P, Ouellette M. Parasite susceptibility to amphotericin B in failures of treatment for visceral leishmaniasis in patients coinfected with HIV type 1 and Leishmania infantum. *Clin Infect Dis*. 2009 Jan 15;48(2):e16-22.

Lee N, Gannavaram S, Selvapandiyan A, Debrabant A. Characterization of metacaspases with trypsin-like activity and their putative role in programmed cell death in the protozoan parasite Leishmania. *Eukaryot Cell*. 2007 Oct;6(10):1745-57.

TH-1832_126106036

Leishman WB. On the possibility of the occurrence of trypanomiasis in India. *Br Med J.* 1903; 1.2213: 1252–1254.

Levkau B, Kenagy RD, Karsan A, Weitkamp B, Clowes AW, Ross R, Raines EW. Activation of metalloproteinases and their association with integrins: an auxiliary apoptotic pathway in human endothelial cells. *Cell Death Differ*. 2002 Dec;9(12):1360-7.

Li JY, Chen LL, Cui YM, Luo QL, Li J, Nan FJ, Ye QZ. Specificity for inhibitors of metal-substituted methionine aminopeptidase. *Biochem Biophys Res Commun*. 2003 Jul 18;307(1):172-9.

Li LY, Luo X, Wang X. Endonuclease G is an apoptotic DNase when released from mitochondria. *Nature*. 2001 Jul 5;412(6842):95-9.

Li X, Chang YH. Evidence that the human homologue of a rat initiation factor-2 associated protein (p67) is a methionine aminopeptidase. *Biochem Biophys Res Commun*. 1996 Oct 3;227(1):152-9.

Liu S, Widom J, Kemp CW, Crews CM, Clardy J. Structure of human methionine aminopeptidase-2 complexed with fumagillin. *Science*. 1998 Nov 13;282(5392):1324-7.

Machado MF, Marcondes MF, Juliano MA, McLuskey K, Mottram JC, Moss CX, Juliano L, Oliveira V. Substrate specificity and the effect of calcium on Trypanosoma brucei metacaspase 2. *FEBS J.* 2013 Jun;280(11):2608-21.

MacMorris-Adix M. Leishmaniasis: A review of the disease and the debate over the origin and dispersal of the causaitive parasite Leishmania, *Macalester Reviews in Biogeography*. 2008;1:1-18.

Madeo F, Herker E, Maldener C, Wissing S, Lächelt S, Herlan M, Fehr M, Lauber K, Sigrist SJ, Wesselborg S, Fröhlich KU. A caspase-related protease regulates apoptosis in yeast. *Mol Cell.* 2002 Apr;9(4):911-7.

Maiuri MC, Le Toumelin G, Criollo A, Rain JC, Gautier F, Juin P, Tasdemir E, Pierron G, Troulinaki K, Tavernarakis N, Hickman JA, Geneste O, Kroemer G. Functional and physical interaction between Bcl-X(L) and a BH3-like domain in Beclin-1. *EMBO J*. 2007 May 16;26(10):2527-39.

Maltezou HC. Drug resistance in visceral leishmaniasis. *J Biomed Biotechnol*. 2010;2010:617521.

Marinho FA, Gonçalves KC, Oliveira SS, Gonçalves DS, Matteoli FP, Seabra SH, Oliveira AC, Bellio M, Oliveira SS, Souto-Padrón T, d'Avila-Levy CM, Santos AL, Branquinha MH. The calpain inhibitor MDL28170 induces the expression of apoptotic markers in Leishmania amazonensis promastigotes. *PLoS One.* 2014 Jan 31;9(1):e87659.

TH-1832_126106036

Marinho Fde A, Gonçalves KC, Oliveira SS, Oliveira AC, Bellio M, d'Avila-Levy CM, Santos AL, Branquinha MH. Miltefosine induces programmed cell death in Leishmania amazonensis promastigotes. *Mem Inst Oswaldo Cruz*. 2011 Jun;106(4):507-9.

Mariño G, Niso-Santano M, Baehrecke EH, Kroemer G. Self-consumption: the interplay of autophagy and apoptosis. *Nat Rev Mol Cell Biol*. 2014 Feb;15(2):81-94.

Martin SJ, Reutelingsperger CP, McGahon AJ, Rader JA, van Schie RC, LaFace DM, Green DR. Early redistribution of plasma membrane phosphatidylserine is a general feature of apoptosis regardless of the initiating stimulus: inhibition by overexpression of Bcl-2 and Abl. *J Exp Med*. 1995 Nov 1;182(5):1545-56.

Masson D, Tschopp J. Isolation of a lytic, pore-forming protein (perforin) from cytolytic T-lymphocytes. *J Biol Chem*. 1985 Aug 5;260(16):9069-72.

Masson D, Zamai M, Tschopp J. Identification of granzyme A isolated from cytotoxic T-lymphocyte-granules as one of the proteases encoded by CTL-specific genes. *FEBS Lett*. 1986 Nov 10;208(1):84-8.

Mattson MP, Chan SL. Calcium orchestrates apoptosis. *Nat Cell Biol*. 2003 Dec;5(12):1041-3.

Mbongo N, Loiseau PM, Billion MA, Robert-Gero M. Mechanism of amphotericin B resistance in Leishmania donovani promastigotes. *Antimicrob Agents Chemother*. 1998 Feb;42(2):352-7

McCall LI, El Aroussi A, Choi JY, Vieira DF, De Muylder G, Johnston JB, Chen S, Kellar D, Siqueira-Neto JL, Roush WR, Podust LM, McKerrow JH. Targeting Ergosterol biosynthesis in Leishmania donovani: essentiality of sterol 14 alpha-demethylase. *PLoS Negl Trop Dis*. 2015 Mar 13;9(3):e0003588.

Medema JP, Toes RE, Scaffidi C, Zheng TS, Flavell RA, Melief CJ, Peter ME, Offringa R, Krammer PH. Cleavage of FLICE (caspase-8) by granzyme B during cytotoxic T lymphocyte-induced apoptosis. *Eur J Immunol*. 1997 Dec;27(12):3492-8

Mehdi S. Cell-penetrating inhibitors of calpain. *Trends Biochem Sci*. 1991 Apr;16(4):150-3.

Mizushima N, Yoshimori T, Ohsumi Y. The role of Atg proteins in autophagosome formation. *Annu Rev Cell Dev Biol*. 2011;27:107-32.

Moreira ME, Del Portillo HA, Milder RV, Balanco JM, Barcinski MA. Heat shock induction of apoptosis in promastigotes of the unicellular organism Leishmania (Leishmania) amazonensis. *J Cell Physiol*. 1996 May;167(2):305-13.

Morowitz MJ, Barr R, Wang Q, King R, Rhodin N, Pawel B, Zhao H, Erickson SA, Sheppard GS, Wang J, Maris JM, Shusterman S. Methionine aminopeptidase 2

TH-1832_126106036

inhibition is an effective treatment strategy for neuroblastoma in preclinical models. *Clin Cancer Res*. 2005 Apr 1;11(7):2680-5.

Mosmann T. Rapid colorimetric assay for cellular growth and survival: application to proliferation and cytotoxicity assays. *J Immunol Methods*. 1983 Dec 16;65(1-2):55-63.

Moss CX, Westrop GD, Juliano L, Coombs GH, Mottram JC. Metacaspase 2 of Trypanosoma brucei is a calcium-dependent cysteine peptidase active without processing. *FEBS Lett*. 2007 Dec 11;581(29):5635-9

Mottram JC, Helms MJ, Coombs GH, Sajid M. Clan CD cysteine peptidases of parasitic protozoa. *Trends Parasitol*. 2003 Apr;19(4):182-7

Mouatt-Prigent A, Karlsson JO, Agid Y, Hirsch EC. Increased M-calpain expression in the mesencephalon of patients with Parkinson's disease but not in other neurodegenerative disorders involving the mesencephalon: a role in nerve cell death? *Neuroscience*. 1996 Aug;73(4):979-87.

Murachi T, Tanaka K, Hatanaka M, Murakami T. Intracellular Ca2+-dependent protease (calpain) and its high-molecular-weight endogenous inhibitor (calpastatin). *Adv Enzyme Regul*. 1980;19:407-24.

Murray HW, Berman JD, Davies CR, Saravia NG. Advances in leishmaniasis. *Lancet*. 2005 Oct 29-Nov 4;366(9496):1561-77.

Nagata S. Apoptotic DNA fragmentation. *Exp Cell Res*. 2000 Apr 10;256(1):12-8.

Nishimura Y, Kawabata T, Kato K. Identification of latent procathepsins B and L in microsomal lumen: characterization of enzymatic activation and proteolytic processing in vitro. *Arch Biochem Biophys.* 1988 Feb 15;261(1):64-71.

Nixon RA, Saito KI, Grynspan F, Griffin WR, Katayama S, Honda T, Mohan PS, Shea TB, Beermann M. Calcium-activated neutral proteinase (calpain) system in aging and Alzheimer's disease. *Ann N Y Acad Sci*. 1994 Dec 15;747:77-91.

Odake S, Kam CM, Narasimhan L, Poe M, Blake JT, Krahenbuhl O, Tschopp J, Powers JC. Human and murine cytotoxic T lymphocyte serine proteases: subsite mapping with peptide thioester substrates and inhibition of enzyme activity and cytolysis by isocoumarins. *Biochemistry*. 1991 Feb 26;30(8):2217-27.

Orlowski RZ. The role of the ubiquitin-proteasome pathway in apoptosis. *Cell Death Differ*. 1999 Apr;6(4):303-13.

Ozols J, Carr SA, Strittmatter P. Identification of the NH2-terminal blocking group of NADH-cytochrome b5 reductase as myristic acid and the complete amino acid sequence of the membrane-binding domain. *J Biol Chem*. 1984 Nov 10;259(21):13349-54.

TH-1832_126106036

Paris C, Loiseau PM, Bories C, Bréard J. Miltefosine induces apoptosis-like death in Leishmania donovani promastigotes. *Antimicrob Agents Chemother*. 2004 Mar;48(3):852-9.

Patel T, Gores GJ, Kaufmann SH. The role of proteases during apoptosis. *FASEB J*. 1996 Apr;10(5):587-97.

Peng BW, Lin J, Lin JY, Jiang MS, Zhang T. Exogenous nitric oxide induces apoptosis in Toxoplasma gondii tachyzoites via a calcium signal transduction pathway. *Parasitology*. 2003 Jun;126(Pt 6):541-50.

Picazarri K, Nakada-Tsukui K, Nozaki T. Autophagy during proliferation and encystation in the protozoan parasite Entamoeba invadens. *Infect Immun*. 2008 Jan;76(1):278-88.

Pinheiro RO, Nunes MP, Pinheiro CS, D'Avila H, Bozza PT, Takiya CM, Côrte-Real S, Freire-de-Lima CG, DosReis GA. Induction of autophagy correlates with increased parasite load of Leishmania amazonensis in BALB/c but not C57BL/6 macrophages. *Microbes Infect*. 2009 Feb;11(2):181-90.

Purkait B, Kumar A, Nandi N, Sardar AH, Das S, Kumar S, Pandey K, Ravidas V, Kumar M, De T, Singh D, Das P. Mechanism of amphotericin B resistance in clinical isolates of Leishmania donovani. *Antimicrob Agents Chemother*. 2012 Feb;56(2):1031-41.

Quan LT, Tewari M, O'Rourke K, Dixit V, Snipas SJ, Poirier GG, Ray C, Pickup DJ, Salvesen GS. Proteolytic activation of the cell death protease Yama/CPP32 by granzyme B. *Proc Natl Acad Sci U S A.* 1996 Mar 5;93(5):1972-6.

Rachidi N, Taly JF, Durieu E, Leclercq O, Aulner N, Prina E, Pescher P, Notredame C, Meijer L, Spath GF. Pharmacological assessment defines Leishmania donovani Casein Kinase 1 as a drug target and reveals important functions in parasite viability and intracellular infection. *Antimicrob. Agents*. 2014;58(3):1501-15.

Raff MC. Social controls on cell survival and cell death. *Nature*. 1992 Apr 2;356(6368):397-400.

Rappoport N, Karsenty S, Stern A, Linial N, Linial M. ProtoNet 6.0: organizing 10 million protein sequences in a compact hierarchical family tree. *Nucleic Acids Res.* 2012 Jan;40(Database issue):D313-20.

Rawlings ND, Waller M, Barrett AJ, Bateman A. MEROPS: the database of proteolytic enzymes, their substrates and inhibitors. *Nucleic Acids Res*. 2014 Jan;42(Database issue):D503-9.

Reithinger R, Dujardin JC, Louzir H, Pirmez C, Alexander B, Brooker S. Cutaneous leishmaniasis. *Lancet Infect Dis*. 2007 Sep;7(9):581-96.

Resh MD. Covalent lipid modifications of proteins. *Curr Biol*. 2013 May 20;23(10):R431-5.

TH-1832_126106036

Roberts LR, Adjei PN, Gores GJ. Cathepsins as effector proteases in hepatocyte apoptosis. *Cell Biochem Biophys.* 1999;30(1):71-88.

Roberts LR, Kurosawa H, Bronk SF, Fesmier PJ, Agellon LB, Leung WY, Mao F, Gores GJ. Cathepsin B contributes to bile salt-induced apoptosis of rat hepatocytes. *Gastroenterology*. 1997 Nov;113(5):1714-26.

Roderick SL, Matthews BW. Structure of the cobalt-dependent methionine aminopeptidase from Escherichia coli: a new type of proteolytic enzyme. *Biochemistry*. 1993 Apr 20;32(15):3907-12.

Romano PS, Arboit MA, Vázquez CL, Colombo MI. The autophagic pathway is a key component in the lysosomal dependent entry of Trypanosoma cruzi into the host cell. *Autophagy*. 2009 Jan;5(1):6-18.

Ross R. Further notes on Leishman's bodies. *Br Med J.* 1903;2(2239):1401.

Rotonda J, Nicholson DW, Fazil KM, Gallant M, Gareau Y, Labelle M, Peterson EP, Rasper DM, Ruel R, Vaillancourt JP, Thornberry NA, Becker JW. The three-dimensional structure of apopain/CPP32, a key mediator of apoptosis. *Nat Struct Biol*. 1996 Jul;3(7):619-25.

Rowan AD, Mason P, Mach L, Mort JS. Rat procathepsin B. Proteolytic processing to the mature form in vitro. *J Biol Chem*. 1992 Aug 5;267(22):15993-9.

Rozen S, Skaletsky H. Primer3 on the WWW for general users and for biologist programmers. *Methods Mol Biol*. 2000;132:365-86.

Sabra R, Branch RA. Amphotericin B nephrotoxicity. *Drug Saf.* 1990 Mar-Apr;5(2):94-108

Saito K, Elce JS, Hamos JE, Nixon RA. Widespread activation of calcium-activated neutral proteinase (calpain) in the brain in Alzheimer disease: a potential molecular basis for neuronal degeneration. *Proc Natl Acad Sci U S A.* 1993 Apr 1;90(7):2628-32.

Sambrook J, Fritschi EF, Maniatis T. Molecular cloning: a laboratory manual. 2nd Ed. *Cold Spring Harbor, NY*. 1989.

Sangueza OP, Sangueza JM, Stiller MJ, Sangueza P. Mucocutaneous leishmaniasis: a clinicopathologic classification. *J Am Acad Dermatol*. 1993 Jun;28(6):927-32.

Sasaki T, Yoshimura N, Kikuchi T, Hatanaka M, Kitahara A, Sakihama T, Murachi T. Similarity and dissimilarity in subunit structures of calpains I and II from various sources as demonstrated by immunological cross-reactivity. *J Biochem*. 1983 Dec;94(6):2055-61.

Saudagar P, Dubey VK. Molecular mechanisms of in vitro betulin-induced apoptosis of Leishmania donovani. *Am J Trop Med Hyg*. 2014 Feb;90(2):354-60.

TH-1832_126106036

Saudagar P, Saha P, Saikia AK, Dubey VK. Molecular mechanism underlying antileishmanial effect of oxabicyclo[3.3.1]nonanones: inhibition of key redox enzymes of the pathogen. *Eur J Pharm Biopharm*. 2013 Nov;85(3 Pt A):569-77.

Savill J, Fadok V. Corpse clearance defines the meaning of cell death. *Nature*. 2000 Oct 12;407(6805):784-8.

Schotte P, Declercq W, Van Huffel S, Vandenabeele P, Beyaert R. Non-specific effects of methyl ketone peptide inhibitors of caspases. *FEBS Lett*. 1999 Jan 8;442(1):117-21.

Schultz AM, Tsai SC, Kung HF, Oroszlan S, Moss J, Vaughan M. Hydroxylamine-stable covalent linkage of myristic acid in G0 alpha, a guanine nucleotide-binding protein of bovine brain. *Biochem Biophys Res Commun*. 1987 Aug 14;146(3):1234-9.

Schultz AM, Henderson LE, Oroszlan S, Garber EA, Hanafusa H. Amino terminal myristylation of the protein kinase p60src, a retroviral transforming protein. *Science*. 1985 Jan 25;227(4685):427–429.

Schwartz MK. Tissue cathepsins as tumor markers. *Clin Chim Acta*. 1995 Jun 15;237(1-2):67-78.

Selvakumar P, Lakshmikuttyamma A, Kanthan R, Kanthan SC, Dimmock JR, Sharma RK. High expression of methionine aminopeptidase 2 in human colorectal adenocarcinomas. *Clin Cancer Res.* 2004 Apr 15;10(8):2771-5.

Sharma AK, Rohrer B. Calcium-induced calpain mediates apoptosis via caspase-3 in a mouse photoreceptor cell line. *J Biol Chem*. 2004 Aug 20;279(34):35564-72.

Sharma U, Singh S. Insect vectors of Leishmania: distribution, physiology and their control. *J Vector Borne Dis*. 2008 Dec;45(4):255-72.

Sheen IS, Jeng KS, Jeng WJ, Jeng CJ, Wang YC, Gu SL, Tseng SY, Chu CM, Lin CH, Chang KM. Fumagillin treatment of hepatocellular carcinoma in rats: an in vivo study of antiangiogenesis. *World J Gastroenterol*. 2005 Feb 14;11(6):771-7.

Shibata M, Kanamori S, Isahara K, Ohsawa Y, Konishi A, Kametaka S, Watanabe T, Ebisu S, Ishido K, Kominami E, Uchiyama Y. Participation of cathepsins B and D in apoptosis of PC12 cells following serum deprivation. *Biochem Biophys Res Commun.* 1998 Oct 9;251(1):199-203.

Shukla AK, Patra S, Dubey VK. Iridoid glucosides from Nyctanthes arbortristis result in increased reactive oxygen species and cellular redox homeostasis imbalance in Leishmania parasite. *Eur J Med Chem*. 2012 Aug;54:49-58

Shusterman S, Grupp SA, Barr R, Carpentieri D, Zhao H, Maris JM. The angiogenesis inhibitor tnp-470 effectively inhibits human neuroblastoma xenograft growth, especially in the setting of subclinical disease. *Clin Cancer Res.* 2001 Apr;7(4):977-84.

TH-1832_126106036

Sin N, Meng L, Wang MQ, Wen JJ, Bornmann WG, Crews CM. The anti-angiogenic agent fumagillin covalently binds and inhibits the methionine aminopeptidase, MetAP-2. *Proc Natl Acad Sci U S A.* 1997 Jun 10;94(12):6099-103.

Singh AN, Yadav P, Dubey VK. cDNA cloning and molecular modeling of procerain B, a novel cysteine endopeptidase isolated from Calotropis procera. *PLoS One*. 2013;8(3):e59806

Singh S, Sarma S, Katiyar SP, Das M, Bhardwaj R, Sundar D, Dubey VK. Probing the molecular mechanism of hypericin-induced parasite death provides insight into the role of spermidine beyond redox metabolism in Leishmania donovani. *Antimicrob Agents Chemother*. 2015 Jan;59(1):15-24.

Smyth MJ, Trapani JA. Granzymes: exogenous proteinases that induce target cell apoptosis. *Immunol Today*. 1995 Apr;16(4):202-6.

Solbiati J, Chapman-Smith A, Miller JL, Miller CG, Cronan JE Jr. Processing of the N termini of nascent polypeptide chains requires deformylation prior to methionine removal. *J Mol Biol*. 1999 Jul 16;290(3):607-14.

Sorimachi H, Saido TC, Suzuki K. New era of calpain research. Discovery of tissue-specific calpains. *FEBS Lett*. 1994 Apr 18;343(1):1-5.

Squìer MK, Miller AC, Malkinson AM, Cohen JJ. Calpain activation in apoptosis. *J Cell Physiol*. 1994 May;159(2):229-37.

Stockdale L, Newton R. A review of preventative methods against human leishmaniasis infection. *PLoS Negl Trop Dis*. 2013 Jun 20;7(6):e2278.

Sundar S, Olliaro PL. Miltefosine in the treatment of leishmaniasis: Clinical evidence for informed clinical risk management. *Ther Clin Risk Manag*. 2007 Oct;3(5):733-40.

Sundar S, Pai K, Kumar R, Pathak-Tripathi K, Gam AA, Ray M, Kenney RT. Resistance to treatment in Kala-azar: speciation of isolates from northeast India. *Am J Trop Med Hyg*. 2001 Sep;65(3):193-6.

Sundar S. Drug resistance in Indian visceral leishmaniasis. *Trop Med Int Health*. 2001 Nov;6(11):849-54

Talanian RV, Yang X, Turbov J, Seth P, Ghayur T, Casiano CA, Orth K, Froelich CJ. Granule-mediated killing: pathways for granzyme B-initiated apoptosis. *J Exp Med*. 1997 Oct 20;186(8):1323-31.

Tang CH, Grimm EA. Depletion of endogenous nitric oxide enhances cisplatin-induced apoptosis in a p53-dependent manner in melanoma cell lines. *J Biol Chem*. 2004 Jan 2;279(1):288-98.

TH-1832_126106036

Thornberry NA, Lazebnik Y. Caspases: enemies within. *Science*. 1998 Aug 28;281(5381):1312-6.

Trapani JA, Smyth MJ. Functional significance of the perforin/granzyme cell death pathway. *Nat Rev Immunol.* 2002 Oct;2(10):735-47.

Tschopp J, Schäfer S, Masson D, Peitsch MC, Heusser C. Phosphorylcholine acts as a Ca2+-dependent receptor molecule for lymphocyte perforin. *Nature*. 1989 Jan 19;337(6204):272-4.

Turk BE, Griffith EC, Wolf S, Biemann K, Chang YH, Liu JO. Selective inhibition of amino-terminal methionine processing by TNP-470 and ovalicin in endothelial cells. *Chem Biol*. 1999 Nov;6(11):823-33.

Urbina JA. Lipid biosynthesis pathways as chemotherapeutic targets in kinetoplastid parasites. *Parasitology*. 1997;114 Suppl:S91-9.

Uren AG, O'Rourke K, Aravind LA, Pisabarro MT, Seshagiri S, Koonin EV, DixitVM. Identification of paracaspases and metacaspases: two ancient families of caspase-like proteins, one of which plays a key role in MALT lymphoma. *Mol Cell.* 2000 Oct;6(4):961-7.

Van de Craen M, Van den Brande I, Declercq W, Irmler M, Beyaert R, Tschopp J, Fiers W, Vandenabeele P. Cleavage of caspase family members by granzyme B: a comparative study in vitro. *Eur J Immunol*. 1997 May;27(5):1296-9.

Vercammen D, van de Cotte B, De Jaeger G, Eeckhout D, Casteels P, Vandepoele K, Vandenberghe I, Van Beeumen J, Inzé D, Van Breusegem F. Type II metacaspases Atmc4 and Atmc9 of Arabidopsis thaliana cleave substrates after arginine and lysine. *J Biol Chem*. 2004 Oct 29;279(44):45329-36.

Verma NK, Dey CS. Possible mechanism of miltefosine-mediated death of Leishmania donovani. *Antimicrob Agents Chemother*. 2004 Aug;48(8):3010-15.

Verma NK, Singh G, Dey CS. Miltefosine induces apoptosis in arsenite-resistant Leishmania donovani promastigotes through mitochondrial dysfunction. *Exp Parasitol.* 2007 May;116(1):1-13.

Villalba JD, Gómez C, Medel O, Sánchez V, Carrero JC, Shibayama M, Ishiwara DG. Programmed cell death in Entamoeba histolytica induced by the aminoglycoside G418. *Microbiology*. 2007 Nov;153(Pt 11):3852-63.

Walker KW, Bradshaw RA. Yeast methionine aminopeptidase I can utilize either Zn^{2+} or Co^{2+} as a cofactor: a case of mistaken identity*? Protein Sci*. 1998 Dec;7(12):2684-7.

Walker NP, Talanian RV, Brady KD, Dang LC, Bump NJ, Ferenz CR, Franklin S, Ghayur T, Hackett MC, Hammill LD, et al. Crystal structure of the cysteine protease interleukin-1 beta-converting enzyme: a (p20/p10)2 homodimer. *Cell*. 1994 Jul 29;78(2):343-52.

TH-1832_126106036

Wang J, Sheppard GS, Lou P, Kawai M, Park C, Egan DA, Schneider A, Bouska J, Lesniewski R, Henkin J. Physiologically relevant metal cofactor for methionine aminopeptidase-2 is manganese. *Biochemistry*. 2003 May 6;42(17):5035-42.

Wang KK. Calpain and caspase: can you tell the difference? *Trends Neurosci.* 2000 Jan;23(1):20-6.

Wang KK. Developing selective inhibitors of calpain. *Trends Pharmacol Sci*. 1990 Apr;11(4):139-42.

Watanabe N, Lam E. Two Arabidopsis metacaspases AtMCP1b and AtMCP2b are arginine/lysine-specific cysteine proteases and activate apoptosis-like cell death in yeast. *J Biol Chem.* 2005 Apr 15;280(15):14691-9.

Waterhouse NJ, Finucane DM, Green DR, Elce JS, Kumar S, Alnemri ES, Litwack G, Khanna K, Lavin MF, Watters DJ. Calpain activation is upstream of caspases in radiation-induced apoptosis. *Cell Death Differ.* 1998 Dec;5(12):1051-61.

Weingärtner A, Kemmer G, Müller FD, Zampieri RA, Gonzaga dos Santos M, Schiller J, Pomorski TG. Leishmania promastigotes lack phosphatidylserine but bind annexin V upon permeabilization or miltefosine treatment. *PLoS One*. 2012;7(8):e42070

Welburn SC, Dale C, Ellis D, Beecroft R, Pearson TW. Apoptosis in procyclic Trypanosoma brucei rhodesiense in vitro. *Cell Death Differ*. 1996 Apr;3(2):229-36.

Williams RA, Mottram JC, Coombs GH. Distinct roles in autophagy and importance in infectivity of the two ATG4 cysteine peptidases of Leishmania major. *J Biol Chem*. 2013 Feb 1;288(5):3678-90.

Wilson KP, Black JA, Thomson JA, Kim EE, Griffith JP, Navia MA, Murcko MA, Chambers SP, Aldape RA, Raybuck SA, et al. Structure and mechanism of interleukin-1 beta converting enzyme. *Nature*. 1994 Jul 28;370(6487):270-5.

Wu GS, Saftig P, Peters C, El-Deiry WS. Potential role for cathepsin D in p53-dependent tumor suppression and chemosensitivity. *Oncogene*. 1998 Apr 30;16(17):2177-83.

Xia W, Wolfe MS. Intramembrane proteolysis by presenilin and presenilin-like proteases. *J Cell Sci.* 2003 Jul 15;116(Pt 14):2839-44.

Xie H, Johnson GV. Ceramide selectively decreases tau levels in differentiated PC12 cells through modulation of calpain I. *J Neurochem*. 1997 Sep;69(3):1020-30.

Yang G, Kirkpatrick RB, Ho T, Zhang GF, Liang PH, Johanson KO, Casper DJ, Doyle ML, Marino JP Jr, Thompson SK, Chen W, Tew DG, Meek TD. Steady-state kinetic characterization of substrates and metal-ion specificities of the full-length and N-terminally truncated recombinant human methionine aminopeptidases (type 2). *Biochemistry*. 2001 Sep 4;40(35):10645-54.

TH-1832_126106036

Yonekawa T, Thorburn A. Autophagy and cell death. *Essays Biochem*. 2013;55:105-17.

Young JD, Hengartner H, Podack ER, Cohn ZA. Purification and characterization of a cytolytic pore-forming protein from granules of cloned lymphocytes with natural killer activity. *Cell*. 1986 Mar 28;44(6):849-59

Yousefi S, Perozzo R, Schmid I, Ziemiecki A, Schaffner T, Scapozza L, Brunner T, Simon HU. Calpain-mediated cleavage of Atg5 switches autophagy to apoptosis. *Nat Cell Biol*. 2006 Oct;8(10):1124-32.

Yu CS, Chen YC, Lu CH, Hwang JK. Prediction of protein subcellular localization. *Proteins*. 2006 Aug 15;64(3):643-51.

Yuan J, Shaham S, Ledoux S, Ellis HM, Horvitz HR. The C. elegans cell death gene ced-3 encodes a protein similar to mammalian interleukin-1 beta-converting enzyme. *Cell*. 1993 Nov 19;75(4):641-52.

Zamzami N, Kroemer G. The mitochondrion in apoptosis: how Pandora's box opens. *Nat Rev Mol Cell Biol*. 2001 Jan;2(1):67-71.

Zangger H, Mottram JC, Fasel N. Cell death in Leishmania induced by stress and differentiation: programmed cell death or necrosis? *Cell Death Differ*. 2002 Oct;9(10):1126-39.

Zuo X, Djordjevic JT, Bijosono Oei J, Desmarini D, Schibeci SD, Jolliffe KA, Sorrell TC. Miltefosine induces apoptosis-like cell death in yeast via Cox9p in cytochrome c oxidase. *Mol Pharmacol*. 2011 Sep;80(3):476-85.

TH-1832_126106036

Publications*

1. **Ritesh Kumar,** Kartikeya Tiwari and Vikash Kumar Dubey **(2017)** Methionine aminopeptidase 2 is a key regulator of apoptotic like cell death in *Leishmania donovani*. ***Scientific Reports*-Nature publishing group,** 7: 95.
   Appeared as "**New drug targets for developing cures for *Kala-azar***" research highlight in **Nature India**, doi: 10.1038/nindia.2017.42, A news letter of **Nature Publishing Group**.

2. **Ritesh Kumar,** Pratyajit Mohapatra and Vikash Kumar Dubey **(2016)** Exploring realm of proteases of *Leishmania donovani* genome and gene expression analysis of proteases under apoptotic condition. ***Journal of Proteomics and Bioinformatics***, 9: 200-208.

3. **Ritesh Kumar** and Vikash Kumar Dubey **(2017)** Understanding the role of methionine aminopeptidase 2 in programmed cell death of *Leishmania donovani* by studying the knockout mutants. (Manuscript submitted for publication).

4. Kartikeya Tiwari, **Ritesh Kumar** and Vikash Kumar Dubey **(2016)** Biochemical characterization of dihydroorotase of *Leishmania donovani*: Understanding pyrimidine metabolism through its inhibition. ***Biochimie***, 131: 45-53.

5. Shalini Singh, Ekta Kumari, Ruchika Bhardwaj, **Ritesh Kumar** and Vikash Kumar Dubey **(2017)** Molecular events leading to death of *Leishmania donovani* under spermidine starvation after hypericin treatment. ***Chemical Biology & Drug Design,*** doi: 10.1111/cbdd.13022.

6. Ruchika Bhardwaj, **Ritesh Kumar**, Sanjeev Kumar Singh, Chandrabose Selvaraj and Vikash Kumar Dubey **(2016)** Understanding the importance of conservative hypothetical protein LdBPK_070020 in *Leishmania donovani* and its role in subsistence of the parasite. ***Archives of Biochemistry and Biophysics***, 596, 10-21.

7. Mousumi Das, **Ritesh Kumar** and Vikash Kumar Dubey **(2015)** Ornithine decarboxylase of *Leishmania donovani*: Biochemical properties and possible role of N-terminal extension. ***Protein and Peptide Letters***, 22, 130-136**.**

8. **Ritesh Kumar[*],** Shalini Singh[*] and Vikash Kumar Dubey **(2015)** Bioinformatics Tools to Analyze Proteome and Genome Data. Advances in the Understanding of Biological Sciences Using Next Generation Sequencing (NGS) Approaches. ***Springer International Publishing,*** 179-194. ([*]Equal Contribution) **(BOOK CHAPTER)**

*** Publications from the work reported in the thesis and from collaborative work**

TH-1832_126106036

Conference Proceedings

1. **Ritesh Kumar** and Vikash Kumar Dubey. Exploring the world of proteases in search of caspase like activity in *Leishmania donovani* at International Conference on "Future Prospects of Advancements in Biological Sciences, Health Issues & Environmental Protection at Indira Gandhi Pratishthan, Lucknow, 07th -08th Feb 2014. (**Best Poster Award**)

2. **Ritesh Kumar** and Vikash Kumar Dubey. MAP2 orchestrates apoptosis: A mechanistic insight of cell death in *Leishmania donovani* parasite at Research Conclave organized by student academic board, IIT Guwahati, 20th March, 2016.

3. **Ritesh Kumar** and Vikash Kumar Dubey. Mechanistic elucidation of apoptosis in Leishmania: the important role of noncaspase proteases at Flow Application on Basic, Applied and Clinical Biology" FABACTCS 2016, IIT Guwahati, 03rd – 05th November, 2016.

4. **Ritesh Kumar** and Vikash Kumar Dubey. Effect of TNP-470 on the apoptotic processes of miltefosine treated *Leishmania donovani.* 57th Annual conference of Association of Microbiologists of India & International Symposium on Microbes and Biosphere: What's new what next at Gauhati University, Guwahati, 24th -27th Nov, 2016.

5. **Ritesh Kumar** and Vikash Kumar Dubey. Understanding the role of methionine aminopeptidase 2 in programmed cell death of *Leishmania donovani* by studying the knockout mutants. 3rd International Conference on perspective of cell signaling and molecular medicine, at Bose Institute, Kolkata, 08th -10th Jan 2016.

6. **Ritesh Kumar** and Vikash Kumar Dubey. Apoptotic mystery in *Leishmania donovani*: An update. Research Conclave organized by student academic board, IIT Guwahati, 16th – 19th March, 2017 **(Best Poster Award)**

TH-1832_126106036